University of the Witwatersrand

Master's Dissertation

Application of the Bivariate Chebyshev Spectral Collocation Quasi-linearisation Method for Non-similar Boundary Layer Equations

Author:
Vuyelwa Makibelo

Supervisor:
Prof C. Harley

A dissertation submitted in attainment of the requirements for the degree of Master of Science

in the

School of Computer Science and Applied Mathematics

February 2017

Declaration of Authorship

I, Vuyelwa Makibelo, affirm that this dissertation entitled, 'Application of the Bivariate Chebyshev Spectral Collocation Quasi-linearisation Method for Non-similar Boundary Layer Equations' and the work produced in it is my own. I attest that:

- This dissertation was completed whilst in candidature for a research degree at the University of the Witwatersrand.
- Where any portion of this work has previously been submitted for any form of qualification at any university or institution, this has been distinctly declared.
- Where I have made use of published work of others, this has been referenced.
- Quotations from the work of others has been clearly stated.
- I have recognized all main sources that aided in the treatise that I have presented.
- In this dissertation where work was done jointly with others and solely by myself, this has been clearly indicated.

Signed: ______________________________

Date: ______________________________

"All things splendid have been achieved by those who dared believe that something inside them was superior to circumstance."

Bruce Barton

UNIVERSITY OF THE WITWATERSRAND

Abstract

Faculty Of Science
School of Computer Science and Applied Mathematics

Master of Science

Application of the Bivariate Chebyshev Spectral Collocation Quasi-linearisation Method for Non-similar Boundary Layer Equations

by Vuyelwa MAKIBELO

In this dissertation the bivariate spectral quasi-linearisation method (BI-SQLM) will be used to solve non-similar boundary layer equations. There are three models examined which are:

(i) Unsteady boundary layer flow adjacent to a permeable stretching surface in a porous medium, which consists of a decoupled non-linear equation.

(ii) Thermal radiation effects on magnetohydrodynamics (MHD) forced convection flow adjacent to a non-isothermal wedge in the presence of a heat source or sink, described by a system of two non-linear decoupled equations.

(iii) Unsteady laminar MHD flow near a forward stagnation point of an impulsively rotating and translating sphere in the presence of buoyancy forces, depicted by a system of three non-linear coupled equations.

The numerical results are graphically shown to examine the effects of the different parametric quantities. Convergence and error analyses are conducted to validate the resolutions obtained.

Keywords: Boundary layer, Unsteady flow, Non-linear, Non-similarity, MHD, BI-SQLM.

Acknowledgements

This dissertation is a great milestone in my academic career. I have been fortunate to grasp theories and concepts through extensive research. I am thankful to a number of people who have guided me and provided abetment throughout my research.

Firstly I would like to acknowledge and thank the School of Computer Science and Applied Mathematics (CSAM) at the University of the Witwatersrand for the research facilities provided to me; this aided the completion of my dissertation. In addition to CSAM, I am grateful to the DST-NRF Centre of Excellence in Mathematical and Statistical Sciences (CoE-MaSS) for the financial support and the weekly thought-provoking academic seminars.
I express a warm heartfelt thanks to my supervisor, Prof C. Harley for taking me on as her student, I also thank her for her time, efforts, support and pearls of wisdom.

I am colossally grateful to Vusi Magagula who, as a friend, was willing to help, provide insight, encouragement and emit the support that I needed. I would like to evince my earnest gratitude to my friends Arielle Mulunge (my person), Mathibele Nchabeleng, Mothusi Ponoesele and Gundo Mukhavhuli, who in their own way incentivised me to strive towards my goal. Their prayers, unceasing encouragement went a long way and I appreciate all the good times I shared with every one of them.
My deepest gratitude goes to my mom, Nocawe Makibelo, for her tower of strength when days were really dark in my life and all the sacrifices made out of love. I would like to also thank my siblings Thembi Makibelo and Mmanoko Makibelo for being awesome in general. Last but definitely not the least, I thank my Lord and Saviour Jesus Christ for being my anchor, provider, strength and friend, for I am because He is.

Contents

Symbols

B_o	Externally imposed magnetic field in the y-direction
c_p	Specific heat constant pressure
C_f	Local skin-friction coefficient
Ec	Eckert number
f	Stream function
f_o	Wall mass transfer parameter
k	Thermal conductivity
K	Mean radiation absorption coeficient
m	Pressure gradient parameter
N_R	Thermal radiation parameter
N_{u_x}	Local Nusselt number
Pr	Prandtl number
q_r	Radiative heat flux
Q_o	Heat generation or absorption coefficient
Re_x	Local Reynolds number
T	Temperature
u	Velocity component in the x-direction
U_∞	Potential flow or free stream velocity
v	Velocity in the y-direction
v_o	Suction or injection velocity
x	Coordinate along the wedge surface
y	Coordinate normal to the wedge surface

Greek letters

α	Thermal diffusivity or buoyancy parameter
β	Angle factor of the wedge
η	Pseudosimilarity variable
ξ	Magnetic variable
ω	Total angle of the wedge

ϕ	Dimensionless heat generation or absorption coefficient
θ	Dimensionless temperature
ρ	Density of fluid
ν	Kinematic viscosity
σ	Electrical conductivity
σ^*	Stefan-Boltzmann constant
ψ	Stream function
λ	Porosity parameter or rotation parameter

Subscripts

w	Condition at the wall
∞	Condition at free stream

Dedicated to my mom, Nocawe Makibelo.

Chapter 1

Introduction

The inception of the terminology "spectral" is not very apparent but stems from the primary use of Fourier[1] sines and cosines as basis functions (Gottlieb and Orszag 1977; Brown and Churchhill 1993) particularly with time series analysis and the fundamental frequencies of a process, namely "spectrum"(Shen et al. 2011). Spectral methods have become popular as a method of solution for large-scale calculations, in areas such as heat-transfer, boundary layers, reacting flows, compressible flows and magnetohydrodynamics [1]. The rudimentary problem of approximating a function by interpolation on an interval has paved the way for spectral methods [2]. These techniques have been found to be successful for approximating and solving ordinary and partial differential equations [3].

Spectral methods are global methods, meaning that the computation at any given point depends not only on information at neighbouring points but information across the entire domain [4]. Some of the benefits of using spectral techniques are rapid convergent approximations and dual representations in the physical and transform space which allows for monitoring of the spectrum solution. Furthermore, if symmetries exist in the solutions then spectral methods allow for the exploitation of these symmetries which leads to small errors [5]. The methods make use of higher order polynomials of Fourier series yielding higher orders of accuracy, which becomes extremely advantageous for large computations where there are several data points. There are some drawbacks to these methods one of which is sensitivity at the boundaries, under these circumstances we may encouter unstable behaviour [6].

Spectral representations have been used since the day of Fourier (1882) [2]. Some spectral methods can be tracked back to the "method of weighted residuals "(MWR) of Finlayson and Scriven (1966) [2]. The fundamental components of MWR are the trial

[1] Jean Baptiste Joseph Fourier (1768-1830) was a French mathematician and physicist well known for the development of the Fourier series and the solution of differential equations notably heat transfer.

functions[2] which are utilized as basis functions for a truncated series expansion of the solution and the test functions[3]. These are used to ensure that the differential equation is satisfied as accurately as possible by the truncated series expansion. Among spectral schemes the three most commonly used are Tau, Galerkin and collocation[4] (also known as pseudo-spectral) methods [4]. The schemes are distinguished by the choice of test functions [4]. The Tau and Galerkin method are implemented in terms of expansion coefficients where as collocation methods are applied in terms of physical space values of unknown functions [7]. The Tau technique is a modification of the Galerkin approach which is suited to problems with non-periodic boundary conditions. The collocation method is the preferred form of the spectral methods as it is very simple to implement. For one-dimensional problems, the case of complex non-linear equations the results provide sufficient smoothness.

Numerical spectral methods were originally developed by meteorologists Blinova, Haurwitz and Graig (1987) [1]. In 1954 the first numerical computations were produced by Silberman [1]. Computing solutions with non-linear terms was problematic until Orszag (1969) and Eliasen et al. (1970) developed transform methods that are still pivotal for many large scale spectral computations [1]. Many useful versions of spectral methods have been formulated since 1971. In this study the BI-SQLM method presented by Motsa et al. [3] will be applied to non-similar boundary layer equations.

Boundary layer theory is frequently used to analyze complicated mass and heat transfer problems that involve chemical reactions. The Keller-box method is a popular method used by many researchers to solve unsteady boundary layer flow problems [8]. The Keller-box method is an implicit based finite difference numerical scheme developed by Cebeci and Bradshaw [9]. The shooting method is another commonly used numerical technique to solve similar boundary layer equations [10]. It has been observed however that using this method to solve boundary layer equations for Non-Newtonian fluids becomes problematic when viscosity is a function of shear rate. Furthermore, the shooting method tends to be unstable where the gradient of velocity distribution approaches zero. Also, when the number of equations coupled increases the shooting method becomes increasingly cumbersome and inefficient.

In this study non-similar boundary layer equations are considered, as they are of interest due to an extensive range of applications in engineering and industry [11]. Non-similarity of boundary layers may stem from a variation in free stream velocity, effect of suction or injection of fluid at the wall, wall temperature and buoyancy force effect; in some cases a combination of these effects may occur to cause a flow to be characterised as

[2]Also called expansion approximating functions.

[3]Also known as weight functions.

[4]Collocation is interchangable with pseudo-spectral. Collocation methods seek an approximate solution to satisfy the underlying equation at a set of collocation points.

non-similar [11]. The existence of non-similar flows arose after Ludwig Prandtl introduced boundary layer theory, such flows could only be resolved experimentally or by means of analytic methods [12]. Now with the use of computers and numerical methods non-similar flows can be computed with greater accuracy. The subsequent methods have been applied to examine non-similar boundary layer flows: *i.* Analytic methods by series expansion was carried out by Howarth (1938), Gertler (1957) and Machin (1961); these types of techniques have become obsolete. *ii.* Approximate integral methods were used by Karman(1921) and Rosenhead (1963); approximate methods comprise of two parts, estimating the velocity and temperature profiles and insertion of experimental relationships in integral parameters. *iii.* Numerical techniques of finite differences or finite elements as originally employed by Spalding (1977) and Keller (1978) and these methods have gained popularity among researchers more especially finite differences. However these numerical methods have some drawbacks such as being tedious and computationally costly for solving systems of equations or maintaining a high level of accuracy.

Non-similar boundary layer equations have been found to be more arduous to solve than similar boundary layer equations, but over the years significant progress has been made by various researchers. In Chen's approach non-similar equations were reduced to ordinary differential equations (ODEs) using perturbation theory[5], the ODEs are then solved using the shooting method [10]. Nakamara formulated a numerical technique to solve non-similar boundary layer equations by means of successive substitution iterations of finite difference schemes. The main idea was to reduce a third-order similar boundary layer equation to a second-order boundary value problem which is solved by a tridiagonal matrix solver [10]. This was first applied when considering the natural convection analysis for a Non-Newtonian fluid using the power law model and also using boundary layer equations for micropolar fluids [10]. The method developed by Nakamara was proven to be successful upon similar boundary layer equations. The derivation of the difference equatons is substantially simpler than that of Cebecci and Bradshaw who set up their difference schemes by means of the Keller-box method [13, 14]. The technique of Nakamara for unsteady similar equations was also made applicable to non-similar boundary layer equations. Kafoussias and Williams further extended the method of Nakamara; their technique is based on the common difference method with central differencing tridiagonal matrix manipulation and an iterative procedure [10, 15].

Recently Hayat et al. [16] used homotopy analysis method (HAM) to solve unsteady three dimensional MHD flow and mass transfer in porous media. This technique has been widely used by researchers with similar non-linear problems [17]. HAM is based on homotopy in topology. This method overcomes the preceding restrictions and limitations of perturbation techniques. The benefit of HAM is the independence of physical

[5]Perturbation theory is applicable when deviation from the unperturbed case is small.

parameters and adjustments of the convergence region, but it is time consuming and very tedious to attain higher-order approximations [18]. Soon after Hayat et al. [14] Motsa et al. [19, 20] made use of the spectral relaxation method (SRM) and the spectral quasi-linearisation method (SQLM) to solve unsteady boundary layer problems which have shown to be more precise, easier to implement and computationally efficient. Spectral techniques are advantageous as they are efficient and have a high degree of accuracy without being computationally taxing. The BI-SQLM will be applied for these reasons to the non-similar boundary layer equations. This will act as an extension to the work conducted by Motsa et al. [3]. Three models are considered in this treatise where two are decoupled non-linear differential equations and the remaining model is emcompassed by coupled non-linear differential equations. In proceeding chapters approximate solutions will be obtained, this will be accompanied by convergence and error analyses, as well as some comparisons to previous results.

1.1 Basic concepts

Boundary Layer: *A boundary layer is a thin layer of viscous fluid close to the solid surface of a wall in contact with a stream that is mobile in which (within it's thickness) the flow velocity varies from zero at the wall (where the "sticks" to the wall because of its viscosity[6]).*

[21] ***Porosity:*** *is a measure of how much of a rock is open in space. This space can be between grains or with cracks or cavities of the rock* [22].

Suction: *A force that causes a fluid or solid to be drawn into an interior space or to adhere to a surface because of the difference between external and internal pressures. The surface should have holes (slots, porous sections, perforations)* [23].

Injection: *Forceful insertion of a substance under pressure* [24].

Hydrodynamic: *This is the motion of fluids and the forces acting on solid bodies immersed in fluids and in motion relative to them* [25].

Thermal: *This notion relates to heat, a consequence of heat transfer between the surface and fluid* [26].

Pressure gradient: *This is a physical quantity that describes which direction pressure changes the most rapidly around a particular location.*

[6] measure of resistance

Magnetic parameter: *This is a dimensionless number that is employed in magnetofluid dynamics, it is equated to the product of the square of the magnetic permeability*[7], *the square of the magnetic field strength*[8], *the electrical conductivity*[9] , *and a characteristic length, divided by the product of the mass density*[10] *and the fluid velocity* [27].

Buoyancy parameter: *Is a parameter that denotes the upward pressure applied by the fluid in which a body is immersed. Furthermore it is the Grashof number*[11] *divided by the square of the Reynolds number*[12] [28].

Prandtl number: *This is a dimensionless number, that is represented as the ratio of momentum diffusivity*[13] *to thermal diffusivity*[14] [29].

Rotation parameter: *This is the action of rotating about an axis or centre, also it defines an angle* [30].

Skin-friction coefficient[15]*: The dimensionless skin-friction coefficient is described as proportional to the frictional force per unit area or the shearing stress applied by wind at the surface and square of the surface wind speed.* [31].

Nusselt number: *This is an important non-dimensional quantity utilized in convection*[16]*heat transfer.* [32].

Eckert number: *The Eckert number is a useful dimensionless quantity in determining the relative importance of heat transfer where the kinetic energy of a flow is depicted.* [33].

[7]This is a constant proportionality that prevails betwixt magnetic induction and magnetic field intensity.

[8]Magnetic field strength can be visualized as magnetic field lines, it also correlates to the density of the field lines.

[9]The capacity of a material to carry the flow of an electric current.

[10]This is the mass (or number of particles) per unit volume of a substance, material or object.

[11]Grashof number is significant in cases of fluid flow due to natural convection, meaning the motion of the fluid is not caused by an external source but by the differences in densities between two points.

[12]This is a dimensionless number that is a measure of the ratio of inertial forces (Forces that resists change in velocity of objects.) to viscous forces (Friction between fluid and boundaries.). The higher the Reynolds number the more the flow is turbulent.

[13]This is the motion of a moving body described as the product of mass and velocity.

[14]Thermal diffusivity is essentially how quickly a material reacts to the change in temperature.

[15]Also known as friction coefficient or drag coefficient.

[16]Transfer of heat through a fluid (liquid or gas) induced by molecular motion.

Chapter 2

Methodology

2.1 Lagrange interpolation

Spectral methods stem from approximating a function by interpolation over an interval. Interpolation is the process of determining a function that takes on specified values at specified points. Interpolation is a prominent method in science and engineering where discrete experimental data is dealt with. In addition, interpolation is used to simplify convoluted functions by sampling data points and interpolating them using a simpler function. Polynomials are generally used for interpolation because they are easier to evaluate, differentiate and integrate rather than trigonometric and exponential series expansions [34]. Algebraic polynomials are one of the most widely used classes of functions, mapping the set of real numbers into itself. The set of functions are of the form

$$P_n(x) = a_n x^n + a_{n-1}x^{n-1} + ... + a_1 x + a_0,$$

where n is a non-negative integer and $a_0, ..., a_n$ are real constants. Polynomial interpolation involves determining a polynomial of order n that passes through $n+1$ data points [35]. Lagrange interpolation is one of the methods used to find this polynomial. Other methods include the Newton divided difference approach and the Direct method. A benefit of Lagrange interpolation in comparison with the Direct method and the Newton divided-difference representation, is its simplicity. The Lagrange interpolating polynomial can be determined without the need to solve the system of simultaneous equations or conducting repetitive calculations as in the case of Newton interpolating polynomials where a table of divided differences is required [35]. Another advantage of Lagrange interpolation is that it does not necessitate evenly spaced points, hence it does not suffer from the Runge phenomenon[17]. However, it is preferable to search for the nearest value in the table and use the lowest order interpolant consistent with the function of the data, as higher order polynomials may cause undesirable and rapid fluctuations. Another setback of Lagrange interpolation, is that it can become expensive to evaluate.

Interpolation Problem Statement

Given $(n+1)$ distinct points as shown in the table below

x	x_0	x_1	...	x_n
y	y_0	y_1	...	y_n

we want to find a polynomial that is defined for all x, and takes on the corresponding value of y_i for each of the $n+1$ distinct x_i's in the table. A polynomial P of which

$$P(x_i) = y_i \qquad \text{when } \; 0 \leq i \leq n$$

is said to **interpolate** the table. The points x_i are known as **nodes**. In general the degree of the polynomial is dependent on the number of nodes.

Theorem 2.1.1 Weierstrass Approximation Theorem [36]

If f is defined and continuous on $[a,b]$ and $\epsilon > 0$ is given, then there exists a polynomial P, defined on $[a,b]$ with the property that

$$|f(x) - P(x)| < \epsilon, \qquad \forall x \in [a,b].$$

Thus a given function can be approximated 'closely' by a polynomial which passes through the points $(x_0, f(x_0)), (x_1, f(x_1)), ..., (x_n, f(x_n))$. Knowing that $f(x_k)$ (written compactly as f_k), $k = 0, 1, ..., n$ are the values of a certain function $y = f(x)$ at x_k, then the most obvious then to do is to construct a polynomial $P_n(x)$ of degree at most n that passes through the $(n+1)$ points:

$$(x_0, f_0), (x_1, f_1), ..., (x_n, f_n).$$

[17] It is a problem of oscillations at the edges of an interval with polynomials of high degree over equispaced interpolation points.

Theorem 2.1.2 Existence and Uniqueness Theorem for Polynomial Interpolation [36]

Given $(n+1)$ distinct points $x_0, x_1, ..., x_n$ and the associated values $f_0, f_1, ..., f_n$ of a function $f(x)$ at these points (i.e if $f(x) = f_i$) there is a unique polynomial $P_n(x)$ of degree at most n such that

$$P_n(x) = f_i, \qquad \textit{for } i = 0, 1, ..., n.$$

As soon as it is known that the interpolating polynomial exists and is unique, the problem then becomes how to construct a polynomial $P_n(x)$ of degree at most n such that

$$P_n(x) = f_i, \qquad i = 0, 1, ..., n.$$

Below the Lagrange way of constructing the interpolation is described. Suppose $n = 1$, this means we have two points $(x_0, f_0), (x_1, f_1)$, then it is easy to see that the linear polynomial

$$P_1(x) = \frac{x - x_1}{x_0 - x_1} f_0 + \frac{x - x_0}{x_1 - x_0} f_1$$

is an interpolating polynomial, because

$$P_1(x_0) = f_0, \quad P_1(x_1) = f_1.$$

For convienience, the polynomial $P_1(x)$ is written in the form

$$P_1(x) = L_0(x) f_0 + L_1(x) f_1,$$

where

$$L_0(x) = \frac{x - x_1}{x_0 - x_1} \quad \text{and} \quad L_1(x) = \frac{x - x_0}{x_1 - x_0}.$$

It is noted that both polynomials $L_0(x)$ and $L_1(x)$ are polynomials of degree one. Therefore P_1 is the unique linear function that passes through (x_0, f_0) and (x_1, f_1). This is shown in Figure 2.1 below.

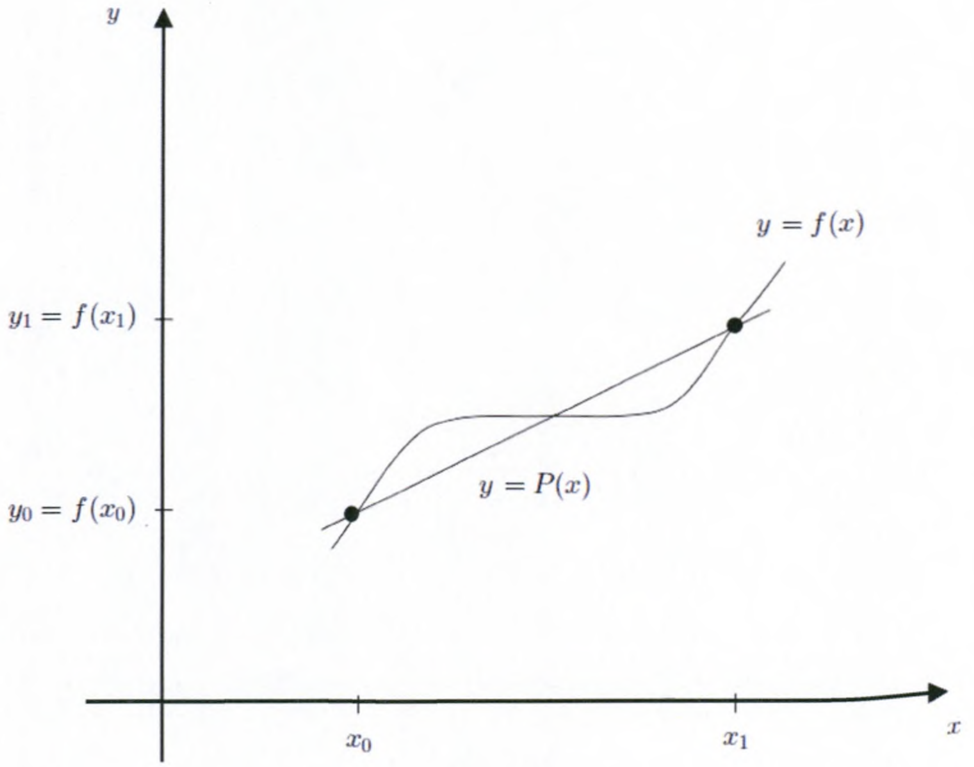

FIGURE 2.1

This concept can be generalized easily for polynomials of higher degrees. To generate polynomials of higher degrees, $\{L_k(x)\}$ is recursively defined as follows:

$$L_k(x) = \frac{(x-x_0)(x-x_1)...(x-x_{k-1})(x-x_{k+1})...(x-x_n)}{(x_k-x_0)(x_k-x_1)...(x_k-x_{k-1})(x_k-x_{k+1})...(x_k-x_n)} = \prod_{0\le m\le n} \frac{x-x_m}{x_k-x_m}, \tag{2.1}$$

where $k = 0, 1, 2, ..., n$ and $m \neq k$. The interpolatng polynomial $P_n(x)$ is defined as follows

$$P_n(x) = L_0(x)f_0 + L_1(x)f_1 + ... + L_n(x)f_n = \sum_{k=0}^{n} L_k(x)f(x_k).^{18} \tag{2.2}$$

To see that $P_n(x)$ expressed in equation (2.2) is an interpolating polynomial, it is noted

$$L_0(x) = \frac{(x-x_1)(x-x_2)...(x-x_n)}{(x_0-x_1)(x_0-x_2)...(x_0-x_n)},$$
$$L_1(x) = \frac{(x-x_0)(x-x_2)...(x-x_n)}{(x_1-x_0)(x_1-x_2)...(x_1-x_n)},$$
$$\vdots$$
$$L_n(x) = \frac{(x-x_0)(x-x_1)...(x-x_{n-1})}{(x_n-x_0)(x_n-x_1)...(x_n-x_{n-1})},$$

[18]The formula was first published by Waring in 1779, then it was rediscovered by Euler in 1783 and published by Lagrange in 1795.

also

$$L_0(x_0) = 1,\ L_0(x_1) = L_0(x_2)...L_0(x_n) = 0,$$
$$L_1(x_1) = 1,\ L_1(x_0) = L_1(x_2)...L_1(x_n) = 0.$$

In general

$$L_k(x_k) = 1 \quad \text{and} \quad L_k(x_i) = 0, \quad i \neq k.$$

The polynomials L_k are known as **cardinal polynomials** and have the property

$$L_i(x_j) = \begin{cases} 0 & \text{if } i \neq j, \\ 1 & \text{if } i = j. \end{cases}$$

Thus

$$\begin{aligned}
P_n(x_0) &= L_0(x_0)f_0 + L_1(x_0)f_1 + ... + L_n(x_0)f_n = f_0 + 0 + ... + 0 = f_0, \\
P_n(x_1) &= L_0(x_1)f_0 + L_1(x_1)f_1 + ... + L_n(x_1)f_n = 0 + f_1 + ... + 0 = f_1, \\
&\vdots \\
P_n(x_n) &= L_0(x_n)f_0 + L_1(x_n)f_1 + ... + L_n(x_n)f_n = 0 + 0 + ... + f_n = f_n,
\end{aligned}$$

where the polynomial $P_n(x)$ has the attribute $P_n(x_k) = f_k$ for $k = 0, 1, ..., n$. $P_n(x)$ is known as the **Lagrange interpolating polynomial**. The BI-SQLM which will be applied to the non-linear equations in this treatise is a Lagrange interpolation based method.

2.2 Chebyshev spectral differentiation matrices

The concept of a differentiation matrix has been a useful tool in the numerical solution of differential equations (Canuto et al. 1988; Fornberg 1996). Differentiation matrices play a substantial role in the implementation of the spectral collocation method. There are shortcomings when using spectral methods as opposed to finite elements or finite difference methods; full matrices replace sparse matrices and stability restrictions may be more severe especially for problems that have irregular domains. However if the solution is smooth, rapid convergence makes up for the disadvantage [37].

The interval considered is $[-1, 1]$ where we let $N \geq 1$ be an integer and let $x_0, ..., x_N$ be the set of distinct points in $[-1, 1]$. For definiteness let the numbering be in reverse orders [5]:

$$1 \geq x_0 > x_1 > ... > x_{N-1} > x_N \geq -1.$$

The following are grids that are often regarded:

- Equispaced points

$$x_j = 1 - \frac{2j}{N}, \qquad 0 \leq j \leq N$$

- Chebyshev zero points[19]

$$x_j = \cos\left(\frac{(j-\frac{1}{2})}{N}\right), \qquad 1 \leq j \leq N$$

- Chebyshev extreme points[20]

$$x_j = \cos\left(\frac{j\pi}{N}\right), \qquad 0 \leq j \leq N$$

- Legendre zero points

$$x_j = j\text{th zero of } P_N, \qquad 1 \leq j \leq N$$

- Legendre extreme points

$$x_j = j\text{th extremum of } P_N, \qquad 0 \leq j \leq N,$$

where P_N is the Legendre polynomial of degree N. The focus will be on Chebyshev extreme points. The Chebyshev Gauss-Lobatto (CGL) points are a popular choice of quadrature points. Since they are given explictly and the transform between the physical space and the spectral space can be expeditiously executed by making use of the Fast Fourier Transform (FFT). In turn, Legendre Gauss-Lobatto (LGL) points[21] are inaccessible in explicit form and for larger N (order of polynomial) substantial round off errors may be experienced[38].

Suppose we want to approximate the derivative of the function $f(x)$. Firstly the function would be approximated using Chebyshev extreme points. Denoting the value of the function $f(x)$ at the grid points by $f_k = f(x_k)$, the function is approximated using Lagrange interpolation polynomials as

$$f(x) \approx P_N(x) = \sum_{k=0}^{N} f_k L_k(x), \tag{2.3}$$

[19] Zero points are also known as Gauss points.

[20] Chebyshev extreme points is interchangable with Chebyshev Gauss-Lobatto nodes.

[21] Legendre extreme points

where L_k are the Lagrange polynomials,

$$L_k(x_j) = \begin{cases} 0 & \text{if } j \neq k, \\ 1 & \text{if } j = k, \end{cases}$$

thus

$$f'(x) = \sum_{k=0}^{N} f_k L'_k(x). \tag{2.4}$$

The process of collocating involves evaluating functions and their derivatives at selected grid points. Assessing (2.4) at nodes $\{x_j\}$ (referred to as collocation points) gives

$$f'(x) = \sum_{k=0}^{N} f_k L'_k(x) = \sum_{k=0}^{N} D_{jk} f_k, \quad j = 0, 1, 2, ..., N, \tag{2.5}$$

where

$$D_{jk} = L'_k(x_j).$$

In vector form equation (2.5) can be expressed as

$$\begin{pmatrix} f'(x_0) \\ f'(x_1) \\ \vdots \\ f'(x_{N-1}) \\ f'(x_N) \end{pmatrix} = \begin{pmatrix} D_{0,0} & D_{0,1} & \cdots & D_{0,N-1} & D_{0,N} \\ D_{1,0} & D_{1,1} & \cdots & D_{1,N-1} & D_{1,N} \\ \vdots & \vdots & \ddots & \vdots & \vdots \\ D_{N-1,0} & D_{N-1,1} & \cdots & D_{N-1,N-1} & D_{N-1,N} \\ D_{N,0} & D_{N,1} & \cdots & D_{N,N-1} & D_{N,N} \end{pmatrix} \begin{pmatrix} f(x_0) \\ f(x_1) \\ \vdots \\ f(x_{N-1}) \\ f(x_N) \end{pmatrix}. \tag{2.6}$$

Equation (2.6) can be compactly written as

$$\mathbf{F}' \approx D\mathbf{F}, \tag{2.7}$$

where $\mathbf{F}' = [f'(x_0), f'(x_1), ..., f'(x_N)]^T$, $\mathbf{F} = [f(x_0), f(x_1), ..., f(x_N)]^T$. The entries of D are D_{jk} for $j, k = 0, 1, 2, ..., N$. Higher order derivatives can be obtained as matrix products of D,

$$\mathbf{F}'' \approx D^2\mathbf{F}, \quad \mathbf{F}''' \approx D^3\mathbf{F}, \text{ etc.} \tag{2.8}$$

We may consider a more explicit example via the differentiation matrix for $N = 1, 2, 3$. When $N = 1$, we have $x_0 = 1$, $x_1 = -1$. Thus

$$P_1(x) = \frac{1}{2}(1+x)f_0 + \frac{1}{2}(1-x)f_1, \quad f'(x) \approx \frac{1}{2}f_0 + \frac{1}{2}f_1,$$

expressed in matrix-vector form as

$$\begin{pmatrix} f'(x_0) \\ f'(x_1) \end{pmatrix} = \begin{pmatrix} \frac{1}{2} & -\frac{1}{2} \\ \frac{1}{2} & \frac{1}{2} \end{pmatrix} \begin{pmatrix} f(x_0) \\ f(x_1) \end{pmatrix}.$$

When $N = 2$, the interpolation points are $x_0 = 1$, $x_1 = 0$, $x_2 = -1$ and the corresponding interpolating polynomial and approximate derivative are

$$P_2(x) = \frac{1}{2}x(x+1)f_0 + (1+x)(1-x)f_1 + \frac{1}{2}x(x-1)f_2, \quad f'(x) \approx \left(x + \frac{1}{2}\right) f_0 - 2xf_1 + \left(x - \frac{1}{2}\right) f_2.$$

Evaluating at collocation points gives

$$\begin{aligned} x_0 = 1, \quad & f'(x_0) = \frac{3}{2}f_0 - 2f_1 + \frac{1}{2}f_2, \\ x_1 = 0, \quad & f'(x_1) = \frac{1}{2}f_0 - \frac{1}{2}f_2, \\ x_2 = -1, \quad & f'(x_2) = -\frac{1}{2}f_0 + 2f_1 - \frac{1}{2}f_2, \end{aligned}$$

which can be written in matrix form as

$$\begin{pmatrix} f'(x_0) \\ f'(x_1) \\ f'(x_2) \end{pmatrix} = \begin{pmatrix} \frac{3}{2} & -2 & \frac{1}{2} \\ \frac{1}{2} & 0 & -\frac{1}{2} \\ -\frac{1}{2} & 2 & \frac{3}{2} \end{pmatrix} \begin{pmatrix} f(x_0) \\ f(x_1) \\ f(x_2) \end{pmatrix}.$$

Similarly for $N = 3$, with collocation points $x_0 = 1$, $x_1 = \frac{1}{2}$, $x_2 = -\frac{1}{2}$, $x_3 = 1$, it can be shown that

$$\begin{pmatrix} f'(x_0) \\ f'(x_1) \\ f'(x_2) \\ f'(x_3) \end{pmatrix} = \begin{pmatrix} \frac{19}{6} & -4 & \frac{4}{3} & -\frac{1}{2} \\ 1 & -\frac{1}{3} & -1 & \frac{1}{3} \\ -\frac{1}{3} & 1 & \frac{1}{3} & -1 \\ \frac{1}{2} & -\frac{4}{3} & 4 & \frac{3}{2} \end{pmatrix} \begin{pmatrix} f(x_0) \\ f(x_1) \\ f(x_2) \\ f(x_3) \end{pmatrix}.$$

In general, for each $N > 1$, the entries of the spectral differentiation matrix D of size $(N+1) \times (N+1)$ are

$$D_{jk} = \frac{c_j(-1)^{j+k}}{c_k x_j - x_k}, \qquad j \neq k;\ j,k = 0,1,...,N, \tag{2.9}$$

$$D_{kk} = \frac{x_k}{2(1-x_k^2)}, \qquad k = 0,1,...,N-1, \tag{2.10}$$

$$D_{00} = \frac{2N^2+1}{6} = D_{NN}, \tag{2.11}$$

with

$$c_k = \begin{cases} 2 & k = 0, N, \\ 1 & -1 \leq k \leq N-1. \end{cases}$$

2.3 Solving linear two-point boundary value problems

To illustrate the application of the spectral collocation method in solving differential equations, the following third order two-point boundary value problem is considered [36],

$$a_0(x)y'''(x) + a_1(x)y''(x) + a_2(x)y'(x) + a_3(x)y(x) = f(x), \tag{2.12}$$

subject to the boundary conditions

$$y(-1) = \alpha, \quad y'(-1) = \beta, \quad y'(1) + \gamma y(1) = \delta, \tag{2.13}$$

where $a_k(x)$ $(k = 0, 1, 2, 3)$ and $f(x)$ are known functions of x. The unknown function is approximated as a sum of Lagrange polynomials defined on the Gauss-Lobatto collocation points as

$$y(x) \approx \sum_{k=0}^{N} y_k L_k(x). \tag{2.14}$$

Assuming that the differential equation (2.12) holds at each collocation point x_j $(j = 0, 1, ..., N)$ then

$$a_0(x_j)y'''(x_j) + a_1(x_j)y''(x_j) + a_2(x_j)y'(x_j) + a_3(x_j)y(x_j) = f(x_j). \tag{2.15}$$

Equation (2.15) can be represented as the matrix vector equation

$$\mathbf{a}_0\mathbf{Y}''' + \mathbf{a}_1\mathbf{Y}'' + \mathbf{a}_2\mathbf{Y}' + \mathbf{a}_3\mathbf{Y} = \mathbf{F}, \tag{2.16}$$

where

$$\mathbf{a}_k = \begin{pmatrix} a_k(x_0) & & & & \\ & a_k(x_1) & & & \\ & & \ddots & & \\ & & & a_k(x_{N-1}) & \\ & & & & a_k(x_N) \end{pmatrix} \quad \mathbf{F} = \begin{pmatrix} f(x_0) \\ f(x_1) \\ \vdots \\ f(x_{N-1}) \\ f(x_N) \end{pmatrix} \quad \mathbf{Y} = \begin{pmatrix} y(x_0) \\ y(x_1) \\ \vdots \\ y(x_{N-1}) \\ y(x_N) \end{pmatrix}, \tag{2.17}$$

for $k = 0, 1, 2, 3$. This is succinctly represented as

$$\mathbf{AY} = \mathbf{F},$$

with

$$\mathbf{A} = \mathbf{a}_0\mathbf{D}^3 + \mathbf{a}_1\mathbf{D}^2 + \mathbf{a}_2\mathbf{D} + \mathbf{a}_3. \tag{2.18}$$

The boundary conditions are shown in terms of collocation points,

$$y(x_N) = \alpha, \quad \sum_{k=0}^{N} y_k L_k'(x_N) = \beta, \quad \sum_{k=0}^{N} y_k L_k'(x_0) + \gamma y(x_0) = \delta, \tag{2.19}$$

which in terms of the differentiation matrix are written as

$$y(x_N) = \alpha, \quad \sum_{k=0}^{N} D_{N,k} y_k = \beta, \quad \sum_{k=0}^{N} D_{0,k} y_k + \gamma y(x_0) = \delta, \tag{2.20}$$

with $L_k'(x_j) = D_{j,k}$. The boundary conditions (2.20) are imposed on the first, second last and last row,

$$\begin{pmatrix} D_{0,0}+\gamma & D_{0,1} & \dots & D_{0,N-1} & D_{0,N} \\ A_{1,0} & A_{1,1} & \dots & A_{1,N-1} & A_{1,N} \\ A_{2,0} & A_{2,1} & \dots & A_{2,N-1} & A_{2,N} \\ \vdots & \vdots & \ddots & \vdots & \vdots \\ A_{N-2,0} & A_{N-2,1} & \dots & A_{N-2,N-1} & A_{N-2,N} \\ D_{N,0} & D_{N,1} & \dots & D_{N,N-1} & D_{N,N} \\ 0 & 0 & \dots & 0 & 1 \end{pmatrix} \begin{pmatrix} y(x_0) \\ y(x_1) \\ y(x_2) \\ \vdots \\ y(x_{N-2}) \\ y(x_{N-1}) \\ y(x_N) \end{pmatrix} = \begin{pmatrix} \delta \\ f(x_1) \\ f(x_2) \\ \vdots \\ f'(x_{N-2}) \\ \beta \\ \alpha \end{pmatrix}. \tag{2.21}$$

The approximate solution of $y(x)$ at the collocation points is obtained by solving (2.21).

2.4 Solving non-linear boundary value problems using the quasi-linearisation method

The quasi-linearisation method is used to simplify non-linear ordinary differential equations to a linearised form. When the spectral technique is applied to the linearised equation, the method is called the spectral quasi-linearisation method (SQLM) [36]. This technique will of use in a later chapter when deriving an initial solution to one of the non-linear equations considered in this dissertation.

To illustrate the manner in which this method is to be implemented, consider the following non-linear ordinary differential equation

$$F[x, y(x), y'(x), .., y^{(n)}(x)] = 0, \quad x \in [a, b], \tag{2.22}$$

with the boundary conditions

$$G_{a,k}[y(a), y'(a), .., y^{(n-1)}(a)] = 0, \quad k = 1, 2, ..., m, \tag{2.23}$$

$$G_{b,k}[y(b), y'(b), .., y^{(n-1)}(b)] = 0, \quad k = m + 1, m + 2, ..., n. \tag{2.24}$$

F is a non-linear operator of $y(x)$ and its n derivatives, $G_{a,k}$, $G_{a,k}$ are non-linear functions of $y(x)$ and its $n - 1$ derivatives at $x = a$ and $x = b$. The quasi-linearisation approach assumes that the difference between the approximation of the solution at the current iteration (denoted by $y_{r+1}(x)$) and the previous iteration (denoted by $y_r(x)$) is small. The QLM determines the approximate solution at the $(r + 1)$ iteration level as the solution of the linear equation

$$F[x, y_r(x), y_r'(x), .., y_r^{(n)}(x)] + \sum_{p=0}^{n} \frac{\partial F}{\partial y^{(p)}}[x, y_r(x), y_r'(x), .., y_r^{(n)}(x)][y_{r+1}^{(p)}(x) - y_r^{(p)}(x)] = 0, \tag{2.25}$$

with linearised boundary conditions

$$G_{a,k}[y_r(a), y_r'(a), .., y_r^{(n)}(a)] + \sum_{p=0}^{n} \frac{\partial G_{a,k}}{\partial y^{(p)}}[y_r(a), y_r'(a), .., y_r^{(n)}(a)][y_{r+1}^{(p)}(a) - y_r^{(p)}(a)] = 0, \tag{2.26}$$

for $k = 1, 2, ..., m$ and

$$G_{b,k}[y_r(b), y_r'(b), .., y_r^{(n)}(b)] + \sum_{p=0}^{n} \frac{\partial G_{b,k}}{\partial y^{(p)}}[y_r(b), y_r'(b), .., y_r^{(n)}(b)][y_{r+1}^{(p)}(b) - y_r^{(p)}(b)] = 0, \tag{2.27}$$

where $k = m+1, ..., n$. Since the Chebyshev spectral collocation method is used to solve the now linear equations (2.22)-(2.24), it is then convenient to write the equations in the form

$$a_{n,r}(x)y_{r+1}^{(n)}(x) + a_{n-1,r}(x)y_{r+1}^{(n-1)}(x) + ... + a_{1,r}(x)y_{r+1}'(x) + a_{0,r}(x)y_{r+1}(x) = R_r(x), \tag{2.28}$$

$$\alpha_{n-1,r}(a)y_{r+1}^{(n-1)}(a) + \alpha_{n-2,r}(a)y_{r+1}^{(n-2)}(a) + ... + \alpha_{1,r}(a)y_{r+1}'(a) + \alpha_{0,r}(a)y_{r+1}(a) = R_{a,k}, \tag{2.29}$$

$$\beta_{n-1,r}(b)y_{r+1}^{(n-1)}(b) + \beta_{n-2,r}(b)y_{r+1}^{(n-2)}(b) + ... + \beta_{1,r}(b)y_{r+1}'(b) + \beta_{0,r}(b)y_{r+1}(b) = R_{b,k}, \tag{2.30}$$

where

$$a_{p,r}(x) = \frac{\partial F}{\partial y^{(n-p)}}[x, y_r(x), y_r'(x), .., y_r^{(n)}(x)], \quad p = 0, 1, 2, ..., n, \tag{2.31}$$

$$R_r(x) = \sum_{p=0}^{n} \frac{\partial F}{\partial y^{(p)}}[x, y_r(x), y_r'(x), .., y_r^{(n)}(x)]y_r^{(p)} - F[x, y_r(x), y_r'(x), .., y_r^{(n)}(x)],$$
$$p = 0, 1, 2, ..., n, \tag{2.32}$$

$$\alpha_{p,k} = \frac{\partial G_{a,k}}{\partial y^{(p)}}[y_r(a), y_r'(a), .., y_r^{(n)}(a)], \quad p = 1, 2, ..., n-1, \quad k = 1, 2, ..., m, \tag{2.33}$$

$$\beta_{p,k} = \frac{\partial G_{b,k}}{\partial y^{(p)}}[y_r(b), y_r'(b), .., y_r^{(n)}(b)], \quad p = 1, 2, ..., n-1, \quad k = m+1, m+2, ..., n,$$

$$R_{a,k} = \sum_{p=0}^{n-1} \frac{\partial G_{b,k}}{\partial y^{(p)}}[y_r(b), y_r'(b), .., y_r^{(n)}(b)]y_r^{(p)}(a) - G_{a,k}[y_r(a), y_r'(a), .., y_r^{(n)}(a)],$$
$$k = 1, 2, ..., m, \tag{2.34}$$

$$R_{b,k} = \sum_{p=0}^{n-1} \frac{\partial G_{b,k}}{\partial y^{(p)}}[y_r(b), y_r'(b), .., y_r^{(n)}(b)]y_r^{(p)}(b) - G_{b,k}[y_r(b), y_r'(b), .., y_r^{(n)}(b)],$$
$$k = m+1, m+2, ..., n. \tag{2.35}$$

Equations (2.28)-(2.30) are solved using the Chebyshev spectral collocation method.

2.5 Bivariate spectral quasi-linearisation method (BI-SQLM)

The bivariate spectral quasi-linearisation method was developed by combining elements of the quasi-linearisation method and chebyshev spectral collocation with bivariate Lagrange interpolation [3]. The BI-SQLM was recently presented by Motsa et al. [3] to solve non-linear evolution partial differential equations. The solutions that were obtained were uniformly accurate and valid in large intervals of space and time domains. As such we introduce this method as a means to provide solutions to the non-linear problems presented in this treatise.

Considering a non-linear partial differential equation

$$\frac{\partial u}{\partial \tau} = H\left(u, \frac{\partial u}{\partial \eta}, \frac{\partial^2 u}{\partial \eta^2}, ..., \frac{\partial^n u}{\partial \eta^n}\right), \tag{2.36}$$

with physical region $\tau \in [0, T]$, $\eta \in [a, b]$ where n is the order of differentiation, $u(\eta, \tau)$ is the required solution and H is a non-linear term. The region $\tau \in [0, T]$ is converted to $t \in [-1, 1]$ using the transformation $\tau = T(t+1)/2$ and $\eta \in [a, b]$ is converted to the region $x \in [-1, 1]$ using the transformation $\eta = 1/2(b-a)x + 1/2(b+a)$. Equation

(2.36) can be expressed as

$$\frac{\partial u}{\partial t} = H\left(u, \frac{\partial u}{\partial x}, \frac{\partial^2 u}{\partial x^2}, ..., \frac{\partial^n u}{\partial x^n}\right), \quad t \in [-1,1], \quad x \in [-1,1]. \tag{2.37}$$

The solution is approximated by the bivariate Lagrange interpolation polynomial of the form

$$u(x,t) \approx \sum_{i=0}^{N_x}\sum_{j=0}^{N_t} u(x_i,t_j)L_i(x)L_j(t), \tag{2.38}$$

which interpolates $u(x,t)$ at selected points in both the x and t directions defined by

$$x_i = \cos\left(\frac{\pi i}{N_x}\right), \quad i = 0,1,2...,N_x, \quad t_j = \cos\left(\frac{\pi j}{N_t}\right), \quad j = 0,1,2...,N_t. \tag{2.39}$$

Before linearising (2.37), it is convenient to split it into its linear and non-linear components[22]

$$F[u,u',...,u^{(n)}] + G[u,u',...,u^{(n)}] - \dot{u} = 0, \tag{2.40}$$

where the dot and primes denote the time and spatial derivatives respectively. F is a linear operator and G is the non-linear operator. Approximating a non-linear operator G using linear terms of the Taylor series expansion we obtain

$$G[u,u',...,u^{(n)}] \approx G[u_r,u_r',...,u_r^{(n)}] + \sum_{k=0}^{n}\frac{\partial G}{\partial u^{(k)}}\left(u_{r+1}^{(k)} - u_r^{(k)}\right). \tag{2.41}$$

Equation (2.41) can be expressed as

$$G[u,u',...,u^{(n)}] \approx G[u_r,u_r',...,u_r^{(n)}]+\sum_{k=0}^{n}\phi_{k,r}[u_r,u_r',...,u_r^{(n)}]u_{r+1}^{(k)}-\sum_{k=0}^{n}\phi_{k,r}[u_r,u_r',...,u_r^{(n)}]u_r^{(k)}, \tag{2.42}$$

where

$$\phi_{k,r}[u_r,u_r',...,u_r^{(n)}] = \frac{\partial G}{\partial u^{(k)}}[u_r,u_r',...,u_r^{(n)}]. \tag{2.43}$$

Substituting (2.42) into (2.40) the following is attained

$$F[u_{r+1},u_{r+1}',...,u_{r+1}^{(n)}] + \sum_{k=0}^{n}\phi_{k,r}u_{r+1}^{(k)} - \dot{u}_{r+1} = R_r[u_r,u_r',...,u_r^{(n)}], \tag{2.44}$$

where

$$R_r[u_r,u_r',...,u_r^{(n)}] = \sum_{k=0}^{n}\phi_{k,r}u_r^{(k)} - G[u_r,u_r',...,u_r^{(n)}]. \tag{2.45}$$

[22]It is also possible to treat equation (2.37) as a non-linear component.

The time derivative and spatial derivatives at Chebyshev-Gauss-Lobatto points (x_i, t_j) are represented as

$$\begin{aligned}\left.\frac{\partial u}{\partial t}\right|_{x=x_i,\, t=t_j} &= \sum_{p=0}^{N_x}\sum_{k=0}^{N_t} u(x_p, t_k)L_p(x_i)\frac{dL_k(t_j)}{dt} \\ &= \sum_{k=0}^{N_t} d_{jk}u(x_i, t_k), \end{aligned} \tag{2.46}$$

where $d_{jk} = dL_k(t_j)/dt$ is the standard first derivative Chebyshev differentiation matrix of size $(N_t + 1) \times (N_t + 1)$. The spatial derivatives at the Chebyshev-Gauss-Lobatto points (x_i, t_j) for $i = 0, 1, 2, ..., N_x$ are given as follows

$$\begin{aligned}\left.\frac{\partial u}{\partial x}\right|_{x=x_i,\, t=t_j} &= \sum_{p=0}^{N_x}\sum_{k=0}^{N_t} u(x_p, t_k)L_p(x_i)\frac{dL_k(t_j)}{dx} \\ &= \sum_{k=0}^{N_x} D_{ip}u(x_i, t_k) = \mathbf{D}\mathbf{U}_j, \end{aligned} \tag{2.47}$$

where $D_{ip} = dL_k(t_j)/dx$, is the standard first Chebyshev differentiation matrix of size $(N_x + 1) \times (N_x + 1)$. The nth order derivative is represented as follows

$$\left.\frac{\partial^n u}{\partial x^n}\right|_{x=x_i,\, t=t_j} = \sum_{k=0}^{N_x} D_{ip}^n u(x_i, t_k) = \mathbf{D}^n\mathbf{U}_j, \quad i = 0, 1, 2, ..., N_x. \tag{2.48}$$

Making the substitutions of the time and spatial derivatives into (2.44), the following is obtained

$$F[\mathbf{U}_{r+1,j}, \mathbf{U}'_{r+1,j}, ..., \mathbf{U}^{(n)}_{r+1,j}] + \sum_{k=0}^{n}\Phi_{k,r}\mathbf{U}^{(k)}_{r+1,j} - \sum_{k=0}^{N_t} d_{jk}\mathbf{U}_{r+1,k} = R_r[\mathbf{U}_{r,j}, \mathbf{U}'_{r,j}, ..., \mathbf{U}^{(n)}_{r,j}], \tag{2.49}$$

for $j = 0, 1, 2, ..., N_t$, where

$$\mathbf{U}^{(n)}_{r+1,j} = \mathbf{D}^n\mathbf{U}_{r+1,j} \tag{2.50}$$

and

$$\Phi_{k,r} = \begin{pmatrix} \phi_k(x_0, t_j) & 0 & 0 & \cdots & 0 \\ 0 & \phi_k(x_1, t_j) & & & 0 \\ 0 & & \ddots & & \vdots \\ \vdots & & & \phi_k(x_{N_x-1}, t_j) & 0 \\ 0 & 0 & \cdots & 0 & \phi_k(x_{N_x}, t_j) \end{pmatrix}. \tag{2.51}$$

The initial condition for (2.37) corresponds to $\tau_{N_t} = -1$ and (2.49) is expressed as

$$F[\mathbf{U}_{r+1,j}, \mathbf{U}'_{r+1,j}, ..., \mathbf{U}^{(n)}_{r+1,j}] + \sum_{k=0}^{n} \Phi_{k,r}\mathbf{U}^{(k)}_{r+1,j} - \sum_{k=0}^{N_t} d_{jk}\mathbf{U}_{r+1,k} = \mathbf{R}_j, \tag{2.52}$$

where

$$\mathbf{R}_j = R_r[\mathbf{U}_{r,j}, \mathbf{U}'_{r,j}, ..., \mathbf{U}^{(n)}_{r,j}] + d_j N_t \mathbf{U}_{N_t}, \quad j = 0, 1, 2, ..., N_t - 1.$$

Equation (2.52) represented in matrix form is given as

$$\begin{pmatrix} A_{0,0} & A_{0,1} & \cdots & A_{0,N_t-1} & A_{0,N_t} \\ A_{1,0} & A_{1,1} & \cdots & A_{1,N_t-1} & A_{1,N_t} \\ \vdots & \vdots & \ddots & \vdots & \vdots \\ A_{N_t-2,0} & A_{N_t-2,1} & \cdots & A_{N_t-2,N-1} & A_{N_t-2,N_t} \end{pmatrix} \begin{pmatrix} \mathbf{U}_0 \\ \mathbf{U}_1 \\ \vdots \\ \mathbf{U}_{N_t-1} \end{pmatrix} = \begin{pmatrix} \mathbf{R}_0 \\ \mathbf{R}_1 \\ \vdots \\ \mathbf{R}_{N_t-1} \end{pmatrix}, \tag{2.53}$$

where

$$A_{i,i} = F[\mathbf{I}, \mathbf{D}, ..., \mathbf{D}^{(n)}] + \sum_{k=0}^{n} \Phi^{(k)}_{k,r} - d_{i,i}\mathbf{I}, \tag{2.54}$$

$$A_{i,j} = d_{i,j}\mathbf{I}, \quad i \neq j. \tag{2.55}$$

Finding the inverse of (2.53) gives the approximate solution to the non-linear partial differential equation (2.37).

Chapter 3

Model I: Unsteady boundary layer flow adjacent to a permeable stretching surface in a porous medium

The flow of a viscous fluid over a stretching sheet plays a significant role in engineering applications such as the extrusion of plastic sheets, boundary layer flows along a liquid film, condensation processes, a cooling metallic plate in a cooling bath and applications in glass and polymer industries [39]. Sakiadis [40] conducted a numerical study of boundary layer flows over a stretched surface moving with constant velocity and the work was validated by Tsou et al. [41] where a combined analytical and experimental study was done on the flow and heat transfer of a continuous moving plate. Soon after several researchers further expanded the study by including other physical features such as suction, injection, magnetic field, rotation of a disk, heat transfer analysis and viscoelasticity of a liquid. The effect of suction or injection on boundary flows due to the stretching of the wall was analysed by Crane [42], where exact solutions were obtained. Banks [43] discussed non-similarity solutions of boundary layer equations for a stretching wall analytically and numerically. Banks and Zaturska [44] focused on boundary layer flow adjacent to the stretching wall and attained analytical solutions for certain eigenvalues and eigenfunctions. In the research conducted by Grubka and Bobba [45], the heat transfer characteristics of a continuous stretching surface with variable temperature was explored, where the power law temperature distribution was solved in terms of Kummer functions and various closed form analytical solutions were found. Similarity solutions for heat transfer characteristics of a continuous stretching plate was reported by Ali [46]. Erickson et al. [47] looked into the flow of a moving continuous plate with suction and injection for cases where the transverse velocty profile is non-zero at the surface; results were acquired numerically through the fourth-order Runge-Kutta formula, the iteration method of Hartree and numerical integration. Elbashbeshy [48] examined heat transfer over a stretching plate with a variable surface heat flux. The equations that govern the two-dimensional laminar flow were solved numerically by applying the Nachtsheim-Swigert scheme, which later brings forth a fourth-order Runge-Kutta scheme. Chen and Char [49] studied the heat transfer of a continuous, stretching surface with suction or blowing and the solutions were expressed in terms of Kummer's functions. Exact solutions were found by Magyari and Keller [50] for a self-similar boundary layer flow brought about by a permeable stretching surface. Chaudhary et al. [51] used numerical intergration to investigate convecton boundary layer flow along a vertical permeable surface. Vajravelu [52] obtained exact solutions for hydromagnetic flow and heat transfer over a continuous mobile permeable flat surface. Nazar et al. [53], Liao and Xu [54] and Liao [55] produced results for unsteady boundary flow equations by means of transformations found by Williams and Rhyne [56] and the Keller-box numerical method.

An unsteady boundary layer flow adjacent to a permeable a stretching surface in a porous medium will be solved using BI-SQLM. This problem was previously analysed by Ali and Mehmood using HAM [57]. An incompressible hydrodynamic viscous fluid bounded by an infinite plate situated at $y = 0$ is considered.

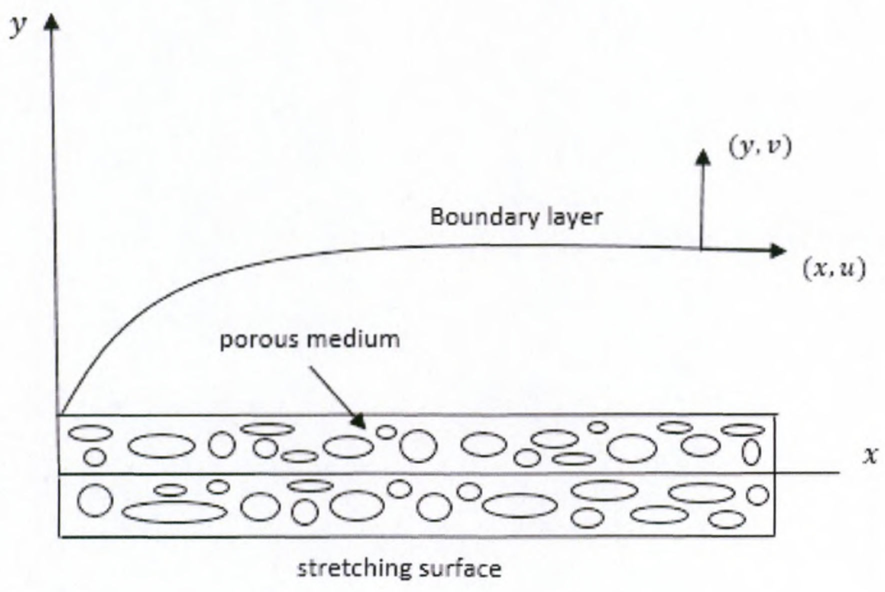

FIGURE 3.1: Visual representation of Model I

Assumptions

- The upper half space of the plate is porous and the fluid lies in this porous region at $y > 0$.

- The plate is a highly elastic membrane and is uniformly porous so that the suction or injection is possible.

- Two equal and opposite forces are applied along the x-axis so that the wall is stretched while keeping the origin fixed.

The following equations describe the boundary layer flow

$$\frac{\partial u}{\partial x} + \frac{\partial v}{\partial y} = 0, \tag{3.1}$$

$$\frac{\partial u}{\partial t} + u\frac{\partial u}{\partial x} + v\frac{\partial u}{\partial y} = \nu\frac{\partial^2 u}{\partial y^2} - \frac{\nu\phi}{k}u, \tag{3.2}$$

subject to the boundary conditions (for $t > 0$)

$$u = ax, \quad v = -V_0^* \quad \text{at} \quad y = 0, \text{ and}$$

$$u \longrightarrow 0 \quad \text{as} \quad y \longrightarrow \infty, \tag{3.3}$$

where $a > 0$ is a constant, and the initial condition for $(t \leq 0)$ is given by

$$u = v = 0, \tag{3.4}$$

at all points (x, y). The similarity transformation is written as

$$\eta = \sqrt{\frac{a}{\nu\xi}}y, \quad \psi = \sqrt{a\nu\xi}xf(\eta,\xi), \quad \xi = 1 - e^{-\tau}, \quad \tau = at, \tag{3.5}$$

where ψ denotes the stream function. Therefore, the governing system (3.1)-(3.4) transforms into

$$\frac{\partial^3 f}{\partial\eta^3} + \frac{1}{2}(1-\xi)\eta\frac{\partial^2 f}{\partial\eta^2} + \xi\left(f\frac{\partial^2 f}{\partial\eta^2} - \left(\frac{\partial f}{\partial\eta}\right)^2\right) - \xi(1-\xi)\frac{\partial^2 f}{\partial\eta\partial\xi} - \lambda\xi\frac{\partial f}{\partial\eta} = 0, \tag{3.6}$$

subject to the following boundary conditions

$$f(\eta, 0) = V_0, \quad \left.\frac{\partial f}{\partial\eta}\right|_{\eta=0} \quad \text{and} \quad \left.\frac{\partial f}{\partial\eta}\right|_{\eta=\infty}, \tag{3.7}$$

where $\lambda = \nu\phi/ak$ is the porosity parameter and $V_0 = V_0^*/\sqrt{a\nu\xi}$ is the dimensionless suction/injection velocity. Here $V_0 > 0$ corresponds to uniform suction whereas $V_0 < 0$ corresponds to uniform injection at the porous wall.

3.1 Deriving an initial solution

An initial approximation is ascertained using equations (3.6-3.7), by letting $\xi = 0$ ($\tau = 0$) then the non-linear partial differential equation (3.6) simplfies to

$$\frac{\partial^3 f}{\partial \eta^3} + \frac{1}{2}\eta\frac{\partial^2 f}{\partial \eta^2} = 0 \tag{3.8}$$

and the boundary conditions become

$$f(0,0) = V_0, \quad f'(0,0) = 1, \quad f'(\infty, 0) = 0. \tag{3.9}$$

Solving (3.8) we obtain

$$\begin{aligned} \Rightarrow f''' &= -\frac{1}{2}\eta f'', \\ \frac{f'''}{f''} &= -\frac{1}{2}\eta, \end{aligned}$$

integrating both sides

$$\begin{aligned} \Rightarrow \ln(f'') &= -\frac{1}{2}\left(\frac{\eta^2}{2}\right) + \mathrm{C}, \\ \ln(f'') &= -\frac{\eta^2}{4} + \mathrm{C}, \\ f'' &= \mathrm{A}\exp\left(-\frac{-\eta^2}{4}\right), \\ f' &= \mathrm{A}\int_0^{\eta/2} \exp(-t^2)\mathrm{dt} + \mathrm{B}, \end{aligned}$$

$$\Rightarrow f' = \mathrm{A}\frac{\sqrt{\pi}}{2}\mathrm{erf}\left(\frac{\eta}{2}\right) + \mathrm{B}, \tag{3.10}$$

where A, B and C are arbitrary constants and erf is the error function defined as

$$\mathrm{erf}(\eta) = \frac{2}{\sqrt{\pi}}\int_0^{\eta} \exp(-z^2)\, dz.$$

Integrating (3.10) further we obtain

$$f(\eta, 0) = \eta\mathrm{erfc}\left(\frac{\eta}{2}\right) + \frac{2}{\sqrt{\pi}}\left(1 - \exp\left(\frac{-\eta^2}{4}\right)\right) + V_0, \tag{3.11}$$

where erfc (η) is the complementary error function delineated as

$$\operatorname{erfc}(\eta) = \frac{2}{\sqrt{\pi}} \int_{\eta}^{\infty} \exp(-z^2)\, dz.$$

The initial solution (3.11) satifies the boundary conditions (3.7).

3.2 Application of the BI-SQLM

The solution of (3.6) is approximated by the bivariate Lagrange interpolation polynomial of the form

$$f(\eta, \xi) \approx \sum_{i=0}^{N_\eta} \sum_{j=0}^{N_\eta} f(\eta_i, \xi_j) L_i(\eta) L_j(\xi), \tag{3.12}$$

which interpolates $f(\eta, \xi)$ at selected points in the η direction. It is convenient to transform the interval $\xi \in [0, L_\xi]$ to $\zeta \in [-1, 1]$, then choose Chebyshev-Gauss-Lobatto points as collocation points as follows

$$\eta_i = \cos\left(\frac{\pi i}{N_\eta}\right), \quad i = 0, 1, 2..., N_\eta, \quad \zeta_j = \cos\left(\frac{\pi j}{N_\xi}\right), \quad j = 0, 1, 2..., N_\xi. \tag{3.13}$$

Letting H be a non-linear operator of (3.6), this implies that

$$H = f''' + \frac{1}{2}(1-\xi)\eta f'' + \xi(ff'' - (f')^2) - \xi(1-\xi)\frac{\partial f'}{\partial \xi} - \lambda \xi f'. \tag{3.14}$$

Approximating a non-linear operator H using linear terms of the Taylor series expansion we obtain

$$H[f, f', ..., f^{(n)}] \approx H[f_r, f_r', ..., f_r^{(n)}] + \sum_{k=0}^{n} \frac{\partial H}{\partial f^{(k)}} \left(f_{r+1}^{(k)} - f_r^{(k)}\right), \tag{3.15}$$

where the primes denote differentiation with respect to η. Differentiating H with respect to f, f', f'', f''', the following coefficients are acquired

$$a_{0,r}(\eta, \xi)[f_r, f_r', f_r'', f_r'''] = \frac{\partial H}{\partial f} = \xi f_r'', \tag{3.16}$$

$$a_{1,r}(\eta, \xi)[f_r, f_r', f_r'', f_r'''] = \frac{\partial H}{\partial f'} = -2\xi f_r' - \lambda \xi \tag{3.17}$$

$$a_{2,r}(\eta, \xi)[f_r, f_r', f_r'', f_r'''] = \frac{\partial H}{\partial f''} = \frac{1}{2}(1-\xi)\eta + \xi f_r', \tag{3.18}$$

$$a_{3,r}(\eta, \xi)[f_r, f_r', f_r'', f_r'''] = \frac{\partial H}{\partial f'''} = 1. \tag{3.19}$$

Equations (3.16-3.19) are substituted into (3.15) to get

$$a_{3,r}(\eta,\xi)f'''_{r+1}+a_{2,r}(\eta,\xi)f''_{r+1}+a_{1,r}(\eta,\xi)f''_{r+1}+a_{0,r}(\eta,\xi)f_{r+1}-\xi(1-\xi)\frac{\partial f'_{r+1}}{\partial \xi}=R_r(\eta,\xi), \tag{3.20}$$

where

$$R_r(\eta,\xi)=\xi(f''_r f_r-(f'_r)^2).$$

The derivative of f with respect to ξ is described as

$$\begin{aligned}\left.\frac{\partial f'}{\partial \xi}\right|_{\xi=\xi_i} &= 2\sum_{j=0}^{N_\xi} d_{i,j}F'_j(\eta)\\ &= \sum_{j=0}^{N_\xi} \mathbf{d}_{i,j}F'_j(\eta), \quad i=1,...,N_\xi,\end{aligned} \tag{3.21}$$

where $\mathbf{d}=\frac{2}{L_\xi}d$ and L_ξ is the length of ξ. Employing the collocation at ξ_i upon (3.20) we get

$$\begin{aligned}&a^{(i)}_{3,r}(\eta,\xi)F'''_{r+1,i}(\eta)+a^{(i)}_{2,r}(\eta,\xi)F''_{r+1,i}(\eta)+a^{(i)}_{1,r}(\eta,\xi)F''_{r+1,i}(\eta)+a^{(i)}_{0,r}(\eta,\xi)F_{r+1,i}(\eta)\\ &\qquad -2\xi_i(1-\xi_i)\sum_{j=0}^{N_\xi}\mathbf{d}_{i,j}F'_j(\eta)=R_r(\eta,\xi).\end{aligned} \tag{3.22}$$

The derivatives with respect to η are characterized in terms of the Chebyshev differentiation matrix

$$\begin{aligned}\left.\frac{d^pF_{r+1,i}}{d\xi^p}\right|_{\eta=\eta_j} &= \left(\frac{2}{L_\eta}\right)^p\sum_{k=0}^{N_\eta} D^p_{j,k}(\tau_k)F_{r+1,i}\\ &= \sum_{k=0}^{N_\eta}\mathbf{D}^p\mathbf{F}_{r+1,i},\end{aligned} \tag{3.23}$$

where $\mathbf{D}=(2/L_\eta)\,D_{j,k}$, p is the order of the derivative and the vector $\mathbf{F}_{r+1,i}$ is construed as

$$\mathbf{F}_{r+1,i}=[F_{r+1,i}(\tau_0),F_{r+1,i}(\tau_1),...,F_{r+1,i}(\tau_{N_\eta})]^T.$$

Substituting (3.23) into (3.22) gives

$$\mathbf{A}^{(i)}\mathbf{F}_{r+1,i}-2\xi_i(1-\xi_i)\sum_{j=0}^{N_\xi-1}d_{i,j}\mathbf{D}\mathbf{F}_{r+1,j}=\mathbf{R}^{(i)}_1, \tag{3.24}$$

where

$$\mathbf{A}^{(i)} = \mathbf{a}_{3,r}^{(i)}\mathbf{D}^3 + \mathbf{a}_{2,r}^{(i)}\mathbf{D}^2\mathbf{a}_{1,r}^{(i)}\mathbf{D} + \mathbf{a}_{0,r}^{(i)},$$
$$\mathbf{R}_1^{(i)} = R_r^{(i)} + 2\xi_i(1-\xi_i)d_{i,N_\xi}\mathbf{D}\mathbf{F}_{r+1,N_\xi}.$$

The boundary conditions are expressed as

$$\sum_{k=0}^{N} D_{0,k}f_k = 0, \quad f_{r+1}(\eta_N) = V_0, \quad \sum_{k=0}^{N} D_{N,k}f_k = 1. \tag{3.25}$$

After establishing the boundary conditions for each $i = 0, 1, ..., N_\xi - 1$, equation (3.24) can be written in matrix form as

$$\begin{pmatrix} A_{0,0} & A_{0,1} & \cdots & A_{0,N_\xi-2} & A_{0,N_\xi-1} \\ A_{1,0} & A_{1,1} & \cdots & A_{1,N_\xi-2} & A_{1,N_\xi-1} \\ \vdots & \vdots & \ddots & \vdots & \vdots \\ A_{N_\xi-1,0} & A_{N_\xi-1,1} & \cdots & A_{N_\xi-1,N_\xi-2} & A_{N_\xi-1,N_\xi-1} \end{pmatrix} \begin{pmatrix} \mathbf{F}_{r+1,0} \\ \mathbf{F}_{r+1,1} \\ \vdots \\ \mathbf{F}_{r+1,N_\xi-1} \end{pmatrix} = \begin{pmatrix} \mathbf{R}_1^{(0)} \\ \mathbf{R}_1^{(1)} \\ \vdots \\ \mathbf{R}_1^{(N_\xi-1)} \end{pmatrix} \tag{3.26}$$

where

$$A_{i,i} = \mathbf{A}^{(i)} - 2\xi_i(1-\xi_i)d_{i,i}\mathbf{D}, \qquad i = 0, 1, ...N_\xi - 1,$$
$$A_{i,j} = -2\xi_i(1-\xi_i)d_{i,i}\mathbf{D} \quad \text{when} \quad i \neq j.$$

By solving (3.26) the solution to equation (3.6) is obtained.

3.3 Results and analysis

In this section we unpack the results, which are presented graphically. The graphs are plotted for dimensionless velocity components f and f' for varying parametric quantities. It is important to note that the initial solution (3.11) was used to arrive to the final solutions presented in the figures below. We also tested the initial guess Ali and Mehmood [57] utilized in their work and similar results were established.

The velocity f' decreases by increasing the porosity parameter λ, see Figure 3.2. Similarly f' diminishes for all the values of suction ($V_0 > 0$) for $\lambda = 0.5$.

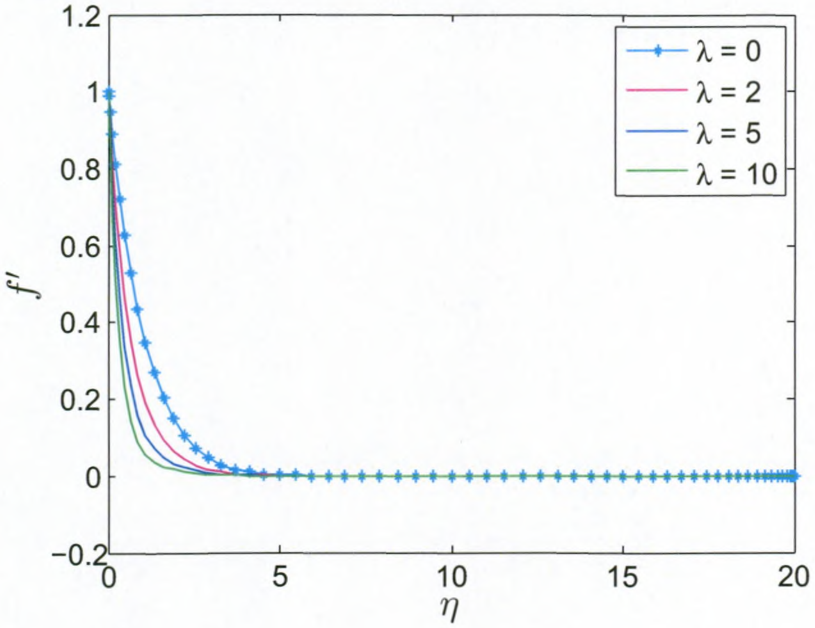

FIGURE 3.2: Distribution of the velocity f' at several values of the porosity parameter λ for $V_0 = 0.5$.

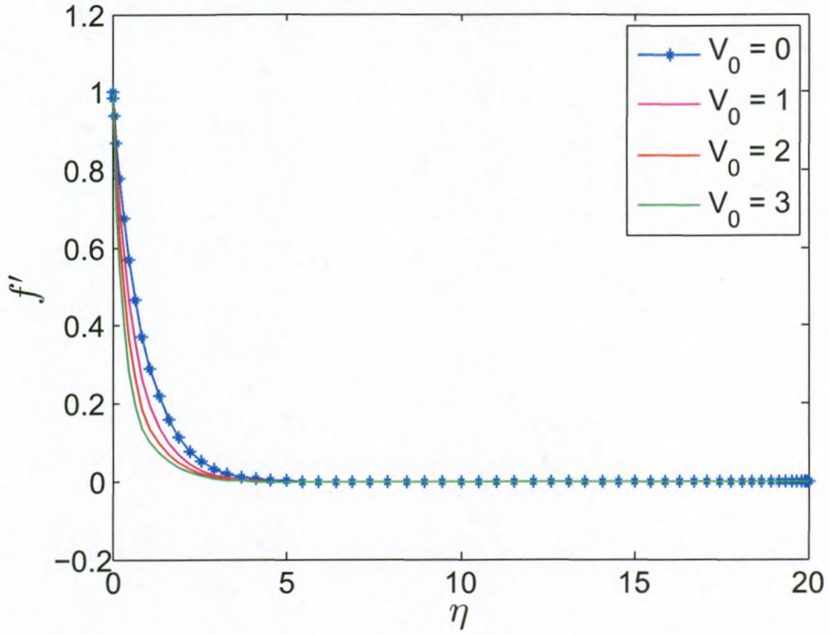

FIGURE 3.3: The effect of suction on velocity f' where $\lambda = 0.5$.

The results are converse to those of suction in Figure 3.3 which is to be expected. The boundary layer thickness reduces by increasing the suction velocity at the wall or by raising the porosity of the medium, but as the porosity further increases the injection at the stretching wall the boundary layer thickness increases.

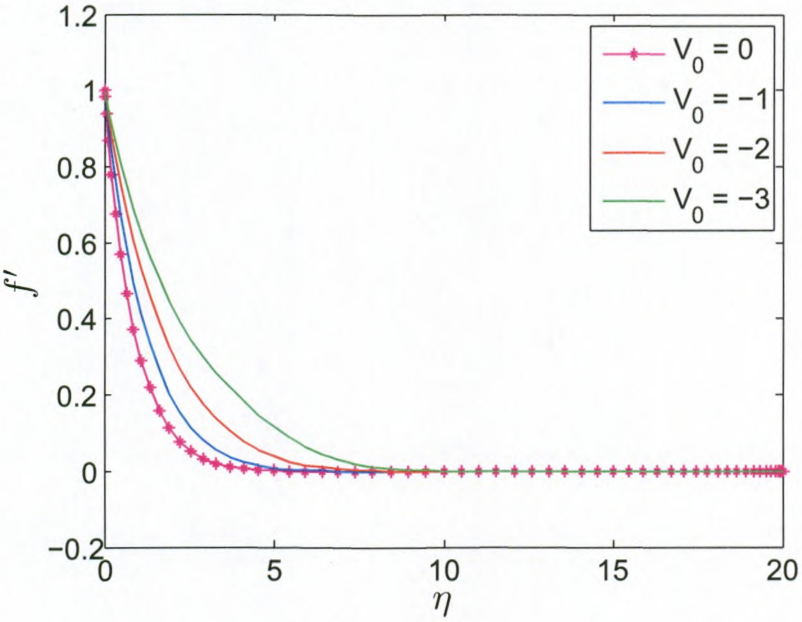

FIGURE 3.4: The effect of injection on velocity f' at the stretching wall when $\lambda = 0.5$.

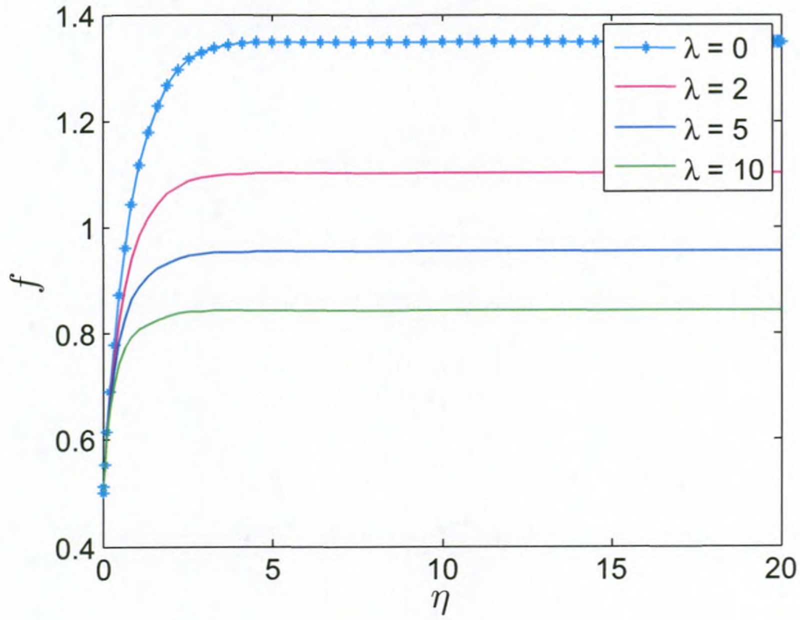

FIGURE 3.5: The impact of the porous medium on the velocity component f where $V_0 = 0.5$.

The consequence of the porosity parameter λ on the velocity component f is similar to that of f'. An increase in λ causes a diminution in the velocity of the fluid. As suction increases the velocity f upsurges at the stretching wall and becomes steady far from the plate.

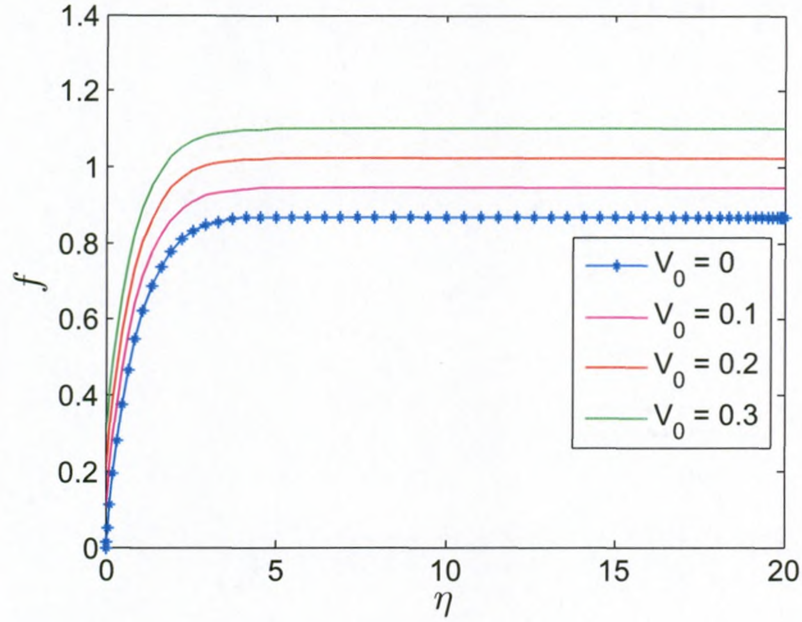

FIGURE 3.6: Velocity profile f for different values of suction parameter V_0 when $\lambda = 0.5$.

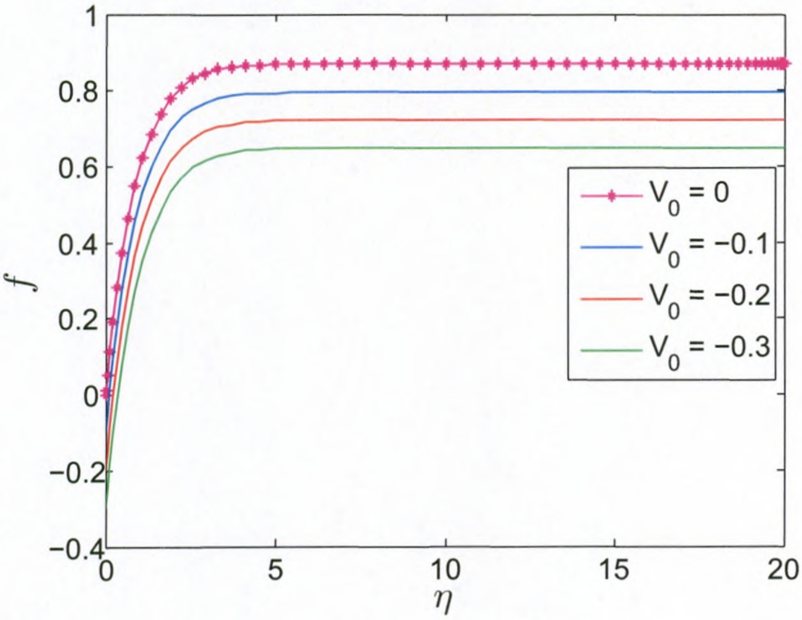

FIGURE 3.7: Velocity profile f for several values of the injection parameter V_0 while $\lambda = 0.5$.

As expected in Figure 3.7, the effect of an increasing injection decreases the velocity f.

3.3.1 Convergence and error analysis

A convergence test is done to see if the estimated solution obtained by means of the BI-SQLM approaches the true solution of equation (3.6). Accompanied by convergence is an evaluation of residual error [23]. The exact solution of equation (3.6) could not be educed from the literature due to the complex nature of the model. The residual error of the numerical solution is derived through a consideration of the numerical representation of the solution, which can be used to obtain approximations to the derivatives - consider (3.21) and (3.23). We observe whether this numerical approximation of the equation, evaluated at each point, provides an answer close to zero at each iteration. The norm of the residual error is accessible during each iteration and can be used in the place of the actual solution error as an indicator of convergence for the algorithm. Convergence with respect to η and ξ is met after five iterations with an elapsed time of 2.87105 seconds and the error is around 10^{-10}. Convergence was also tested using the initial guess Ali and Mehmood [57] employed in their paper and convergence was reached after five iterations; the elapsed time was 4.569710 seconds which is slower compared to when the initial solution was used; the error was roughly 10^{-10}.

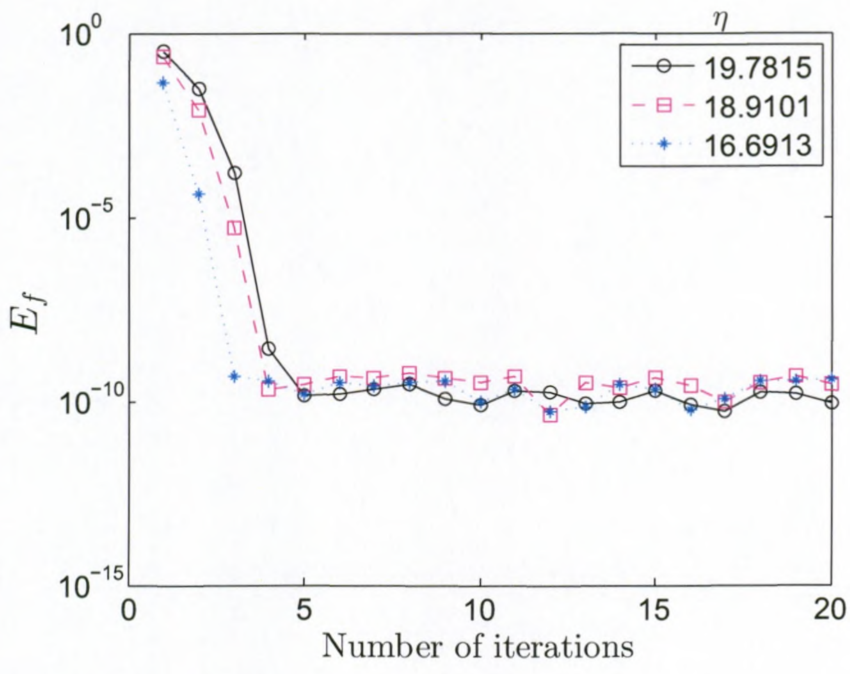

FIGURE 3.8: Convergence and residual error of f with respect to η.

[23] Is the disparity of the observed value and the estimated value.

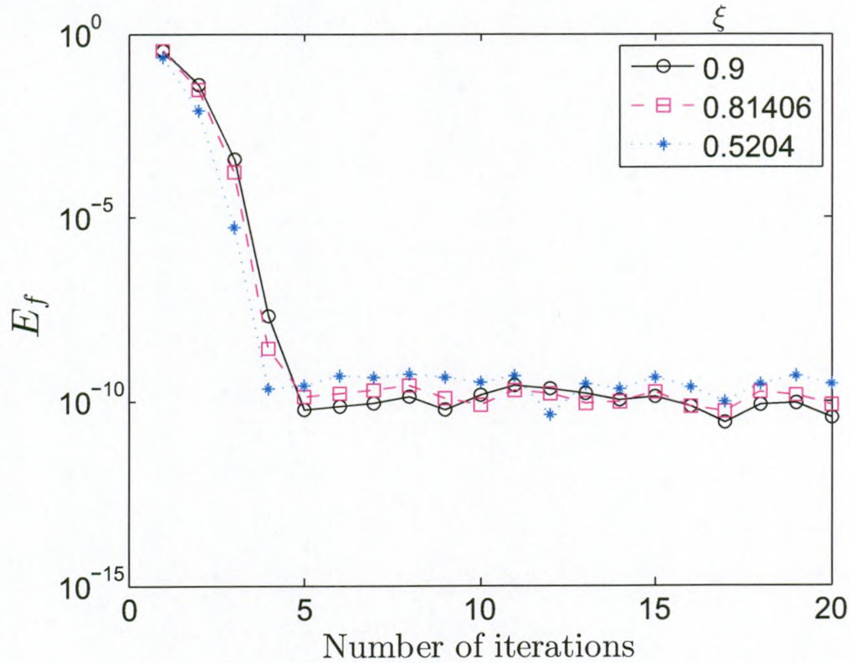

FIGURE 3.9: Convergence and residual error of f with respect to ξ.

The convergence and error of the derivative f plotted against η and ξ in Figures 3.10 and 3.11 follow a similar trend to that of f.

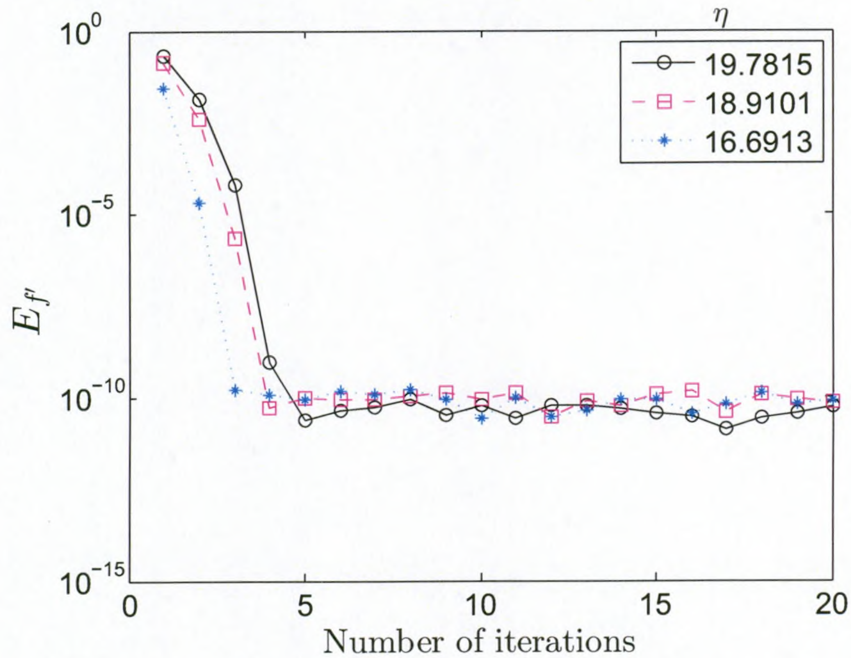

FIGURE 3.10: Convergence and residual error of f' apropos η.

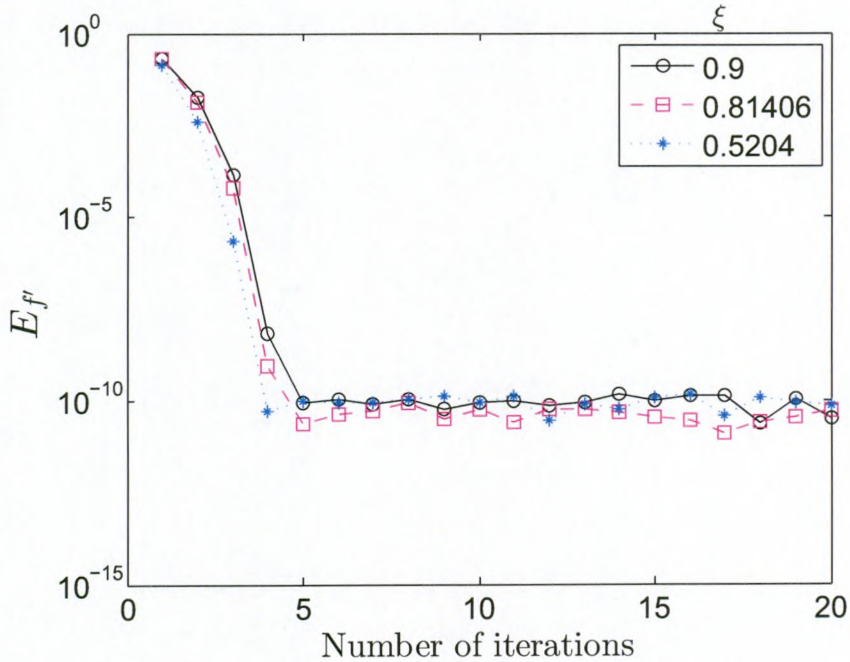

FIGURE 3.11: Convergence and error of f' apropos ξ.

Chapter 4

Model II: Thermal radiation effects on magnetohydrodynamics (MHD) forced convection flow adjacent to a non-isothermal wedge in the presence of a heat source or sink

Thermal radiation plays an important role on flow and heat transfer processes such as the design of many advanced energy conversion systems functioning at a great temperature. In 1998 Raptis [59] looked at the impacts of thermal radiation on the flow of a micropolar fluid past a continuously moving plate. Upon the two-dimensional flow Raptis approximated the temperature with the Taylor series to order four and neglected higher order terms. Transformations were then applied to get a system of three equations that were solved numerically. Similarly in the same year Raptis examined the two-dimensional steady free convection flow through a porous medium in the presence of thermal radiation [60]. MHD forced convection flow adjacent to a non-isothermal wedge with the effects of viscous dissipation and stress was investigated by Yih (1999) [61] numerically, using the Keller-box method. Chamkha et al. [62] generalized the work of Yih [61] by employing an implicit finite difference method. The BI-SQLM will be applied to the non-linear problem that was discussed by Chamkha et al. [62]. A steady, laminar, two-dimensional hydromagnetic boundary layer flow and heat transfer over a permeable non-isothermal wedge in the presence of thermal radiation and heat generation or absorption effects is examined.

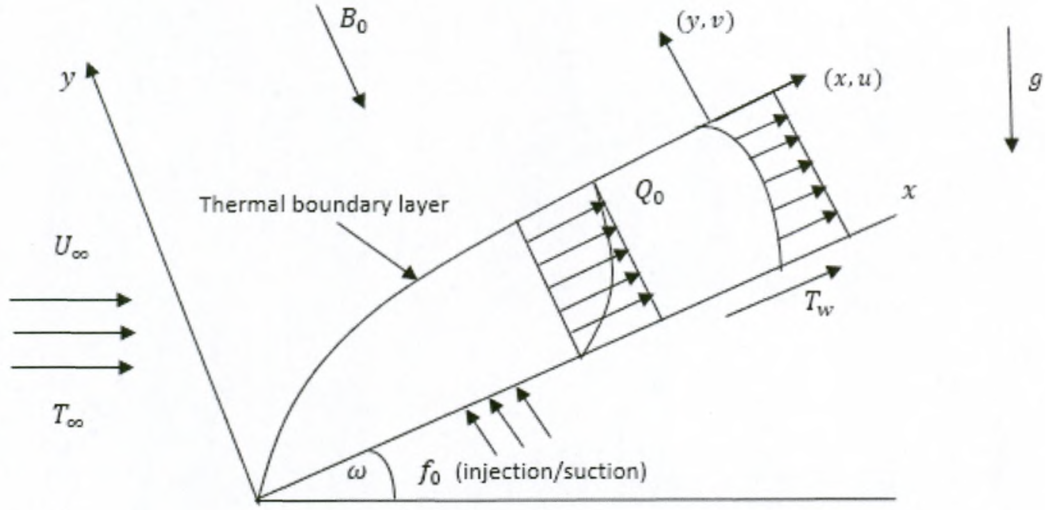

FIGURE 4.1: Visual representation of Model II

Assumptions

- Fluid suction or injection is enforced at the surface of the wedge.
- The applied magnetic field is uniform and is in the direction normal to the surface.
- Fluid properties are constant
- The Reynolds number is small, so that the magnetic field can be ignored.
- The electric field does not exist.

The equations governing this boundary-layer forced convection flow are established on the balance laws of mass, linear momentum and energy. They are written as

$$\frac{\partial u}{\partial x} + \frac{\partial v}{\partial y} = 0, \tag{4.1}$$

$$u\frac{\partial u}{\partial x} + v\frac{\partial u}{\partial y} = \nu\frac{\partial^2 u}{\partial y^2} + U_\infty\frac{dU_\infty}{dx} + \frac{\sigma B_o^2}{\rho}\left(U_\infty - u\right), \tag{4.2}$$

$$u\frac{\partial T}{\partial x} + \frac{\partial T}{\partial y} = \alpha\frac{\partial^2 T}{\partial y^2} + \frac{Q_o}{\rho c_p}\left(T - T_\infty\right) + \frac{1}{\rho c_p}\frac{\partial q_r}{\partial y} + \frac{\nu}{c_p}\left(\frac{\partial u}{\partial y}\right)^2$$

$$-\frac{u}{c_p}\left(U_\infty\frac{dU_\infty}{dx}+\frac{\sigma B_o^2}{\rho}U_\infty\right)+\frac{\sigma B_o^2 u^2}{\rho c_p}. \tag{4.3}$$

The physics of the problem depicts the following boundary conditions

$$y=0: \quad u=0, \quad v=-v_o, \quad T=T_w(x)=T_\infty+Ax^{2m}, \tag{4.4}$$

$$y\longrightarrow\infty: \quad u\longrightarrow U_\infty=Cx^m, \quad T\longrightarrow T_\infty, \tag{4.5}$$

where x and y are coordinates measured along and normal to the surface, respectively; u and v are the velocity components in the x and y directions respectively. In addition the radioactive heat flux q_r is employed according to the Rosseland approximation such that

$$q_r=-\frac{4\sigma *}{3K}\frac{\partial T^4}{\partial y}. \tag{4.6}$$

The fluid-phase temperature within the fluid flow is assumed to be sufficiently small so that T^4 may be defined as a linear function of temperature. This is done by expanding T^4 in a Taylor series about the free stream temperature T_∞ and abridging higher-order terms to give

$$T^4=4T_\infty^3T-3T_\infty^4. \tag{4.7}$$

By substituting (4.6) and (4.7) in (4.3), the following is attained

$$u\frac{\partial T}{\partial x}+\frac{\partial T}{\partial y}=\alpha\frac{\partial^2 T}{\partial y^2}+\frac{Q_o}{\rho c_p}(T-T_\infty)-\frac{16\sigma * T_\infty^3}{3K\rho c_p}\frac{\partial^2 T}{\partial y^2}+\frac{\nu}{c_p}\left(\frac{\partial u}{\partial y}\right)^2$$

$$-\frac{u}{c_p}\left(U_\infty\frac{dU_\infty}{dx}+\frac{\sigma B_o^2}{\rho}U_\infty\right)+\frac{\sigma B_o^2}{\rho c_p}. \tag{4.8}$$

The stream function is expressed as

$$u=\frac{\partial\psi}{\partial y} \quad \text{and} \quad v=-\frac{\partial\psi}{\partial x}. \tag{4.9}$$

These transformations along with the following dimensionless variables

$$\xi=\frac{\sigma B_o^2 x}{\rho U_\infty}, \quad \eta=\frac{y}{x}\left(\frac{U_\infty x}{\nu}\right)^{1/2}, \tag{4.10}$$

$$f(\xi,\eta)=\frac{\psi}{(U_\infty x\nu)^{1/2}}, \quad \theta(\xi,\eta)=\frac{T-T_\infty}{T_w-T_\infty}, \tag{4.11}$$

are substituted into equations (4.1), (4.2) and (4.8). The following non-similar equations are then obtained

$$f'''+\left(\frac{1+m}{2}\right)ff''+m\left(1-(f')^2\right)+\xi(1-f')=(1-m)\xi\left(f'\frac{\partial f'}{\xi}-f''\frac{\partial f}{\partial\xi}\right), \tag{4.12}$$

$$\frac{(1+N_{\mathrm{R}})}{\mathrm{Pr}}\theta'' + \left(\frac{1+m}{2}\right) f\theta' - 2mf'\theta + \phi\xi\theta + Ec\left((f'')^2 - (m+\xi)f' + \xi(f')^2\right)$$
$$= (1-m)\xi\left(f'\frac{\partial \theta}{\partial \xi} - \theta'\frac{\partial f}{\partial \xi}\right), \tag{4.13}$$

where

$$\mathrm{Pr} = \frac{\nu}{\alpha}, \quad N_{\mathrm{R}} = \frac{16\rho^* T_\infty^3}{3Kk}, \quad \phi = \frac{Q_o}{\sigma c_p B_o^2}, \quad Ec = \frac{C}{c_p A}, \tag{4.14}$$

are defined to be the Prandtl number, thermal radiation parameter, dimensionless heat generation or absorption coefficient and the Eckert number respectively. The corresponding boundary conditions are

$$\eta = 0: \quad f' = 0, \quad f = \left(\frac{2}{1+m}\right) f_o \xi^{1/2}, \quad \theta = 1, \tag{4.15}$$

$$\eta \longrightarrow \infty: \quad f' \longrightarrow 1, \quad \theta \longrightarrow 0. \tag{4.16}$$

where f_o is the dimensionless suction or injection parameter.

4.1 Determining the initial guess for $f(\eta,\xi)$ and $\theta(\eta,\xi)$

Deriving the initial solution for $f(\eta,\xi)$, we let $\xi = 0$ from (4.12) giving

$$\Rightarrow f_0''' + \left(\frac{1+m}{2}\right) f_0 f_0'' + m(1 - (f_0')^2) = 0, \tag{4.17}$$

where $f_0 = f_0(\eta)$ and boundary conditions (4.15)-(4.16) are transformed to

$$f_0'(0) = 0, \quad f_0(0) = 0, \quad f_0'(\infty) = 0, \qquad \eta \in [0,\infty). \tag{4.18}$$

Equation (4.17) is solved numerically by applying the spectral quasi-linearisation method (SQLM) for non-linear ordinary differential equations. The initial resolution for (4.17) is

$$f_0(\eta) = \eta - \exp(-\eta) - 1, \tag{4.19}$$

which satisfies the newly transformed boundary conditions (4.18). Applying the SQLM to (4.17), we let

$$F_0[\eta, f_0(\eta), f_0'(\eta), f_0''(\eta), f_0'''(\eta)] = f_0''' + \left(\frac{1+m}{2}\right) f_0 f_0'' + m\left(1 - (f_0')^2\right), \quad \eta \in [0,\infty). \tag{4.20}$$

Thus the SQLM scheme becomes

$$a_{0_{3,r}} f_{0_{r+1}}'''(\eta) + a_{0_{2,r}} f_{0_{r+1}}''(\eta) + a_{0_{1,r}} f_{0_{r+1}}'(\eta) + a_{0_{0,r}} f_{0_{r+1}}(\eta) = R_{f_{0_r}}(\eta), \tag{4.21}$$

where coefficients are defined to be

$$
\begin{aligned}
a_{0_{3,r}} &= \frac{\partial F_0}{\partial f_0'''}[\eta, f_{0_r}(\eta), f_{0_r}'(\eta), f_{0_r}''(\eta), f_{0_r}'''(\eta)] = 1,\\
a_{0_{2,r}} &= \frac{\partial F_0}{\partial f_0''}[\eta, f_{0_r}(\eta), f_{0_r}'(\eta), f_{0_r}''(\eta), f_{0_r}'''(\eta)] = \left(\frac{1+m}{2}\right) f_{0_r},\\
a_{0_{1,r}} &= \frac{\partial F_0}{\partial f_0'}[\eta, f_{0_r}(\eta), f_{0_r}'(\eta), f_{0_r}''(\eta), f_{0_r}'''(\eta)] = -2mf_{0_r}',\\
a_{0_{0,r}} &= \frac{\partial F_0}{\partial f_0}[\eta, f_{0_r}(\eta), f_{0_r}'(\eta), f_{0_r}''(\eta), f_{0_r}'''(\eta)] = \left(\frac{1+m}{2}\right) f_{0_r}''',
\end{aligned}
$$

and

$$
\begin{aligned}
R_{f_{0_r}}(\eta) &= \sum_{p=0}^{3} \frac{\partial F_0}{\partial f_0^{(p)}}[\eta, f_{0_r}(\eta), f_{0_r}'(\eta), f_{0_r}''(\eta), f_{0_r}'''(\eta)] f_{0_r}^{(p)}(\eta) - F_0[\eta, f_{0_r}(\eta), f_{0_r}'(\eta), f_{0_r}''(\eta), f_{0_r}'''(\eta)]\\
&= \left(\frac{1+m}{2}\right) f_{0_r}'' f_{0_r} + \left(-2mf_{0_r}'\right) f_{0_r}' + \left(\frac{1+m}{2}\right) f_{0_r} f_{0_r}'' + \left(\frac{1+m}{2}\right) f_{0_r}''' f_{0_r} + f_{0_r}'''\\
&- \left(f_{0_r}''' + \left(\frac{1+m}{2}\right) f_{0_r} f_{0_r}'' + m\left(1 - (f_{0_r}')^2\right)\right)\\
&= \left(\frac{1+m}{2}\right) f_{0_r} f_{0_r}'' - m - m(f_{0_r}')^2.
\end{aligned}
$$

Employing spectral collocation on (4.21) gives

$$\mathbf{A}_0 \mathbf{F}_{0_{r+1}} = \mathbf{R}_{f_{0_r}}, \tag{4.22}$$

with

$$\mathbf{A}_0 = \mathbf{D}^3 + \mathbf{a}_{0_{2,r}} \mathbf{D}^2 + \mathbf{a}_{0_{1,r}} \mathbf{D} + \mathbf{a}_{0_{0,r}}, \tag{4.23}$$

where

$$
\begin{aligned}
\mathbf{F}_0 &= [f_0(\eta_0), f_0(\eta_1), f_0(\eta_2), ..., f_0(\eta_N)]^{\mathrm{T}},\\
\mathbf{R}_{f_{0_r}} &= [R_{f_{0_r}}(\eta_0), R_{f_{0_r}}(\eta_1), R_{f_{0_r}}(\eta_2), ..., R_{f_{0_r}}(\eta_N)]^{\mathrm{T}}
\end{aligned}
$$

and

$$\mathbf{a}_{0_{p,r}} = [a_{0_{p,r}(\eta_0)}, a_{0_{p,r}(\eta_1)}, a_{0_{p,r}(\eta_2)}, ..., a_{0_{p,r}(\eta_N)}]^T$$

are diagonal matrices. The boundary conditions are represented as follows

$$\sum_{k=0}^{N} D_{0,k} f_{0_k} = 1, \quad f_{0_{r+1}}(\eta_N) = 0, \quad \sum_{k=0}^{N} D_{N,k} f_{0_k} = 0, \tag{4.24}$$

to be implemented on the first, second last and last row of (4.22)

$$\begin{pmatrix} D_{0,0} & D_{0,1} & \cdots & D_{0,N-1} & D_{0,N} \\ A_{0_{1,0}} & A_{0_{1,1}} & \cdots & A_{0_{1,N-1}} & A_{0_{1,N}} \\ A_{0_{2,0}} & A_{0_{2,1}} & \cdots & A_{0_{2,N-1}} & A_{0_{2,N}} \\ \vdots & \vdots & \ddots & \vdots & \vdots \\ A_{0_{N-2,0}} & A_{0_{N-2,1}} & \cdots & A_{0_{N-2,N-1}} & A_{0_{N-2,N}} \\ D_{N,0} & D_{N,1} & \cdots & D_{N,N-1} & D_{N,N} \\ 0 & 0 & \cdots & 0 & 1 \end{pmatrix} \begin{pmatrix} f_0(\eta_0) \\ f_0(\eta_1) \\ f_0(\eta_2) \\ \vdots \\ f_0(\eta_{N-2}) \\ f_0(\eta_{N-1}) \\ f_0(\eta_N) \end{pmatrix} = \begin{pmatrix} 1 \\ R_{f_{0_r}}(\eta_1) \\ R_{f_{0_r}}(\eta_2) \\ \vdots \\ R_{f_{0_r}}(\eta_{N-2}) \\ 0 \\ 0 \end{pmatrix}. \tag{4.25}$$

The initial solution for f is obtained by solving (4.25). Similarly the initial guess for θ is determined by letting $\xi = 0$ so that equation (4.13) is represented as

$$\left(\frac{1+N_R}{\Pr}\right)\theta_0'' + \left(\frac{1+m}{2}\right) f_0\theta_0' - 2mf_0'\theta_0 = -Ec\left(\left(f_0''\right)^2 - mf_0'\right), \qquad \eta \in [0,\infty), \tag{4.26}$$

where $\theta_0 = \theta_0(\eta)$ and the boundary conditions are as follows

$$\theta_0(\eta) = 1 \quad \text{and} \quad \theta_0(\infty) = 0. \tag{4.27}$$

In order to apply the spectral collocation method upon (4.26), $\{\eta_0, \eta_1, \ldots, \eta_{N-1}, \eta_N\}$ are represented as grid points. The function $\theta_0(\eta)$ is approximated by an interpolating polynomial, formulated in terms of values of θ at each collocaton point. Thus

$$\theta_0 = \{\theta_{0_0}, \theta_{0_1}, \ldots, \theta_{0_{N-1}}\theta_{0_N}\}^T$$

is the vector of unknowns. The derivatives at collocation points are expressed as

$$\left.\frac{d\theta_0}{d\eta}\right|_{\eta=\eta_i} = \mathbf{D}\theta_0 \quad \text{and} \quad \left.\frac{d^2\theta_0}{d\eta^2}\right|_{\eta=\eta_i} = \mathbf{D}^2\theta_0, \quad i = 0, 1, \ldots, N. \tag{4.28}$$

Substituting (4.28) into (4.26) gives

$$\begin{pmatrix} B_{0_{0,0}} & B_{0_{0,1}} & \cdots & B_{0_{0,N-1}} & B_{0_{0,N}} \\ B_{0_{1,0}} & B_{0_{1,1}} & \cdots & B_{0_{1,N-1}} & B_{0_{1,N}} \\ B_{0_{2,0}} & B_{0_{2,1}} & \cdots & B_{0_{2,N-1}} & B_{0_{2,N}} \\ \vdots & \vdots & \ddots & \vdots & \vdots \\ B_{0_{N-2,0}} & B_{0_{N-2,1}} & \cdots & B_{0_{N-2,N-1}} & B_{0_{N-2,N}} \\ B_{0_{N-1,0}} & B_{0_{N-1,1}} & \cdots & B_{0_{N-1,N-1}} & B_{0_{N-1,N}} \\ B_{0_{N,0}} & B_{0_{N,1}} & \cdots & B_{0_{N,N-1}} & B_{0_{N,N}} \end{pmatrix} \begin{pmatrix} \theta_0(\eta_0) \\ \theta_0(\eta_1) \\ \theta_0(\eta_2) \\ \vdots \\ \theta_0(\eta_{N-2}) \\ \theta_0(\eta_{N-1}) \\ \theta_0(\eta_N) \end{pmatrix} = \begin{pmatrix} R_{\theta_{0_r}}(\eta_0) \\ R_{\theta_{0_r}}(\eta_1) \\ R_{\theta_{0_r}}(\eta_2) \\ \vdots \\ R_{\theta_{0_r}}(\eta_{N-2}) \\ R_{\theta_{0_r}}(\eta_{N-1}) \\ R_{\theta_{0_r}}(\eta_N) \end{pmatrix}, \tag{4.29}$$

compactly written as

$$\mathbf{B}_0\Theta_0 = \mathbf{R}_{\theta_0}, \tag{4.30}$$

where

$$\mathbf{B}_0 = \left(\frac{1+N_R}{\mathrm{Pr}}\right)\mathbf{D}^2 + \left(\frac{1+m}{2}\right) f_{0_r}\mathbf{D} - 2mf'_{0_r} + \mathbf{I},$$
$$\mathbf{R}_{\theta_0} = -Ec\left((f''_0)^2 - mf'_0\right)$$

and $\mathbf{I}$ is the identity matrix of size $(N_\eta + 1) \times (N_\eta + 1)$. The boundary conditions

$$\theta_0(\eta_0) = 0 \quad \text{and} \quad \theta_0(\eta_N) = 1$$

are imposed on the first and last row of (4.29) to give

$$\begin{pmatrix} 1 & 0 & \dots & 0 & 0 \\ B_{0_{1,0}} & B_{0_{1,1}} & \dots & B_{0_{1,N-1}} & B_{0_{1,N}} \\ B_{0_{2,0}} & B_{0_{2,1}} & \dots & B_{0_{2,N-1}} & B_{0_{2,N}} \\ \vdots & \vdots & \ddots & \vdots & \vdots \\ B_{0_{N-2,0}} & B_{0_{N-2,1}} & \dots & B_{0_{N-2,N-1}} & B_{0_{N-2,N}} \\ B_{0_{N-1,0}} & B_{0_{N-1,1}} & \dots & B_{0_{N-1,N-1}} & B_{0_{N-1,N}} \\ 0 & 0 & \dots & 0 & 1 \end{pmatrix} \begin{pmatrix} \theta_0(\eta_0) \\ \theta_0(\eta_1) \\ \theta_0(\eta_2) \\ \vdots \\ \theta_0(\eta_{N-2}) \\ \theta_0(\eta_{N-1}) \\ \theta_0(\eta_N) \end{pmatrix} = \begin{pmatrix} 0 \\ R_{\theta_{0_r}}(\eta_1) \\ R_{\theta_{0_r}}(\eta_2) \\ \vdots \\ R_{\theta_{0_r}}(\eta_{N-2}) \\ R_{\theta_{0_r}}(\eta_{N-1}) \\ 1 \end{pmatrix}. \tag{4.31}$$

Solving (4.31), θ_0 is then obtained.

4.2 Solution to the two equation system of partial differential equations using the BI-SQLM

We consider equation (4.12) and let H be the non-linear operator of the equation,

$$H = f''' + \left(\frac{1+m}{2}\right) ff'' + m\left(1-(f')^2\right) + \xi(1-f') - (1-m)\xi\left(f'\frac{\partial f'}{\xi} - f''\frac{\partial f}{\partial \xi}\right), \tag{4.32}$$

where $H = H[\eta, f(\eta), f'(\eta), f''(\eta), f'''(\eta)]$ and $f = f(\eta, \xi)$. The linearised equation is shown to be

$$a_{3,r}(\eta,\xi)f'''_{r+1} + a_{2,r}(\eta,\xi)f''_{r+1} + a_{1,r}(\eta,\xi)f''_{r+1} + a_{0,r}(\eta,\xi)f_{r+1} + a_{4,r}(\eta,\xi)\frac{\partial f_{r+1}}{\partial \xi} + a_{5,r}(\eta,\xi)\frac{\partial f'_{r+1}}{\partial \xi}$$

$$-\xi(1-m)f''_r\frac{\partial f_{r+1}}{\partial \xi} + \xi(1-m)f'_r\frac{\partial f'_{r+1}}{\partial \xi} = R_r(\eta,\xi), \tag{4.33}$$

where

$$a_{0,r}(\eta,\xi)[f_r, f_r', f_r'', f_r'''] = \frac{\partial H}{\partial f} = \left(\frac{1+m}{2}\right) f_r'',$$
$$a_{1,r}(\eta,\xi)[f_r, f_r', f_r'', f_r'''] = \frac{\partial H}{\partial f'} = -2mf_r' - \xi - (1-m)\xi\frac{\partial f_r'}{\partial \xi},$$
$$a_{2,r}(\eta,\xi)[f_r, f_r', f_r'', f_r'''] = \frac{\partial H}{\partial f''} = \left(\frac{1+m}{2}\right) f_r + (1-m)\xi\frac{\partial f_r}{\partial \xi},$$
$$a_{3,r}(\eta,\xi)[f_r, f_r', f_r'', f_r'''] = \frac{\partial H}{\partial f'''} = 1,$$
$$a_{4,r}(\eta,\xi)[f_r, f_r', f_r'', f_r'''] = (1-m)\xi f_r'',$$
$$a_{5,r}(\eta,\xi)[f_r, f_r', f_r'', f_r'''] = -(1-m)\xi f_r',$$

and

$$\begin{aligned}
R_{f_r}(\eta) &= \sum_{p=0}^{3} \frac{\partial F}{\partial f^{(p)}}[\eta, f_r(\eta), f_r'(\eta), f_r''(\eta), f_r'''(\eta)] f_r^{(p)}(\eta) + (1-m)\xi f_r''\frac{\partial f_r}{\partial \xi} - (1-m)\xi f_r''\frac{\partial f_r'}{\partial \xi} \\
&\quad - H[\eta, f_r(\eta), f_r'(\eta), f_r''(\eta), f_r'''(\eta)] \\
&= \left(\frac{1+m}{2}\right) f_r'' f_r + \left(-2mf_r' - \xi - (1-m)\xi f_r''\frac{\partial f_r'}{\partial \xi}\right) f_r' \\
&\quad + \left(\left(\frac{1+m}{2}\right) f_r + (1-m)\xi f_r''\frac{\partial f_r}{\partial \xi}\right) f_r'' + f_r''' + (1-m)\xi f_r''\frac{\partial f_r}{\partial \xi} - (1-m)\xi f_r''\frac{\partial f_r'}{\partial \xi} \\
&\quad - f_r''' - \left(\frac{1+m}{2}\right) f_r f_r'' - m\left(1 - (f_r')^2\right) - \xi(1 - f_r') + (1-m)\xi\left(f_r'\frac{\partial f_r'}{\xi} + f_r''\frac{\partial f_r}{\partial \xi}\right) \\
&= -m(f_r')^2 + \left(\frac{1+m}{2}\right) f_r f_r'' + (1+m)\xi f_r''\frac{\partial f_r}{\partial \xi} - (1-m)\xi f_r'\frac{\partial f_r'}{\partial \xi} - m - \xi.
\end{aligned}$$

Applying the collocation at ξ_i in (4.33) we attain

$$\begin{aligned}
&a_{3,r}^{(i)}(\eta,\xi)F_{r+1,i}'''(\eta) + a_{2,r}^{(i)}(\eta,\xi)F_{r+1,i}''(\eta) + a_{1,r}^{(i)}(\eta,\xi)F_{r+1,i}''(\eta) + a_{0,r}^{(i)}(\eta,\xi)F_{r+1,i}(\eta) + a_{4,r}^{(i)}\sum_{j=0}^{N_\xi} \mathrm{d}_{i,j}F_j(\eta) \\
&+ 2a_{5,r}^{(i)}\sum_{j=0}^{N_\xi} \mathbf{d}_{i,j}F_j'(\eta) - 2\xi_i(1-m)F_{r,i}''\sum_{j=0}^{N_\xi} \mathbf{d}_{i,j}F_j(\eta) + 2\xi_i(1-m)F_{r,i}'\sum_{j=0}^{N_\xi} \mathbf{d}_{i,j}F_j'(\eta) = R_{f_r}(\eta,\xi),
\end{aligned} \tag{4.34}$$

where

$$\left.\frac{\partial f}{\partial \xi}\right|_{\xi=\xi_i} = \sum_{j=0}^{N_\xi} \mathbf{d}_{i,j}F_j(\eta) \quad \text{and} \quad \left.\frac{\partial f'}{\partial \xi}\right|_{\xi=\xi_i} = \sum_{j=0}^{N_\xi} \mathbf{d}_{i,j}F_j'(\eta), \quad i = 1, ..., N_\xi,$$

is the derivative of f and f' with respect to ξ. The derivatives with respect to η are expressed as

$$\left.\frac{d^p F_{r+1,i}}{d\xi^p}\right|_{\eta=\eta_j} = \sum_{k=0}^{N_\eta} \mathbf{D}^p \mathbf{F}_{r+1,i}, \tag{4.35}$$

where p is the order of the derivative. Substituting (4.35) into (4.34) gives

$$\mathbf{A}^{(i)} \mathbf{F}_{r+1,i} = \mathbf{R}_1^{(i)}, \tag{4.36}$$

where

$$\begin{aligned}
\mathbf{A}^{(i)} &= \mathbf{a}_{3,r}^{(i)} \mathbf{D}^3 + \mathbf{a}_{2,r}^{(i)} \mathbf{D}^2 + \mathbf{a}_{1,r}^{(i)} \mathbf{D} + \mathbf{a}_{0,r}^{(i)} \mathbf{I}, \\
\mathbf{R}_1^{(i)} &= R_{f_r}^{(i)} + (1-m)\xi_i d_{i,N_\xi} \mathbf{D} \mathbf{F}_{r+1,N_\xi} - (1-m)\xi_i d_{i,N_\xi} \mathbf{F}_{r+1,N_\xi}.
\end{aligned}$$

The boundary conditions are depicted as

$$\sum_{k=0}^{N} D_{0,k} f_k = 1, \quad f_{r+1}(\eta_N) = 0, \quad \sum_{k=0}^{N} D_{N,k} f_k = 0. \tag{4.37}$$

Accounting for the boundary conditions (4.37) for each $i = 0, 1, ..., N_\xi - 1$ in (4.36) gives

$$\begin{pmatrix}
A_{0,0} & A_{0,1} & \cdots & A_{0,N_\xi-2} & A_{0,N_\xi-1} \\
A_{1,0} & A_{1,1} & \cdots & A_{1,N_\xi-2} & A_{1,N_\xi-1} \\
\vdots & \vdots & \ddots & \vdots & \vdots \\
A_{N_\xi-1,0} & A_{N_\xi-1,1} & \cdots & A_{N_\xi-1,N_\xi-2} & A_{N_\xi-1,N_\xi-1}
\end{pmatrix}
\begin{pmatrix}
\mathbf{F}_{r+1,0} \\ \mathbf{F}_{r+1,1} \\ \vdots \\ \mathbf{F}_{r+1,N_\xi-1}
\end{pmatrix}
=
\begin{pmatrix}
\mathbf{R}_1^{(0)} \\ \mathbf{R}_1^{(1)} \\ \vdots \\ \mathbf{R}_1^{(N_\xi-1)}
\end{pmatrix}, \tag{4.38}$$

where

$$\begin{aligned}
A_{i,i} &= \mathbf{A}^{(i)}, & i = 0, 1, ...N_\xi - 1, \\
A_{i,j} &= -(1-m)\xi_i d_{i,N_\xi} \mathbf{D} + (1-m)\xi_i d_{i,N_\xi} & \text{when} \quad i \neq j.
\end{aligned}$$

The approximate solution for (4.12) is attained by solving for $\mathbf{F}$. Thus knowing the solution to $f(\eta, \xi)$ equation (4.13) may be solved. Letting G be a non-linear operator for (4.13), the following coeffients are acquired

$$\begin{aligned}
b_{0,r}(\eta,\xi)[\theta_r, \theta_r', \theta_r''] &= \frac{\partial G}{\partial \theta} = -2mf_r + \phi\xi, \\
b_{1,r}(\eta,\xi)[\theta_r, \theta_r', \theta_r''] &= \frac{\partial G}{\partial \theta'} = \left(\frac{1+m}{2}\right) f_r + (1-m)\,\xi \frac{\partial f}{\partial \xi}, \\
b_{2,r}(\eta,\xi)[\theta_r, \theta_r', \theta_r''] &= \frac{\partial G}{\partial \theta''} = \frac{(1+N_{\mathrm{R}})}{\mathrm{Pr}}, \\
b_{3,r}(\eta,\xi)[\theta_r, \theta_r', \theta_r''] &= \frac{\partial G}{\partial \frac{\partial \theta}{\partial \xi}} = -\,(1-m)\,\xi f_r'
\end{aligned}$$

and

$$\begin{aligned}
R_{\theta_r}(\eta,\xi)[\theta_r,\theta_r',\theta_r''] &= \sum_{l=0}^{2} b_{l,r}\theta_r^{(l)} - G[\theta_r,\theta_r',\theta_r''] \\
&= \left(-2mf_r+\phi\xi\right)\theta_r + \left(\left(\frac{1+m}{2}\right)f_r + (1-m)\,\xi\frac{\partial f}{\partial \xi}\right)\theta_r' + \left(\frac{(1+N_{\mathrm{R}})}{\mathrm{Pr}}\right)\theta_r'' \\
&- \left((1-m)\,\xi f_r'\right)\frac{\partial \theta_r}{\partial \xi} - \left(\frac{(1+N_{\mathrm{R}})}{\mathrm{Pr}}\right)\theta_r'' - \left(\frac{1+m}{2}\right)f_r\theta_r' + 2mf_r'\theta_r' \\
&- \phi\xi\theta_r - Ec\left(\left(f_r''\right)^2 - (m+\xi)\,f_r' + \xi\left(f_r'\right)^2\right) + (1-m)\,\xi\left(f_r'\frac{\partial \theta_r}{\partial \xi} - \theta_r'\frac{\partial f_r}{\partial \xi}\right) \\
&= -Ec\left(\left(f_r''\right)^2 - (m+\xi)\,f_r' + \xi\left(f_r'\right)^2\right).
\end{aligned}$$

Therefore the linearised equation can be expressed as

$$b_{3,r}\frac{\partial \theta_{r+1}}{\partial \xi} + b_{2,r}\theta_{r+1}'' + b_{1,r}\theta_{r+1}' + b_{0,r}\theta_{r+1} = R_{\theta_r}, \tag{4.39}$$

where the derivatives with respect to ξ are respresented as

$$\left.\frac{\partial \theta}{\partial \xi}\right|_{\xi=\xi_i} = \sum_{j=0}^{N_\xi} \mathbf{d}_{i,j}\Theta_j(\eta),$$

Applying collocation at ξ_i we get

$$b_{3,r}^{(i)}\sum_{j=0}^{N_\xi} \mathrm{d}_{i,j}\Theta_j(\eta) + b_{2,r}^{(i)}\Theta_{r+1}''(\eta) + b_{1,r}^{(i)}\Theta_{r+1}'(\eta) + b_{0,r}^{(i)}\Theta_{r+1} = R_{\theta_r}^{(i)}. \tag{4.40}$$

Since the solution at $\xi = 0$ is known, $N_\xi - 1$ is only evaluated, thus

$$b_{3,r}^{(i)}\sum_{j=0}^{N_\xi-1} \mathbf{d}_{i,j}\Theta_j(\eta) + b_{2,r}^{(i)}\Theta_{r+1}''(\eta) + b_{1,r}^{(i)}\Theta_{r+1}'(\eta) + b_{0,r}^{(i)}\Theta_{r+1} = R_{\theta_r}^{(i)} - b_{3,r}^{(N_\xi)}d_{i,j}\Theta_{N_\xi}(\eta). \tag{4.41}$$

The derivatives with respect to η are set in terms of the chebyshev differentiation matrix are

$$\left.\frac{\partial \Theta_{r+1,i}}{\partial \eta}\right|_{\eta=\eta_i} = \sum_{k=0}^{N_\eta} D_{i,j}^{p}\Theta_j(\eta) = \mathbf{D}^p\Theta_{r+1,i}. \tag{4.42}$$

Substituting (4.42) into (4.41) gives

$$\mathbf{B}^{(i)}\Theta_{r+1,i} + b_{3,r}^{(i)}\sum_{j=0}^{N_\xi-1} d_{i,j}\Theta_{r+1,j} = \mathbf{R}_2^{(i)}, \tag{4.43}$$

where

$$\mathbf{B}^{(i)} = b_{2,r}^{(i)}\mathbf{D}^2 + b_{1,r}^{(i)}\mathbf{D} + b_{0,r}^{(i)}\mathbf{I},$$
$$\mathbf{R}_2^{(i)} = R_{\theta_r}^{(i)} - b_{3,r}^{(N_\xi)} d_{i,N_\xi}\Theta_{r+1,N_\xi}$$

and $\mathbf{I}$ is the identity matrix. The boundary conditions are as follows

$$\theta_{r+1}(\eta_0) = 0 \quad \text{and} \quad \theta_{r+1}(\eta_N) = 1. \tag{4.44}$$

Equation (4.43) can be written in matrix form

$$\begin{pmatrix} B_{0,0} & B_{0,1} & \dots & B_{0,N_\xi-2} & B_{0,N_\xi-1} \\ B_{1,0} & B_{1,1} & \dots & B_{1,N_\xi-2} & B_{1,N_\xi-1} \\ \vdots & \vdots & \ddots & \vdots & \vdots \\ B_{N_\xi-1,0} & B_{N_\xi-1,1} & \dots & B_{N_\xi-1,N_\xi-2} & B_{N_\xi-1,N_\xi-1} \end{pmatrix} \begin{pmatrix} \Theta_{r+1,0} \\ \Theta_{r+1,1} \\ \vdots \\ \Theta_{r+1,N_\xi-1} \end{pmatrix} = \begin{pmatrix} \mathbf{R}_2^{(0)} \\ \mathbf{R}_2^{(1)} \\ \vdots \\ \mathbf{R}_2^{(N_\xi-1)} \end{pmatrix}, \tag{4.45}$$

where

$$B_{i,i} = \mathbf{B}^{(i)} + b_{3,r}^{(i)} d_{i,N_\xi}, \qquad i = 0, 1, ..., N_\xi - 1,$$
$$B_{i,j} = b_{3,r}^{(i)} d_{i,N_\xi}, \qquad i \neq j.$$

Solving for Θ gives the approximate solution for $\theta(\eta, \xi)$.

4.3 Results and analysis

The solutions of equations (4.12)-(4.13) are graphically illustrated. The diagrams show the impact of the assorted parameters on velocity and temperature profiles, as well as the local skin-friction coefficient and Nusselt number.

In the work Chamkha et al. [62] published, initial guesses for equations (4.12)-(4.13) were not specified, hence we made use of the initial solutions that were calculated in the earlier section 4.1. We also make comparisons to some results that previous researchers achieved to confirm the validity of the BI-SQLM.

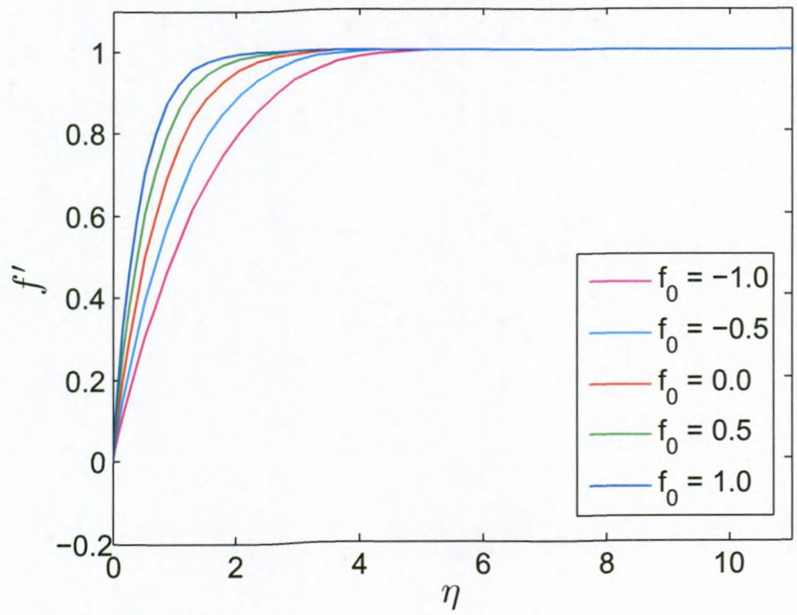

FIGURE 4.2: The influence of f_0 (suction and injection) on the velocity profiles, where $m = 0.3333$, $\Pr = 0.733$, $Ec = 0$, $\phi = 0$, $N_{\mathrm{R}} = 0$ and $\xi = 1.0$.

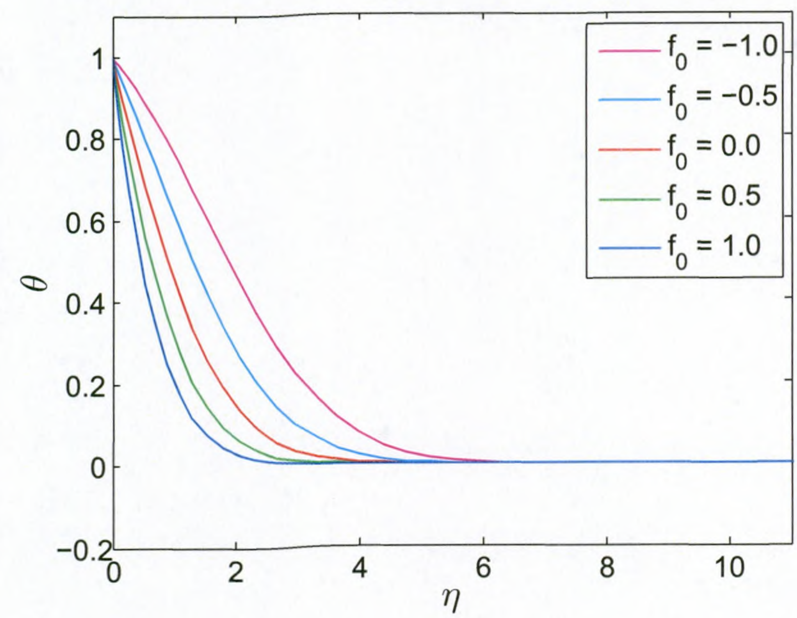

FIGURE 4.3: The consequence of f_0 (suction and injection) on the temperature profiles, when $m = 0.3333$, $\Pr = 0.733$, $Ec = 0$, $\phi = 0$, $N_{\mathrm{R}} = 0$ and $\xi = 1.0$.

The effects of suction reduces both hydrodynamic and thermal boundary layers. This means that there is an increase in fluid velocity and a decrease in fluid temperature. It is anticipated that the opposite effect occurs when injection is imposed.

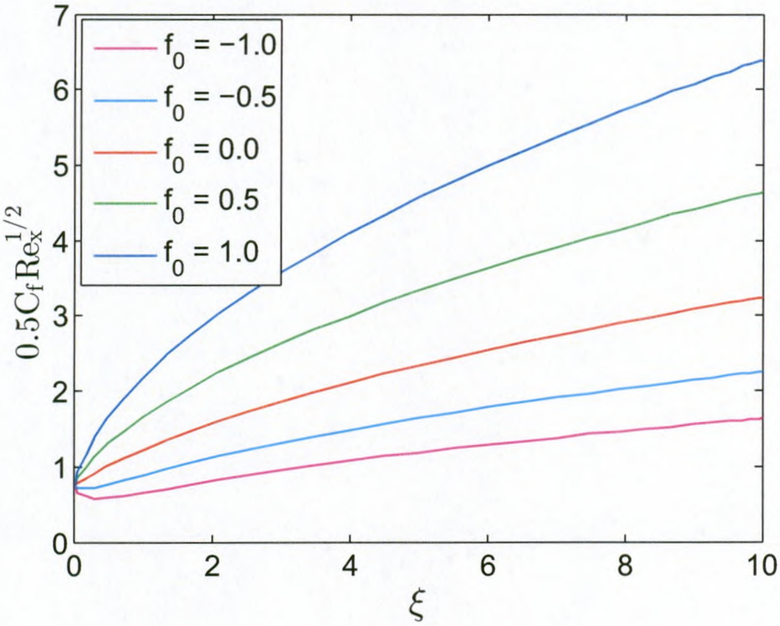

FIGURE 4.4: The repercussions of f_0 upon the skin-friction coefficient, where $m = 0.3333$, $\mathrm{Pr} = 0.733$, $Ec = 0$, $\phi = 0$, $N_\mathrm{R} = 0$ and $\eta = 16$.

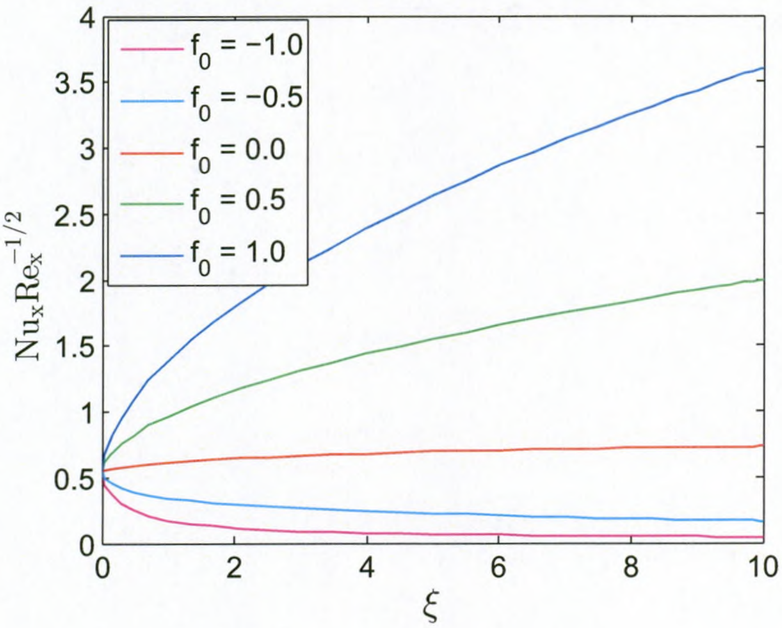

FIGURE 4.5: The response of the Nusselt number for varied f_0, when $m = 0.3333$, $\mathrm{Pr} = 0.733$, $Ec = 0$, $\phi = 0$, $N_\mathrm{R} = 0$ and $\eta = 16$.

In Figures 4.4 and 4.5 the local Nusselt number and skin-friction coefficient upsurges when $f > 0$ and reduces when $f < 0$ over the region ξ. An increment in suction causes a relatively higher Nusselt number, hence this indicates convection considerably dominating the transfer of thermal energy at the surface.

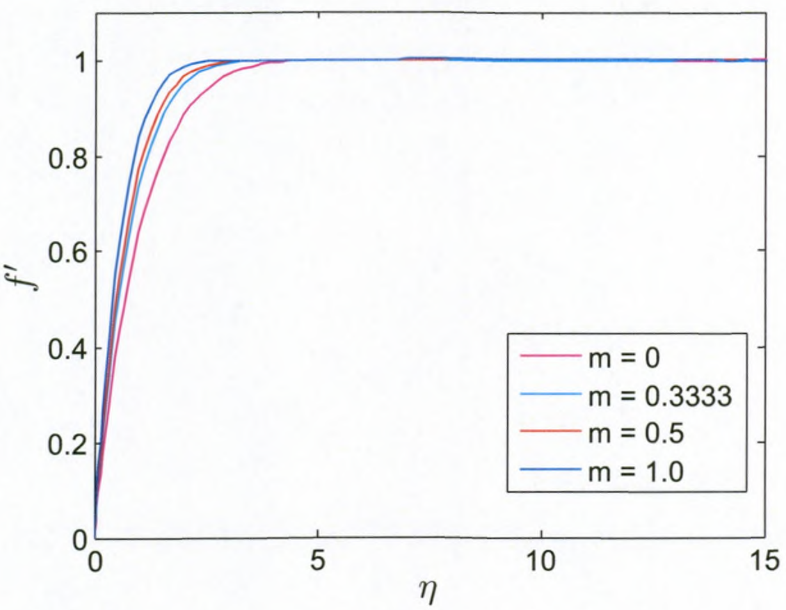

FIGURE 4.6: Effects of pressure gradient m on the velocity profiles, while $Ec = 0.0$, $f_0 = 0.0$, $N_R = 5.0$, $\Pr = 0.733$, $\phi = 0.0$ and $\xi = 1.0$.

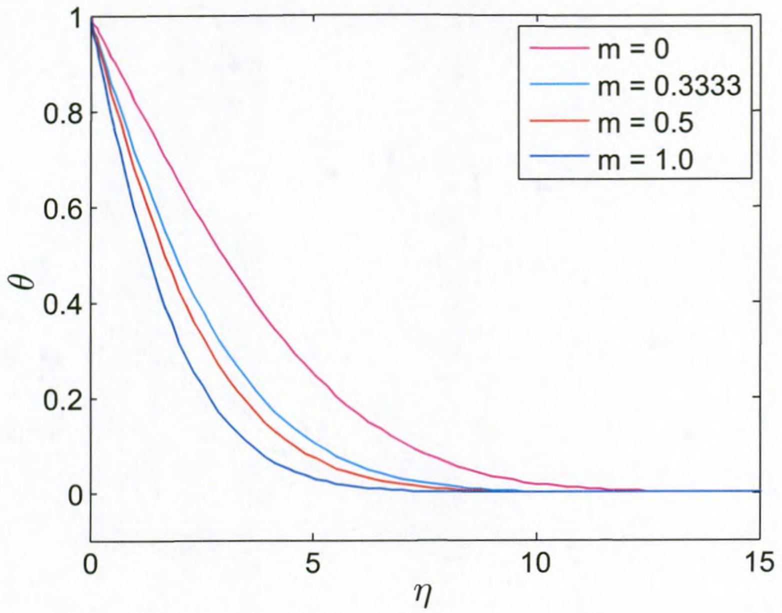

FIGURE 4.7: The impact of pressure gradient m on the temperature profiles, where $Ec = 0.0$, $f_0 = 0.0$, $N_R = 5.0$, $\Pr = 0.733$, $\phi = 0.0$ and $\xi = 1.0$.

As the pressure gradient increases both the velocity and temperature are predicted to diminish. This is accompanied by an increase in the hydrodynamic boundary layer and a decrease in the thermal boundary layer.

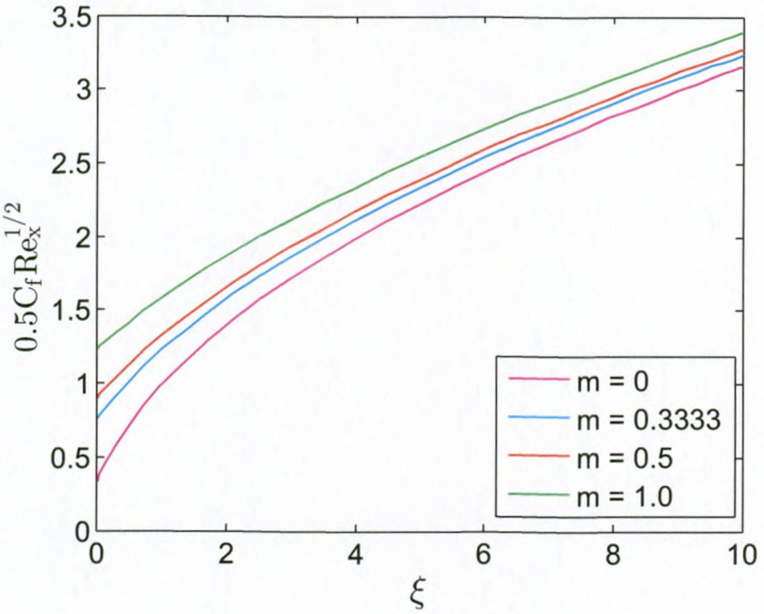

FIGURE 4.8: The influence of the pressure gradient m on the drag coefficient, whilst $Ec = 0.0$, $f_0 = 0.0$, $N_{\mathrm{R}} = 0$, $\mathrm{Pr} = 0.733$, $\phi = 0.0$ and $\eta = 16$.

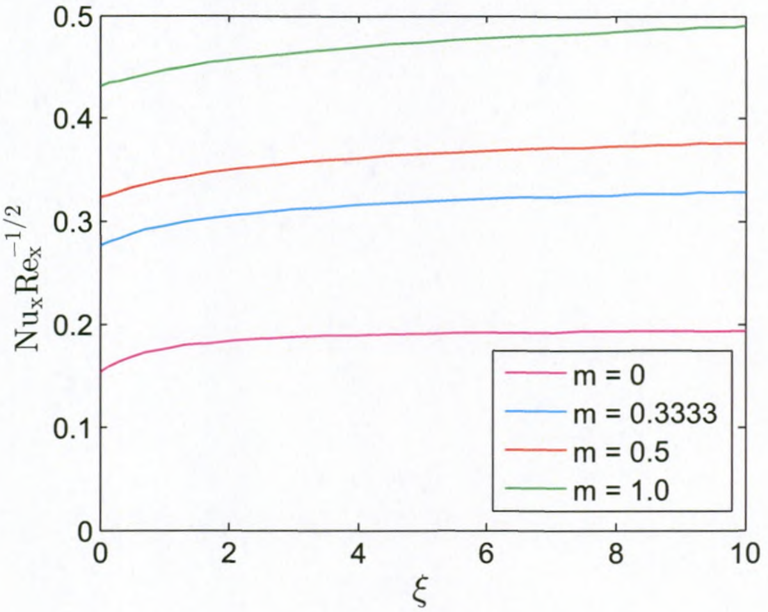

FIGURE 4.9: The consequence of the pressure gradient m upon the Nusselt number, where $Ec = 0.0$, $f_0 = 0.0$, $N_{\mathrm{R}} = 0$, $\mathrm{Pr} = 0.733$, $\phi = 0.0$ and $\eta = 16$.

An accretion of m increases the skin-friction coefficient as well as the Nusselt number.

In figure 4.10, when N_{R} (thermal radiation parameter) rises, this increases the conduction effect of the thermal boundary layer. This causes the temperature to rise at every point away from the wedge surface.

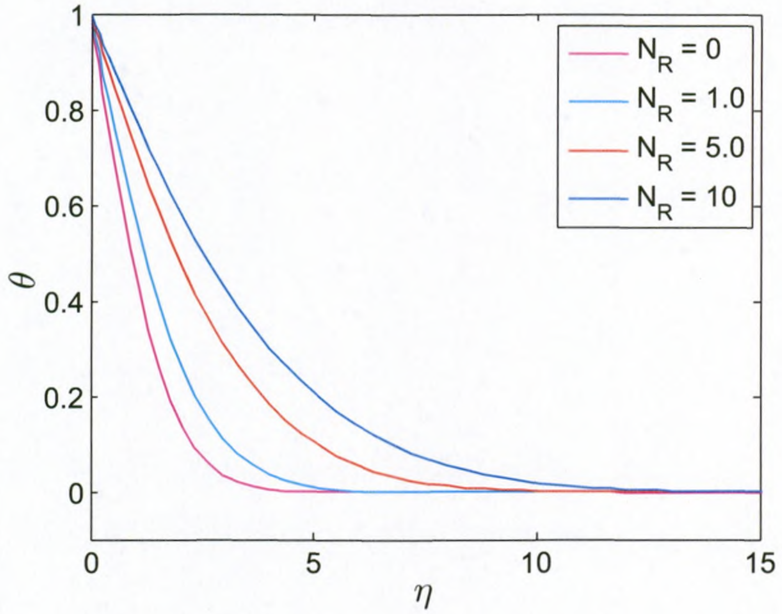

FIGURE 4.10: The impact of thermal radiation N_{R} on the temperature profiles, when $Ec = 0.0$, $f_0 = 0.0$, $m = 0.3333$, $\mathrm{Pr} = 0.733$, $\phi = 0.0$ and $\xi = 1.0$.

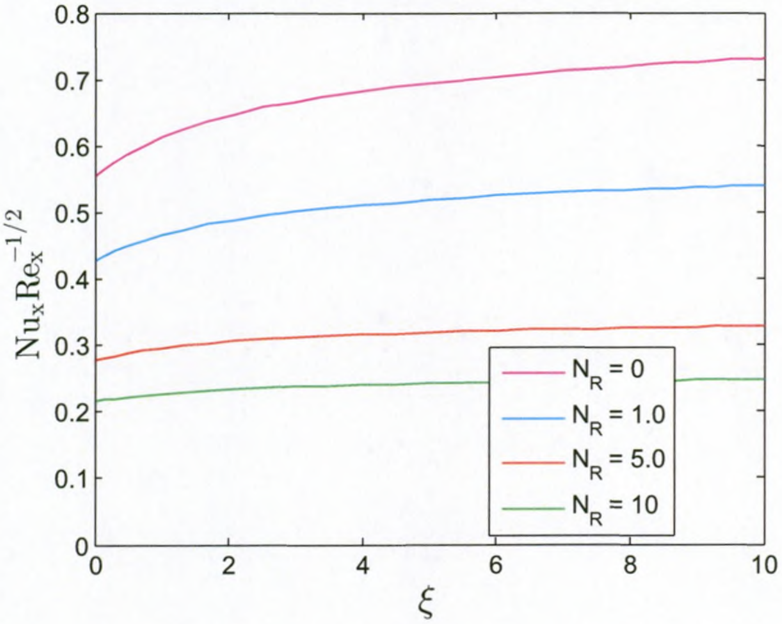

FIGURE 4.11: The effect of thermal radiation N_{R} upon the Nusselt number, while $Ec = 0.0$, $f_0 = 0.0$, $m = 0.3333$, $\mathrm{Pr} = 0.733$, $\phi = 0.0$ and $\eta = 16$.

An increment in N_{R} decreases the local Nusselt number due to it being negatively related to the value of the wall of the temperature profile.

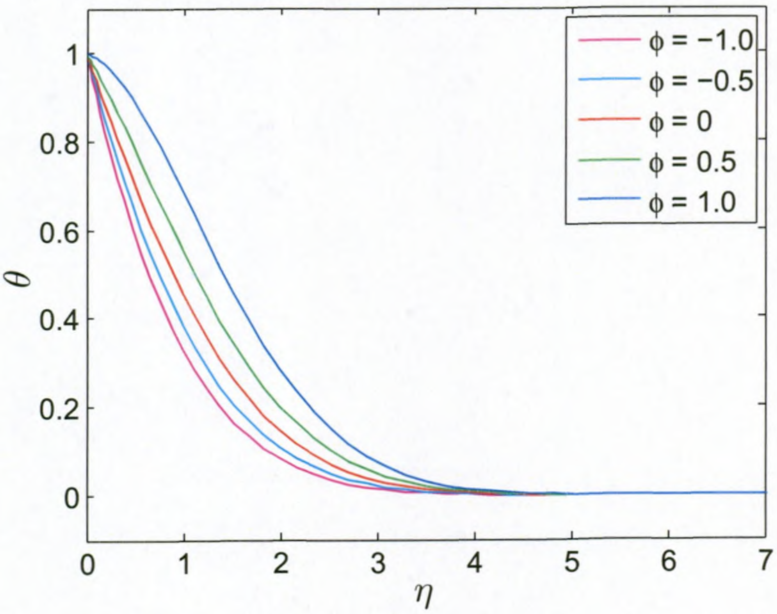

FIGURE 4.12: Effects of ϕ (heat generation or absorption) on the temperature profiles for $Ec = 0.0$, $f_0 = 0.0$, $m = 0.3333$, $N_{\mathrm{R}} = 0.0$, $\Pr = 0.733$, and $\xi = 1.0$.

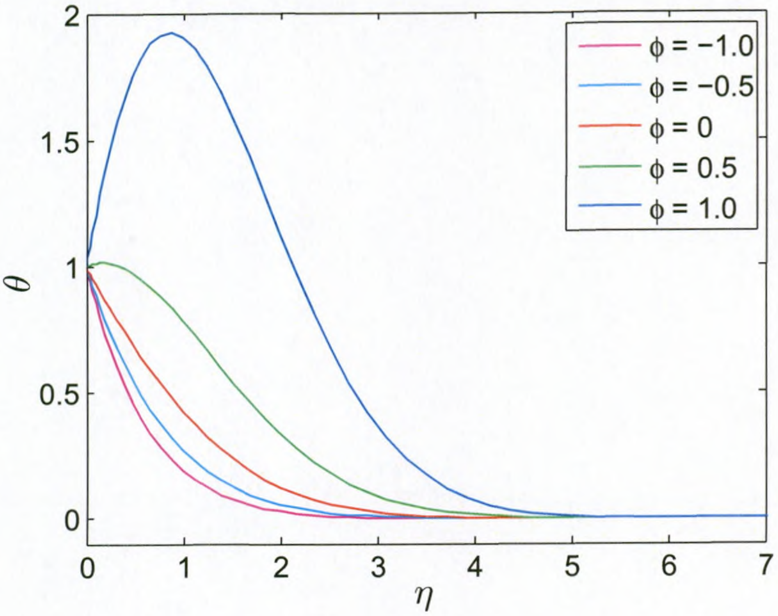

FIGURE 4.13: Effects of ϕ (heat generation or absorption) on the temperature profiles for $Ec = 0.0$, $f_0 = 0.0$, $m = 0.3333$, $N_{\mathrm{R}} = 0.0$, $\Pr = 0.733$, and $\xi = 3.0$.

Figures 4.12 and 4.13 illustrate the changes that are brought about in temperature profiles at $\xi = 1.0$ and $\xi = 3.0$. The presence of a heat source within the flow has a propensity to increase the thermal state of the fluid. This is depicted by an increase in the temperature profile at every point away from the wedge surface as ϕ increases.

On the contrary the presence of a heat sink ($\phi < 0$) in the flow reduces the temperature of the fluid away from the wall. The increase in heat generation or the absorption coefficient ϕ appears to have no effect on the thermal boundary layer for $\xi = 1.0$. However for $\xi = 3.0$ a peak is exhibited; the peak value is higher than that of the wall.

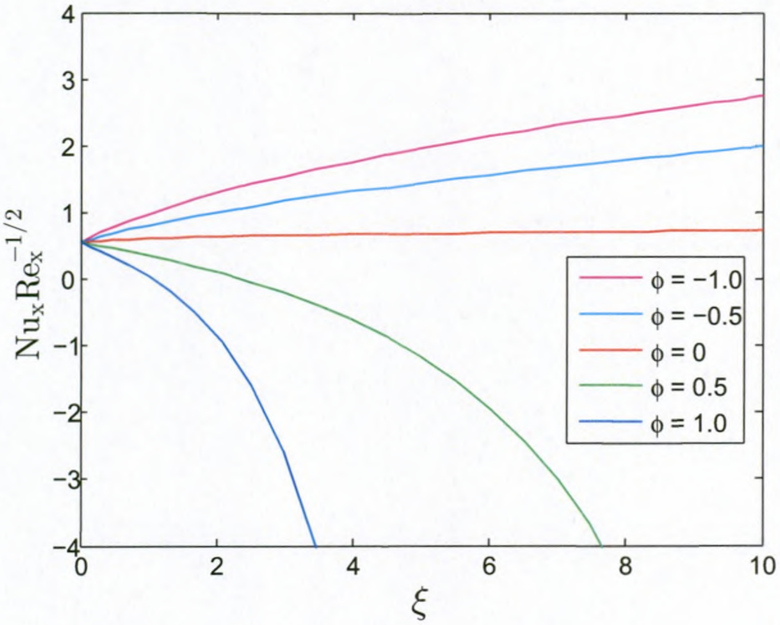

FIGURE 4.14: The results of the Nusselt number for several values of ϕ (heat generation or absorption), whilst $Ec = 0.0,\ f_0 = 0.0,\ m = 0.3333,\ N_{\mathrm{R}} = 0.0,\ \mathrm{Pr} = 0.733$, and $\eta = 16$.

It is observed that heat absorption causes the local Nusselt number to be enhanced where as the the heat generation diminishes $\mathrm{NU_x Re_x^{1/2}}$.

An increasing Eckert number has an incremental influence on the Nusselt number in the presence and in the absence of thermal radiation but more so when $N_{\mathrm{R}} = 0$; see Figures 4.15 and 4.16. This is contrary to what author Yih (1999) obtained.

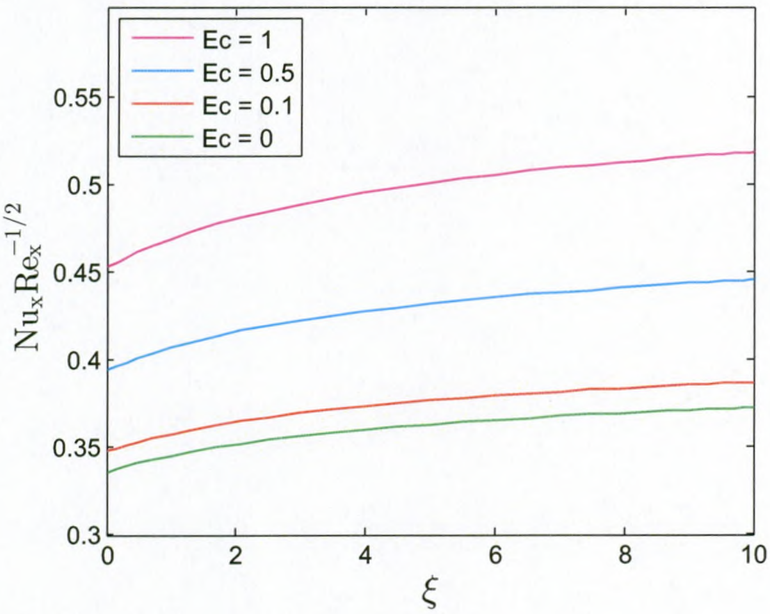

FIGURE 4.15: The impact of the Eckert number upon the Nusselt number, where $f_0 = 0.0$, $m = 1$, $N_{\mathrm{R}} = 10$, $\mathrm{Pr} = 0.733$, $\phi = 0.0$ and $\eta = 16$.

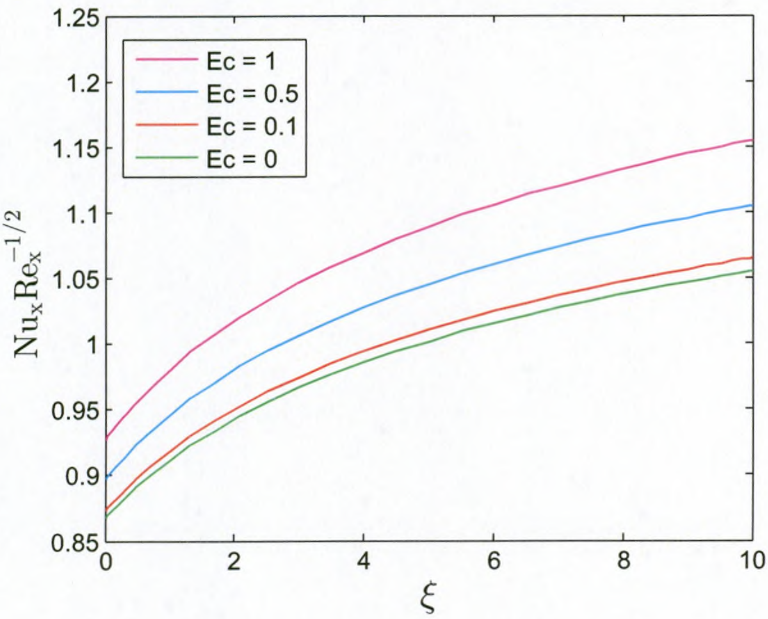

FIGURE 4.16: The effect of the Eckert number upon the Nusselt number, where $f_0 = 0.0$, $m = 1$, $N_{\mathrm{R}} = 0.0$, $\mathrm{Pr} = 0.733$, $\phi = 0.0$ and $\eta = 16$.

It is shown in Table 4.1 and 4.2 that the results of the BI-SQLM compare favourably with previous resolutions obtained. This further validates the credibility and accuracy of the numerical technique applied.

TABLE 4.1: Comparison of the values of $f''(\xi, 0)$ for $m = 1$, $f_0 = 0$.

ξ	Sparrow et al. (1962)	Ariel (1994)	Yih (1999)	Chamkha et al. (2003)	BI-SQLM (Present results)
0	1.231	1.232588	1.232588	1.232710	1.23258766
1	1.584	1.585331	1.585331	1.585480	1.57354438
4	2.345	2.346663	2.346663	2.341002	2.35821589
9	-	3.240950	3.240950	3.240992	3.24342037
25	-	5.147965	5.147964	5.148002	5.15565377
100	-	10.074741	10.074741	10.075001	10.07474113

TABLE 4.2: Comparison of the values of $-\theta(\xi, 0)$ for different values of Pr and Ec where $m = 0$, $f_0 = 0$, $N_{\mathrm{R}} = 0$ and $\phi = 0$.

		Watanabe and Pop (1994)		Yih (1999)		Chamkha et al. (2003)		BI-SQLM (Present results)	
Pr	ξ	$Ec = 0$	$Ec = 1$	$Ec = 0$	$Ec = 1$	$Ec = 0$	$Ec = 1$	$Ec = 0$	$Ec = 1$
0.733	0.0	0.29755	0.12395	0.297526	0.170272	0.297600	0.170184	0.297526	0.170272
	0.5	0.35699	0.20871	0.357022	0.210072	0.357040	0.209858	0.356980	0.210045
	1.0	0.38336	0.22857	0.382588	0.228813	0.383191	0.229000	0.382553	0.228786
	1.5	0.39959	0.24122	0.398264	0.240798	0.399980	0.241002	0.398239	0.240772
	2.0	0.41091	0.25022	0.409168	0.249316	0.409450	0.249307	0.409148	0.249298
1	0.0	0.33206	0.16603	0.332057	0.166027	0.332173	0.166302	0.332057	0.166029
	0.5	0.40280	0.20144	0.402864	0.201452	0.403103	0.201630	0.402816	0.201426
	1.0	0.43446	0.21727	0.433607	0.216814	0.433901	0.216721	0.433567	0.216787
	1.5	0.45413	0.22710	0.452634	0.226323	0.452808	0.226313	0.452604	0.226296
	2.0	0.46798	0.23401	0.465987	0.232988	0.466111	0.233102	0.465963	0.232981

4.3.1 Convergence and error analysis

The application of BI-SQLM upon equations (4.12)-(4.13) results in convergence with respect to η and ξ to be reached after five iterations for both f and θ. The elapsed time is 0.3353 seconds and the error is below 10^{-11}.

Convergence as well as residual error for the derivatives of f and θ are also shown, akin results are attained.

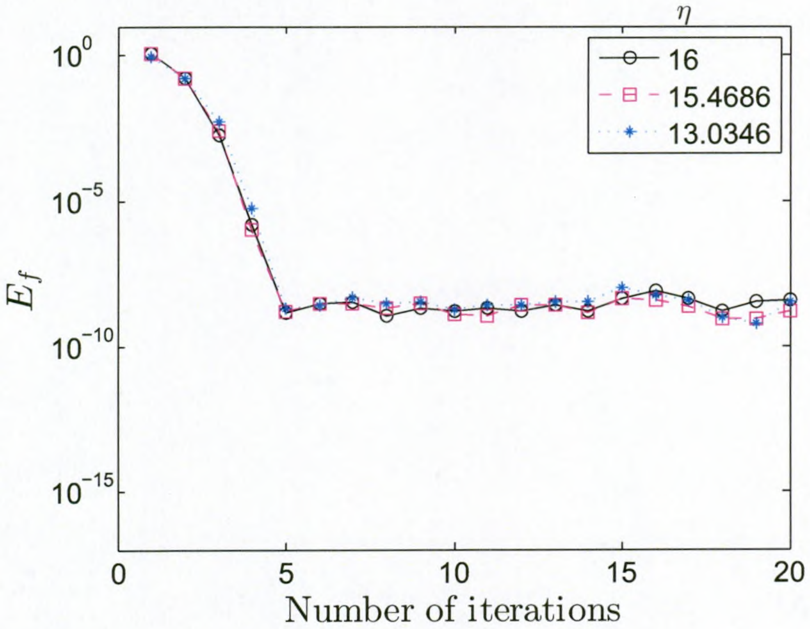

FIGURE 4.17: Convergence and residual error of f with respect to η.

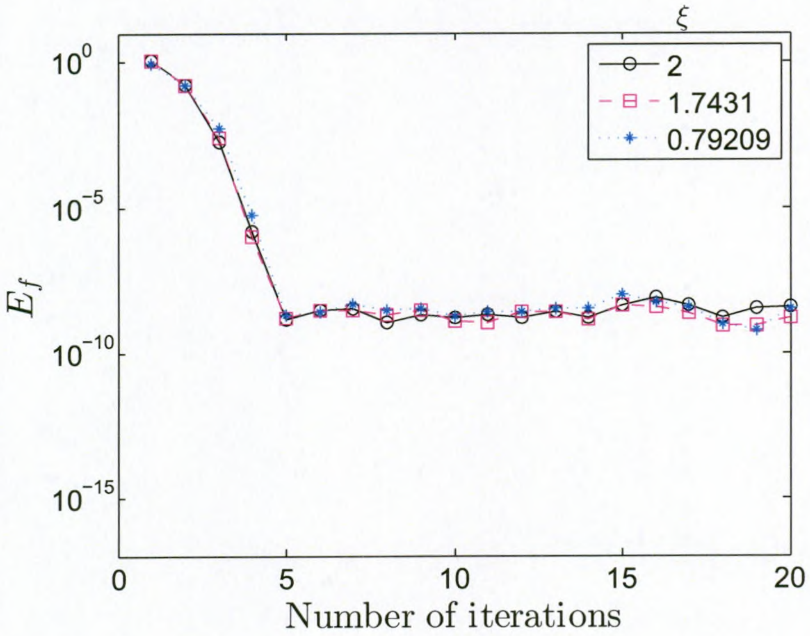

FIGURE 4.18: Convergence and residual error of f with regards to ξ.

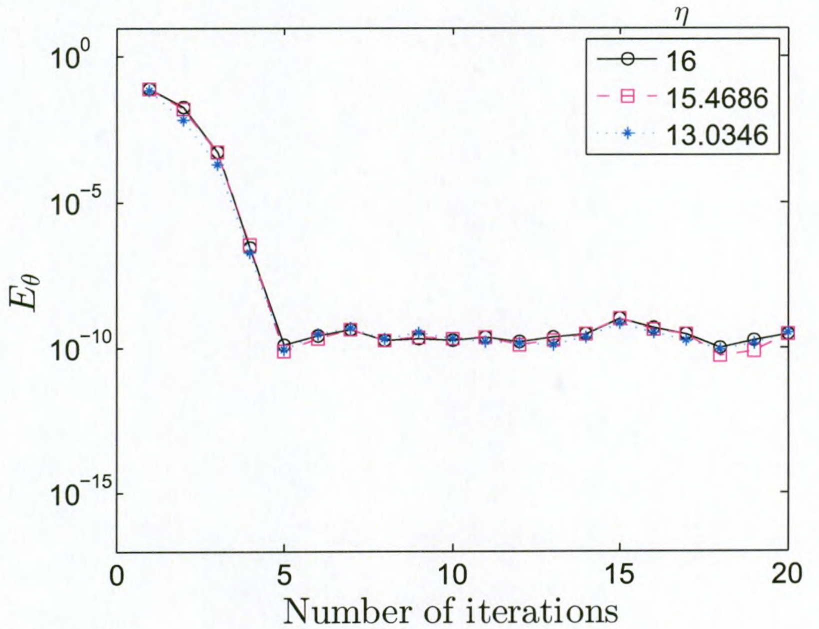

FIGURE 4.19: Convergence and residual error of θ with respect to η.

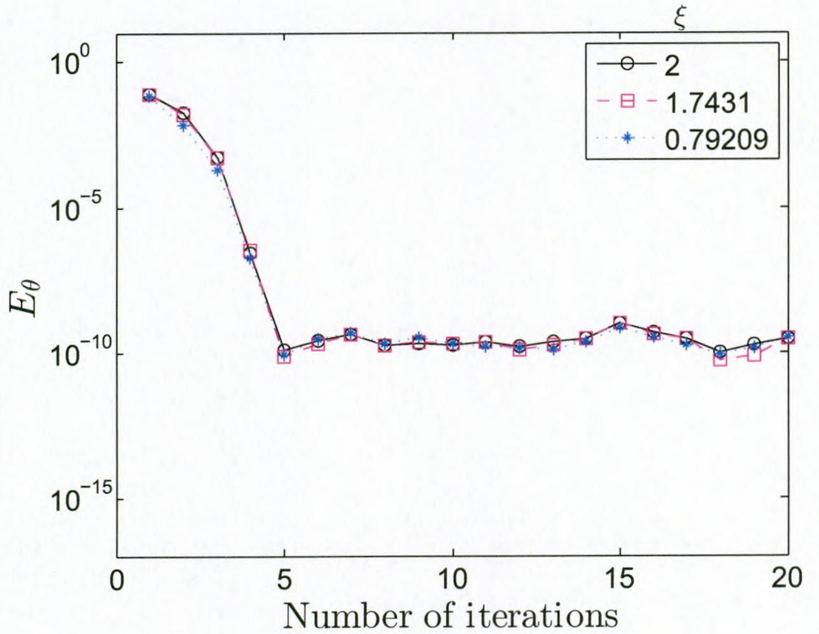

FIGURE 4.20: Convergence and residual error of θ with regards to ξ.

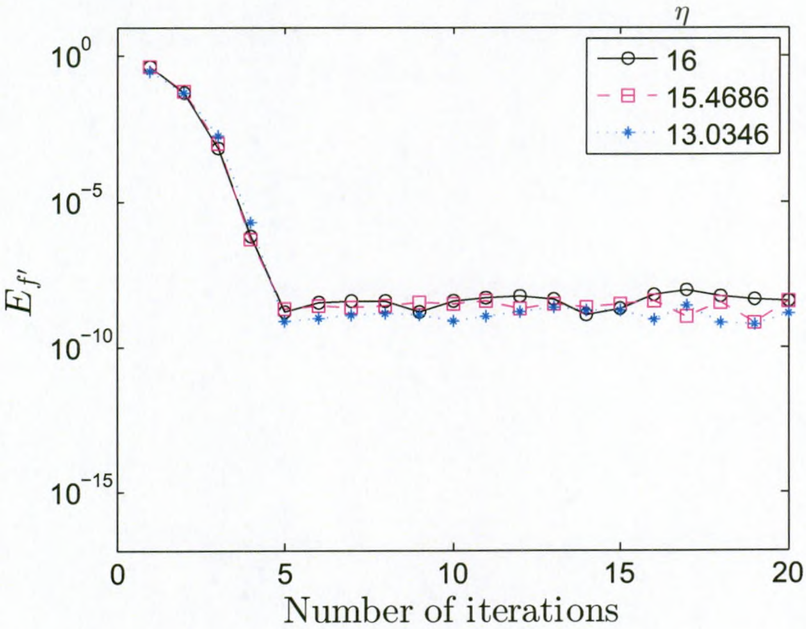

FIGURE 4.21: Convergence and residual error of f' with respect to η.

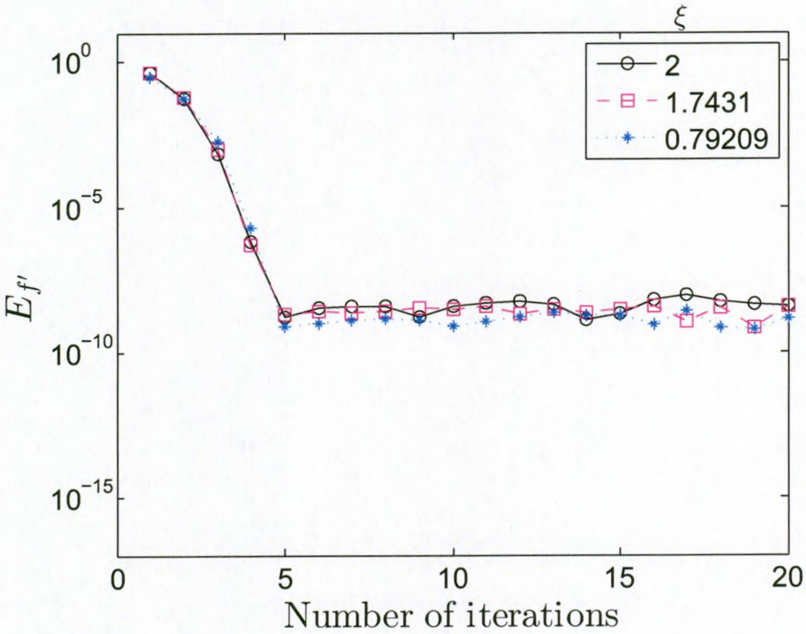

FIGURE 4.22: Convergence and residual error of f' apropos ξ.

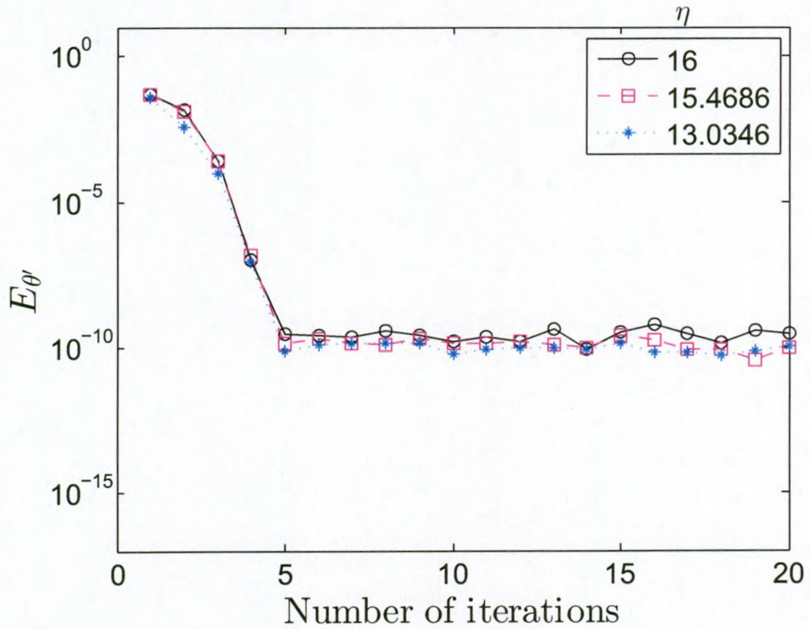

FIGURE 4.23: Convergence and residual error of θ' with respect to η.

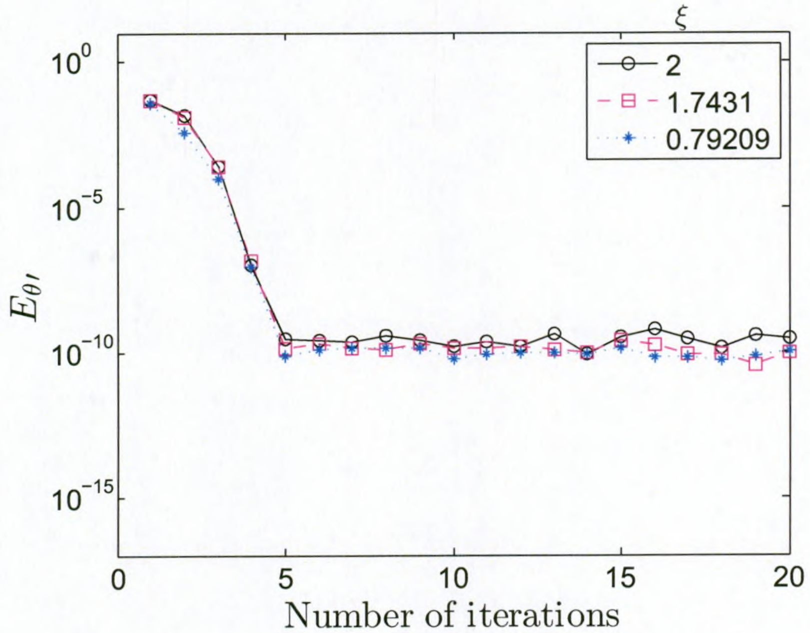

FIGURE 4.24: Convergence and residual error of θ' apropos ξ.

Chapter 5

Model III: Unsteady laminar MHD flow near a forward stagnation point of an impulsively rotating and translating sphere in the presence of buoyancy forces

The study of flow and heat transfer on rotating bodies has an importance in may engineering applications such as projectile motion, re-entry missile design of rotating machinery and fiber coating. Rajasekan and Palekar [63] used the shooting method to obtain solutions to a model describing a mixed convection flow about a rotating sphere. Then Hatzikostantinou [64] looked into the consequences of viscous dissipation on forced[25] and combined[26] convection of an unsteady incompressible flow about a rotating sphere; this was done through the utilization of finite difference approximations. Ece [65] analysed initial boundary layer flow past a translating and spinning rotational symmetric body and acquired first-order solutions analytically and second-order results numerically. HAM was applied to MHD flow near a rotational sphere with buoyancy forces by Dinarvand et al. [66]. In this work the BI-SQLM will be employed to this problem.

Unsteady laminar incompressible boundary layer flow close to the front stagnation point of a rotating sphere where magnetic fields and buoyancy forces are present. Before $t = 0$, the sphere is immobile and plunged in an ambient fluid with surface temperature T_∞

[25] Forced convection is when fluid is forced to flow over a surface or in a tube, induced by external factors such as a pump or fan.

[26] Combined convection is a combination of natural and forced convection, where natural convection is when a fluid moves by itself due to temperature.

which is tantamount to that of a rotating fluid. At time $t = 0$, an abrupt motion is transferred to the ambient fluid and the sphere is incontinently rotated with constant angular velocity Ω. A unvarying magnetic field B is applied in the z direction [66].

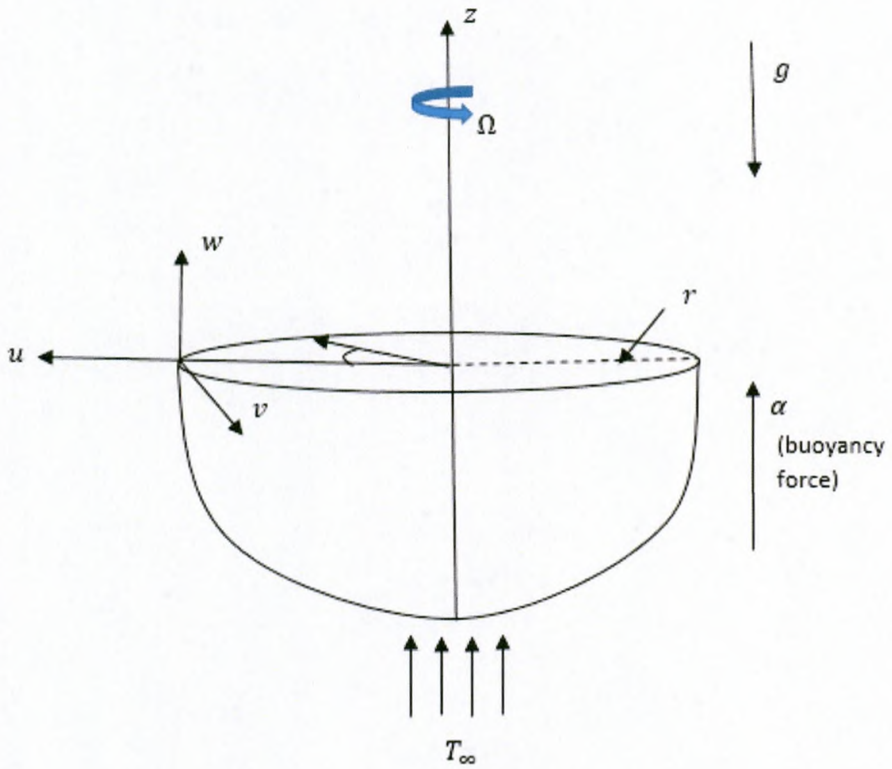

FIGURE 5.1: Visual representation of Model III

Assumptions

- The Reynolds number $R_m = \mu_0 \sigma V L \ll 1$, where μ_0 is the magnetic permeability, σ the electrical conductivity, V and L are the characteristic velocity and length respectively.

- The induced magnetic field is neglected.

- The wall and free stream temperature are taken as coefficients.

- The dissipation terms, Ohmic heating and surface curvature, are disregarded in the locality of the stagnation point.

- The fluid has constant thermophysical properties except for those that cause density changes that generate the buoyancy force, under the Boussinesq approximation.

- The effect of the buoyancy-induced stream-wise pressure gradient terms on the flow and temperature fields are inconsequential.

The boundary layer equations governing the axisymmetric flow are [65]

$$\frac{\partial(ux)}{\partial x} + \frac{\partial(wx)}{\partial z} = 0, \tag{5.1}$$

$$\frac{\partial u}{\partial t} + u\frac{\partial u}{\partial x} + w\frac{\partial u}{\partial z} - \frac{v^2}{x} = u_e\frac{du_e}{dx} + v\frac{\partial^2 u}{\partial z^2} + \bar{g}\beta\left(T - T_\infty\right)\frac{x}{R} - \frac{\sigma B^2}{\rho}\left(u - u_e\right), \tag{5.2}$$

$$\frac{\partial v}{\partial t} + u\frac{\partial v}{\partial x} + w\frac{\partial v}{\partial z} + \frac{uv}{x} = v\frac{\partial^2 w}{\partial z^2} - \frac{\sigma B^2}{\rho}v, \tag{5.3}$$

$$\frac{\partial T}{\partial t} + u\frac{\partial T}{\partial x} + w\frac{\partial T}{\partial z} = \frac{k}{\rho c_p}\frac{\partial^2 T}{\partial z^2}, \tag{5.4}$$

where x is the distance along the meridian from the forward stagnation point, y represents the distance in the direction of rotation, z is the distance normal to the surface; u, v and w are the velocity components along x, y and z directions accordingly. B is the magnetic field, Ω denotes the angular velocity of the sphere, with β being the coefficient of thermal expansion. R is defined to be the raduis of the sphere, $\bar{g}$ is referred to as the acceleration due to gravity, k is the thermal conductivity and the subscripts e, w and ∞ represent conditions of the edge of the boundary layer on a free stream respectively. The initial conditions are

$$u(x, z, t) = v(x, z, t) = w(x, z, t) = 0, \tag{5.5}$$

$$T(x, z, t) = T_\infty, \quad \text{for} \quad t < 0 \tag{5.6}$$

and the corresponding boundary conditions are as follows

$$u(x, 0, t) = 0, \quad v(x, 0, t) = \Omega x, \quad T(x, 0, t) = T_w, \tag{5.7}$$

$$u(x, \infty, t) = u_e(x), \quad v(x, \infty, t) = 0, \quad T(x, \infty, t) = T_\infty. \tag{5.8}$$

The transformations [56]

$$u(x, z, t) = ax\frac{\partial f(\eta, \xi)}{\partial \eta}, \quad v(x, z, t) = \Omega x g(\eta, \xi) \quad \text{and} \quad w(x, z, t) = -(2av)^{\frac{1}{2}}\xi^{\frac{1}{2}}f(\eta, \xi) \tag{5.9}$$

transform equations (5.1)-(5.4) into a system of non-linear partial differential equations [66]

$$\frac{\partial^3 f}{\partial \eta^3} + \frac{1}{4}\eta(1-\xi)\frac{\partial^2 f}{\partial \eta^2} + \xi f\frac{\partial^2 f}{\partial \eta^2} + \frac{1}{2}\xi\left(1 - \left(\frac{\partial f}{\partial \eta}\right)^2 + \lambda g^2\right) + \frac{1}{2}M\xi\left(1 - \frac{\partial f}{\partial \eta}\right)$$
$$+ \frac{1}{2}\alpha\xi\theta - \frac{1}{2}\xi(1-\xi)\frac{\partial^2 f}{\partial \xi \partial \eta} = 0, \tag{5.10}$$
$$\frac{\partial^2 g}{\partial \eta^2} + \frac{1}{4}\eta(1-\xi)\frac{\partial g}{\partial \eta} + \xi\left(f\frac{\partial g}{\partial \eta} - g\frac{\partial f}{\partial \eta}\right) - \frac{1}{2}M\xi g - \frac{1}{2}\xi(1-\xi)\frac{\partial g}{\partial \xi} = 0, \tag{5.11}$$
$$\frac{\partial^2 \theta}{\partial \eta^2} + \frac{1}{4}Pr\eta(1-\xi)\frac{\partial \theta}{\partial \eta} + Pr\xi f\frac{\partial \theta}{\partial \eta} - \frac{1}{2}Pr\xi(1-\xi)\frac{\partial \theta}{\partial \xi} = 0, \tag{5.12}$$

subject to the following boundary conditions

$$f(0,\xi) = 0, \quad \left.\frac{\partial f(\eta,\xi)}{\partial \eta}\right|_{\eta=0} = 0, \quad \left.\frac{\partial f(\eta,\xi)}{\partial \eta}\right|_{\eta=\infty} = 1, \tag{5.13}$$
$$g(0,\xi) = 1, \quad g(\infty,\xi) = 0, \tag{5.14}$$
$$\theta(0,\xi) = 1, \quad \theta(\infty,\xi) = 0. \tag{5.15}$$

Here η is the transformed variable, ξ represents dimensionless time, $\partial f/\partial \eta$ and g are the dimensionless velocity components along the x and y directions respectively, θ denotes the dimensionless temperature, a is the velocity gradient at the edge of the boundary layer, whilst Pr is the Prandtl number and Gr_{R} and Re_{R} are the Grashof and Reynolds number in that given order. Lastly α represents the buoyancy parameter.

5.1 Deriving the initial solutions

Starting with equation (5.10), let $\xi = 0$ then

$$f''' + \frac{1}{4}\eta f'' = 0, \tag{5.16}$$

which may be rearranged to obtain

$$\frac{f'''}{f''} = -\frac{\eta}{4}. \tag{5.17}$$

Integrating both sides of (5.17) twice we find that

$$f' = \mathrm{A}_2\frac{\sqrt{\pi}}{2}\mathrm{erf}\left(\frac{\eta}{\sqrt{8}}\right) + \mathrm{B}_2, \tag{5.18}$$

with A_2 and B_2 being arbitrary constants, erf is the error function denoted as

$$\mathrm{erf}\,(\eta) = \frac{2}{\sqrt{\pi}} \int_0^{\eta} \exp\left(-z^2\right)\, dz.$$

Imposing the boundary condtions to obtain the value of the constants defined in equation (5.18), we find

- $f(0,0) = 0$ implies that

  $B_2 = 0$,

- $f'(\infty, 0) = 1$ implies that

  $A_2 = \frac{2}{\sqrt{\pi}}$.

Equation (5.19) is then reduced to

$$f'(\eta) = \mathrm{erf}\left(\frac{\eta}{\sqrt{8}}\right), \tag{5.19}$$

which upon integration yields

$$f(\eta) = \eta \mathrm{erf}\left(\frac{\eta}{2\sqrt{2}}\right) + 2\exp\left(-\frac{\eta^2}{8}\right)\sqrt{\frac{2}{\pi}} + C_2, \tag{5.20}$$

with C_2 being an arbitrary constant. Imposing the boundary condition $f(0,0) = 0$ we find that

$$C_2 = -2\sqrt{\frac{2}{\pi}}.$$

Thus the initial guess for f is

$$f(\eta) = \eta \mathrm{erf}\left(\frac{\eta}{2\sqrt{2}}\right) + 2\exp\left(-\frac{\eta^2}{8}\right)\sqrt{\frac{2}{\pi}} - 2\sqrt{\frac{2}{\pi}}. \tag{5.21}$$

Similarly for equation (5.11) we let $\xi = 0$ to obtain

$$g'' + \frac{\eta}{4} g' = 0, \tag{5.22}$$

an ordinary differential equation which by integrating both sides twice gives

$$g(\eta) = A_3 \frac{\sqrt{\pi}}{2} \mathrm{erf}\left(\frac{\eta}{\sqrt{8}}\right) + B_3, \tag{5.23}$$

with A_3 and B_3 being arbitrary constants. Applying the boundary conditions on (5.14) the values of the constants are obtained as before to be: $A_3 = -2/\sqrt{\pi}$ and $B_3 = 1$.

The initial solution for g is

$$g(\eta) = \text{erfc}\left(\frac{\eta}{\sqrt{8}}\right). \tag{5.24}$$

Finding the initial resolution for θ, $\xi = 0$ is imposed upon equation (5.12) which gives

$$\theta'' + \frac{Pr\eta}{4}\theta' = 0. \tag{5.25}$$

Integrating both sides of (5.25) twice, the result is a general solution similar to that of equation (5.23)

$$\theta(\eta) = \mathrm{A}_4\frac{\sqrt{\pi}}{2}\text{erf}\left(\frac{\eta\sqrt{Pr}}{\sqrt{8}}\right) + B_4, \tag{5.26}$$

with A_4 and B_4 as arbitrary constants. Once again, via our boundary conditions we are able to get the values of A_4 and B_4 which provides the initial guess as

$$\theta(\eta) = \text{erfc}\left(\frac{Pr\eta}{\sqrt{8}}\right). \tag{5.27}$$

5.2 Application of the BI-SQLM to the three equation coupled system of partial differential equations

Beginning with equation (5.10), which is equated to a non-linear operator FF,

$$\begin{aligned} &f''' + \frac{1}{4}\eta(1-\xi)f'' + \xi f f'' + \frac{1}{2}\xi\left(1 - (f')^2 + \lambda g^2\right) + \frac{1}{2}M\xi(1-f') \\ &+ \frac{1}{2}\alpha\xi\theta - \frac{1}{2}\xi(1-\xi)\frac{\partial f'}{\partial \xi} = FF, \end{aligned} \tag{5.28}$$

where $FF = FF[\eta, f(\eta), f'(\eta), f''(\eta), f'''(\eta)]$. The linearised equation becomes

$$\begin{aligned} &a_{0,r}(\eta,\xi)f'''_{r+1} + a_{1,r}(\eta,\xi)f''_{r+1} + a_{2,r}(\eta,\xi)f''_{r+1} + a_{3,r}(\eta,\xi)f_{r+1} + a_{4,r}(\eta,\xi)\frac{\partial f'_{r+1}}{\partial \xi} \\ &+ a_{5,r}(\eta,\xi)g_{r+1} + a_{6,r}(\eta,\xi)\theta_{r+1} = R_f = R_1 \end{aligned} \tag{5.29}$$

where

$$\begin{aligned}
a_{0,r}(\eta,\xi)[f_r,f_r',f_r'',f_r'''] &= \frac{\partial FF}{\partial f'''} = 1,\\
a_{1,r}(\eta,\xi)[f_r,f_r',f_r'',f_r'''] &= \frac{\partial FF}{\partial f''} = \frac{\eta}{4}(1-\xi)+\xi f_r,\\
a_{2,r}(\eta,\xi)[f_r,f_r',f_r'',f_r'''] &= \frac{\partial FF}{\partial f'} = -\xi f_r - \frac{1}{2}M\xi,\\
a_{3,r}(\eta,\xi)[f_r,f_r',f_r'',f_r'''] &= \frac{\partial FF}{\partial f} = \xi f_r,\\
a_{4,r}(\eta,\xi)[f_r,f_r',f_r'',f_r'''] &= \frac{\partial FF}{\partial\left(\frac{\partial f'}{\partial \xi}\right)} = -\frac{1}{2}\xi(1-\xi),\\
a_{5,r}(\eta,\xi)[f_r,f_r',f_r'',f_r'''] &= \frac{\partial FF}{\partial g} = \xi\lambda g_r,\\
a_{6,r}(\eta,\xi)[f_r,f_r',f_r'',f_r'''] &= \frac{\partial FF}{\partial g} = \frac{1}{2}\alpha\xi,
\end{aligned}$$

and

$$\begin{aligned}
R_f &= a_{0,r}(\eta,\xi)f_r''' + a_{1,r}(\eta,\xi)f_r'' + a_{2,r}(\eta,\xi)f_r'' + a_{3,r}(\eta,\xi)f_r + a_{4,r}(\eta,\xi)\frac{\partial f_r'}{\partial \xi}\\
&+ a_{5,r}(\eta,\xi)g_r + a_{6,r}(\eta,\xi)\theta_r - FF\\
&= f_r''' + \left(\frac{\eta}{4}(1-\xi)+\xi f_r\right)f_r'' + \left(-\xi f_r - \frac{1}{2}M\xi\right)f_r' + \xi f_r'' f_r - \frac{1}{2}\xi(1-\xi)\frac{\partial f_r'}{\partial \xi}\\
&+ \xi\lambda g_r^2 + \frac{1}{2}\alpha\xi\theta_r - f_r''' - \frac{\eta}{4}(1-\xi)f_r'' - \xi f_r f_r'' - \frac{1}{2}\xi\left(1-(f_r')^2+\lambda g_r^2\right)\\
&- \frac{1}{2}M\xi(1-f_r') - \frac{1}{2}\alpha\xi\theta_r + \frac{1}{2}\xi(1-\xi)\frac{\partial f_r'}{\partial \xi}\\
&= -\frac{1}{2}\xi(f_r')^2 + \xi f_r'' f_r - \frac{1}{2}\xi(1+M). \qquad (5.30)
\end{aligned}$$

Similarly for equation (5.11) a non-linear operator GG represents,

$$g'' + \frac{1}{4}\eta(1-\xi)g + \xi(fg - gf') - \frac{1}{2}M\xi g - \frac{1}{2}\xi(1-\xi)\frac{\partial g}{\partial \xi} = GG, \qquad (5.31)$$

where $GG = GG[\eta, g(\eta), g'(\eta), g''(\eta)]$. The linear form of GG is,

$$\begin{aligned}
&b_{0,r}(\eta,\xi)g_{r+1}'' + b_{1,r}(\eta,\xi)g_{r+1}' + b_{2,r}(\eta,\xi)g_{r+1} + b_{3,r}(\eta,\xi)\frac{\partial g_{r+1}}{\partial \xi} + b_{4,r}(\eta,\xi)f_{r+1}\\
&+ b_{5,r}(\eta,\xi)f_{r+1}' = R_g = R_2 \qquad (5.32)
\end{aligned}$$

and the coefficients are defined as

$$
\begin{aligned}
b_{0,r}(\eta,\xi)[g_r,g_r',g_r''] &= \frac{\partial GG}{\partial g''} = 1,\\
g_{1,r}(\eta,\xi)[g_r,g_r',g_r''] &= \frac{\partial GG}{\partial g'} = \frac{\eta}{4}(1-\xi)+\xi f_r,\\
b_{2,r}(\eta,\xi)[g_r,g_r',g_r''] &= \frac{\partial GG}{\partial g} = -\xi f_r' - \frac{1}{2}M\xi,\\
b_{3,r}(\eta,\xi)[g_r,g_r',g_r''] &= \frac{\partial GG}{\partial\left(\frac{\partial g}{\partial \xi}\right)} = -\frac{1}{2}\xi(1-\xi),\\
b_{4,r}(\eta,\xi)[g_r,g_r',g_r''] &= \frac{\partial GG}{\partial f} = \xi g_r',\\
b_{5,r}(\eta,\xi)[g_r,g_r',g_r''] &= \frac{\partial GG}{\partial f'} = -\xi g_r,
\end{aligned}
$$

with

$$
\begin{aligned}
R_g = {} & b_{0,r}(\eta,\xi)g_r'' + b_{1,r}(\eta,\xi)g_r' + b_{2,r}(\eta,\xi)g_r + b_{3,r}(\eta,\xi)\frac{\partial g_r}{\partial \xi} + b_{4,r}(\eta,\xi)f_r\\
& + b_{5,r}(\eta,\xi)f_r' - GG
\end{aligned}
$$

$$
\begin{aligned}
&= g_r'' + \left(\frac{1}{2}\eta(1-\xi)+\xi f_r\right)g_r' + \left(-\xi f_r' - \frac{1}{2}M\xi\right)g_r - \frac{1}{2}\xi(1-\xi)\frac{\partial g_r}{\partial \xi}\\
&+ \xi g_r' f_r - \xi g_r f_r - g_r'' - \frac{1}{2}\eta(1-\xi)g_r' - \xi\left(f_r g_r' - g_r f_r'\right) + \frac{1}{2}M\xi g_r + \frac{1}{2}\xi(1-\xi)\frac{\partial g}{\partial \xi}\\
&= \xi\left(g_r f_r' + f_r g_r'\right).
\end{aligned}
\tag{5.33}
$$

Equation (5.12) is also equated to a non-linear operator $\Theta\Theta$,

$$
\theta'' + \frac{1}{4}Pr\eta(1-\xi)\theta' + Pr\xi f\theta' - \frac{1}{2}Pr\xi(1-\xi)\frac{\partial\theta}{\partial\xi} = \Theta\Theta, \tag{5.34}
$$

where $\Theta\Theta = \Theta\Theta[\eta,\theta(\eta),\theta'(\eta),\theta''(\eta)]$. The linearised equation of (5.34) is

$$
c_{0,r}(\eta,\xi)\theta_{r+1}'' + c_{1,r}(\eta,\xi)\theta_{r+1}' + c_{2,r}(\eta,\xi)\theta_{r+1} + c_{3,r}(\eta,\xi)\frac{\partial\theta_{r+1}}{\partial\xi} + c_{4,r}(\eta,\xi)f_{r+1} = R_\theta = R_3, \tag{5.35}
$$

where

$$
\begin{aligned}
c_{0,r}(\eta,\xi)[\theta_r,\theta_r',\theta_r''] &= \frac{\partial \Theta\Theta}{\partial \theta''} = 1,\\
c_{1,r}(\eta,\xi)[\theta_r,\theta_r',\theta_r''] &= \frac{\partial \Theta\Theta}{\partial \theta'} = \frac{\eta}{4} Pr\,(1-\xi) + \xi Pr f_r,\\
c_{2,r}(\eta,\xi)[\theta_r,\theta_r',\theta_r''] &= \frac{\partial \Theta\Theta}{\partial \theta} = 0,\\
c_{3,r}(\eta,\xi)[\theta_r,\theta_r',\theta_r''] &= \frac{\partial \Theta\Theta}{\partial \left(\frac{\partial \theta}{\partial \xi}\right)} = -\frac{1}{2} Pr\xi\,(1-\xi)\,,\\
c_{4,r}(\eta,\xi)[\theta_r,\theta_r',\theta_r''] &= \frac{\partial GG}{\partial f} = \xi Pr\theta_r',
\end{aligned}
$$

and

$$
\begin{aligned}
R_\theta &= c_{0,r}(\eta,\xi)\theta_r'' + c_{1,r}(\eta,\xi)\theta_r' + c_{2,r}(\eta,\xi)\theta_r + c_{3,r}(\eta,\xi)\frac{\partial \theta_r}{\partial \xi} + c_{4,r}(\eta,\xi)f_r - \Theta\Theta\\
&= \theta_r'' + \frac{1}{4}Pr\eta\,(1-\xi)\,\theta_r' + Pr\xi f_r\theta_r' - \frac{1}{2}Pr\xi\,(1-\xi)\,\frac{\partial \theta_r}{\partial \xi} + Pr\xi\theta_r' f_r\\
&- \theta_r'' - \frac{1}{4}Pr\eta\,(1-\xi)\,\theta_r' - Pr\xi f_r\theta_r' + \frac{1}{2}Pr\eta\,(1-\xi)\,\frac{\partial \theta_r}{\partial \xi}\\
&= Pr\xi\theta_r' f_r.
\end{aligned}
\tag{5.36}
$$

We now set up equations (5.10)-(5.12) in the form of matrices.

Matrices for equation (5.10) are

$$
\begin{aligned}
\mathbf{A}_{11}^{(i)} &= \mathbf{a}_{0,r}\mathbf{D}^3 + \mathbf{a}_{1,r}\mathbf{D}^2 + \mathbf{a}_{2,r}\mathbf{D} + \mathbf{a}_{3,r}\mathbf{I},\\
\mathbf{A}_{12}^{(i)} &= \mathbf{a}_{5,r}\mathbf{I},\\
\mathbf{A}_{13}^{(i)} &= \mathbf{a}_{6,r}\mathbf{I},
\end{aligned}
$$

therefore

$$
\mathbf{A}_{11}^{(i)}F_i + \mathbf{a}_{4,r}\sum_{j=0}^{N_\xi} d_{i,j}\mathbf{D}F_j + \mathbf{A}_{12}^{(i)}G_i + A_{13}^{(i)}\Theta_i = \mathbf{R}_{1,i}, \tag{5.37}
$$

where $i = 0, 1, ..., N_\xi - 1$.

In matrix notation equation (5.11) is represented as

$$
\begin{aligned}
\mathbf{A}_{21}^{(i)} &= \mathbf{b}_{5,r}\mathbf{D} + \mathbf{b}_{4,r}\mathbf{I},\\
\mathbf{A}_{22}^{(i)} &= \mathbf{b}_{0,r}\mathbf{D}^2 + \mathbf{b}_{1,r}\mathbf{D} + \mathbf{b}_{2,r}\mathbf{I},\\
\mathbf{A}_{23}^{(i)} &= 0.\mathbf{I},
\end{aligned}
$$

thus

$$\mathbf{A}_{21}^{(i)}F_i + \mathbf{A}_{22}^{(i)}G_i + \mathbf{b}_{3,r}\sum_{j=0}^{N_\xi} d_{i,j}G_j = \mathbf{R}_{2,i}, \qquad i = 0, 1, ..., N_\xi - 1. \tag{5.38}$$

Lastly for equation (5.12) we obtain

$$\begin{aligned}
\mathbf{A}_{31}^{(i)} &= \mathbf{c}_{4,r}\mathbf{I}, \\
\mathbf{A}_{32}^{(i)} &= 0.\mathbf{I}, \\
\mathbf{A}_{33}^{(i)} &= \mathbf{c}_{0,r}\mathbf{D}^2 + \mathbf{c}_{1,r}\mathbf{D} + \mathbf{c}_{2,r}\mathbf{I},
\end{aligned}$$

hence

$$\mathbf{A}_{31}^{(i)}F_i + \mathbf{A}_{33}^{(i)}\Theta_i + \mathbf{c}_{3,r}\sum_{j=0}^{N_\xi} d_{i,j}\Theta_j = \mathbf{R}_{2,i}, \qquad i = 0, 1, ..., N_\xi - 1. \tag{5.39}$$

The $\mathbf{B}_{i,i}$ matrices are incorporated as they depict the time direction,

$$\begin{aligned}
\mathbf{B}_{11}^{(ii)} &= \mathbf{A}_{11}^{(i)} + \mathbf{a}_{4,r}d_{i,i}\mathbf{D}, \\
\mathbf{B}_{12}^{(ii)} &= \mathbf{A}_{12}^{(i)}, \\
\mathbf{B}_{13}^{(ii)} &= \mathbf{A}_{13}^{(i)}, \\
\mathbf{B}_{21}^{(ii)} &= \mathbf{A}_{21}^{(i)}, \\
\mathbf{B}_{22}^{(ii)} &= \mathbf{A}_{22}^{(i)} + \mathbf{b}_{3,r}d_{i,i}\mathbf{I}, \\
\mathbf{B}_{23}^{(ii)} &= \mathbf{A}_{23}^{(i)}, \\
\mathbf{B}_{31}^{(ii)} &= \mathbf{A}_{31}^{(i)}, \\
\mathbf{B}_{32}^{(ii)} &= \mathbf{A}_{32}^{(i)}, \\
\mathbf{B}_{33}^{(ii)} &= \mathbf{A}_{33}^{(i)} + \mathbf{c}_{3,r}d_{i,i}\mathbf{I}.
\end{aligned}$$

where $i = 0, 1, ..., N_\xi - 1$.

The off-diagonal elements of $\mathbf{B}$ are as follows

$$\begin{aligned}
\mathbf{B}_{11}^{(ij)} &= \mathbf{a}_{4,r}d_{i,i}\mathbf{D}, \\
\mathbf{B}_{12}^{(ij)} &= 0.\mathbf{I}, \\
\mathbf{B}_{13}^{(ij)} &= 0.\mathbf{I}, \\
\mathbf{B}_{21}^{(ij)} &= 0.\mathbf{I},
\end{aligned}$$

$$\mathbf{B}_{22}^{(ij)} = \mathbf{b}_{3,r} d_{i,i}\mathbf{I},$$
$$\mathbf{B}_{23}^{(ii)} = 0.\mathbf{I},$$
$$\mathbf{B}_{31}^{(ii)} = 0.\mathbf{I},$$
$$\mathbf{B}_{32}^{(ii)} = 0.\mathbf{I},$$
$$\mathbf{B}_{33}^{(ii)} = \mathbf{c}_{3,r} d_{i,i}\mathbf{I}.$$

where $i = 0, 1, ..., N_\xi - 1$. The matrix representation of the above is given as

$$\begin{pmatrix} \mathbf{B}_{11} & \mathbf{B}_{12} & \mathbf{B}_{13} \\ \mathbf{B}_{21} & \mathbf{B}_{22} & \mathbf{B}_{23} \\ \mathbf{B}_{31} & \mathbf{B}_{32} & \mathbf{B}_{33} \end{pmatrix} \begin{pmatrix} F_0 \\ G_0 \\ \Theta_0 \end{pmatrix} = \begin{pmatrix} \mathbf{R}_{1,0} \\ \mathbf{R}_{2,0} \\ \mathbf{R}_{3,0} \end{pmatrix}, \tag{5.40}$$

where the boundary conditions for f, g and θ are represented as follows

$$\sum_{k=0}^{N} D_{0,k} f_k = 1, \quad f_{r+1}(\eta_N) = 0, \quad \sum_{k=0}^{N} D_{N,k} f_k = 0, \tag{5.41}$$

$$g_{r+1}(\eta_0) = 0, \quad g_{r+1}(\eta_N) = 1, \tag{5.42}$$

$$\theta_{r+1}(\eta_0) = 0, \quad \text{and} \quad \theta_{r+1}(\eta_N) = 1. \tag{5.43}$$

In solving (5.40) solutions for f, g and θ are obtained.

5.3 Results and analysis

Similarly to model I and II the results are shown using diagrams for various parameters. The initial solutions calculated in section 5.1 are employed when computing solutions presented in this section. We did test the initial guesses that Dinarvand et al. [66] used and the resolutions were connate to the results displayed below; however the elapsed time for convergence is 4.01345 seconds which is slower compared to the 3.96527 seconds we obtained when we harness the initial solutions in section 6.1.

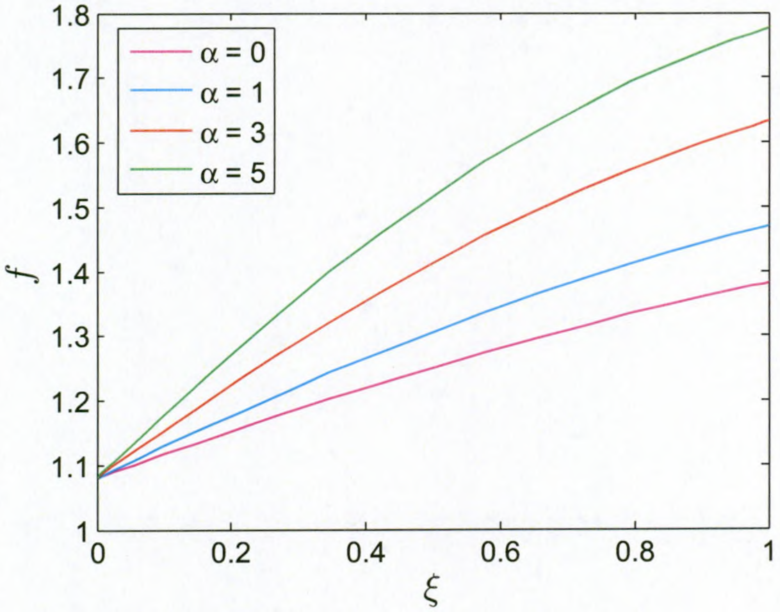

FIGURE 5.2: The influence of α (buoyancy parameter) on f plotted against ξ where $\alpha = 1$, $\mathrm{Pr} = 0.7$ and $\lambda = 1$.

In Figure 5.2 the effect of an increase in the buoyancy parameter increases f, which means that there is a strong presence of the pressure gradient which accelerates the fluid.

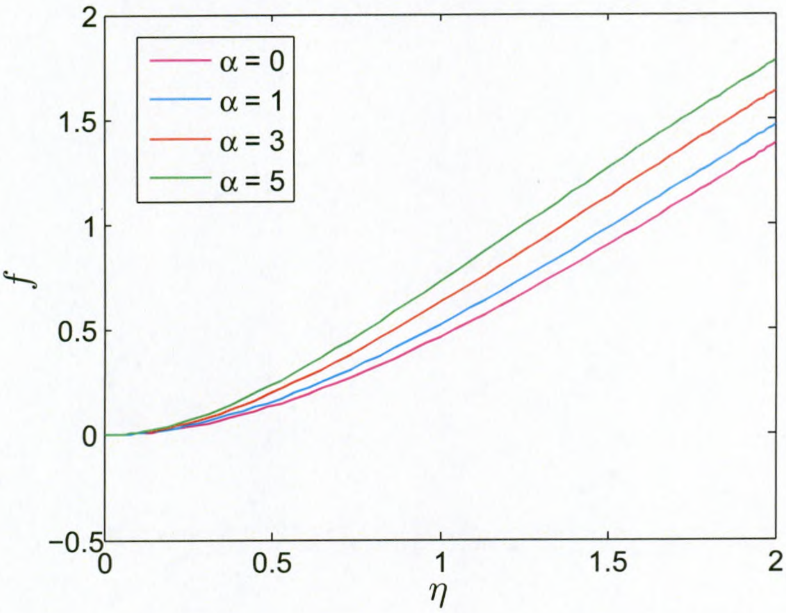

FIGURE 5.3: The impact of α on f plotted against η where $M = 1$, $\mathrm{Pr} = 0.7$ and $\lambda = 1$.

A similar effect is exhibited in Figure 5.2 when f is plotted against η.

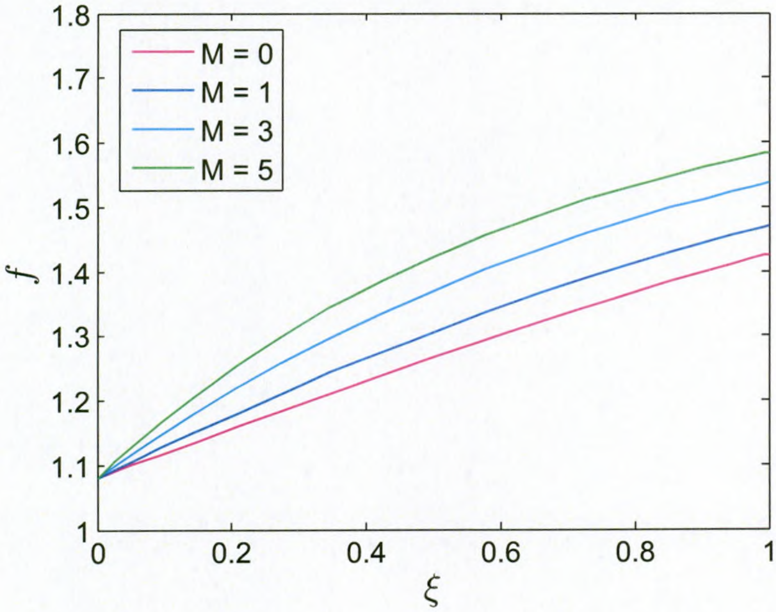

FIGURE 5.4: The effect of M on f plotted against ξ where $\alpha = 1$, $\Pr = 0.7$ and $\lambda = 1$.

In Figure 5.4 variations of M (magnetic parameter) show that f increases as the magnetic parameter increases. Also when we plot f against η for several values of M it increases.

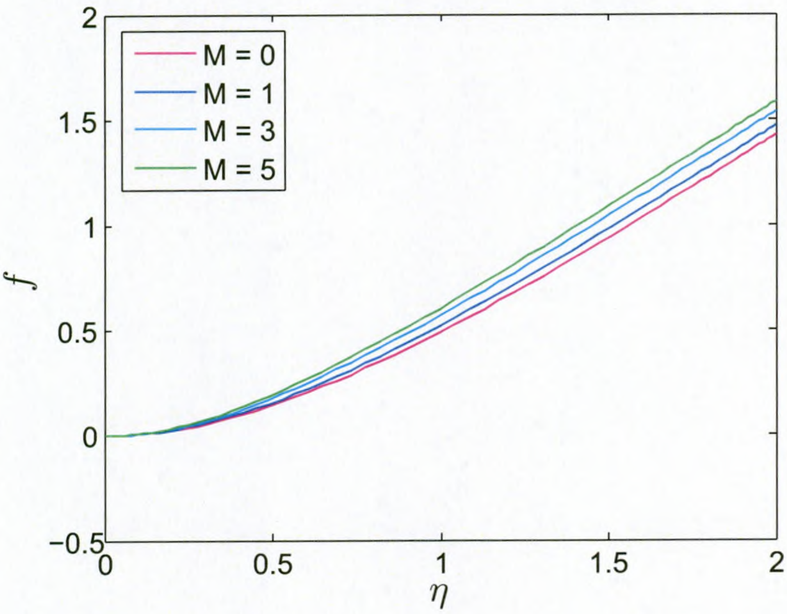

FIGURE 5.5: The effect of M (magnetic parameter) on f plotted against η where $\alpha = 1$, $\Pr = 0.7$ and $\lambda = 1$.

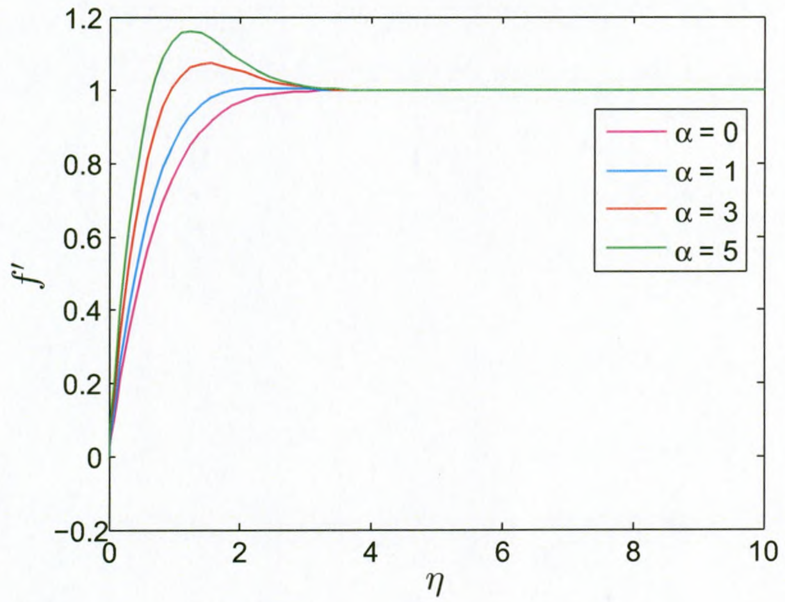

FIGURE 5.6: The velocity distribution plotted against η for several values of α where M = 1, Pr = 0.7 and $\lambda = 1$.

Initially f' increases rapidly as α increases; peaks for $\alpha = 3$ and $\alpha = 5$ are quite visible and a substantial presence of the buoyancy force is experienced by the velocity distribution when $\alpha = 5$. This is because positive buoyancy forces operate as a favourable pressure gradient which expedites the fluid in the buoyancy layer. So the higher the value of α the greater the velocity.

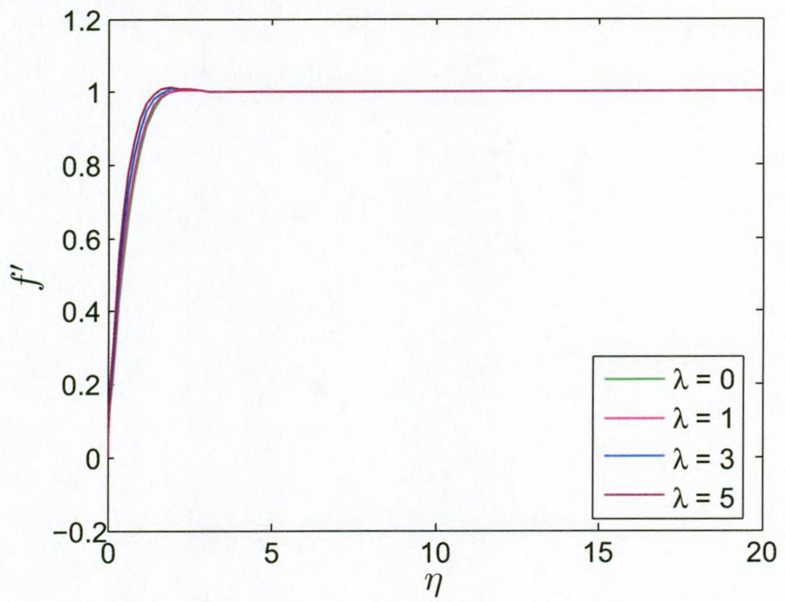

FIGURE 5.7: f' plotted against η for different values of λ where M = 1, Pr = 0.7 and $\alpha = 1$.

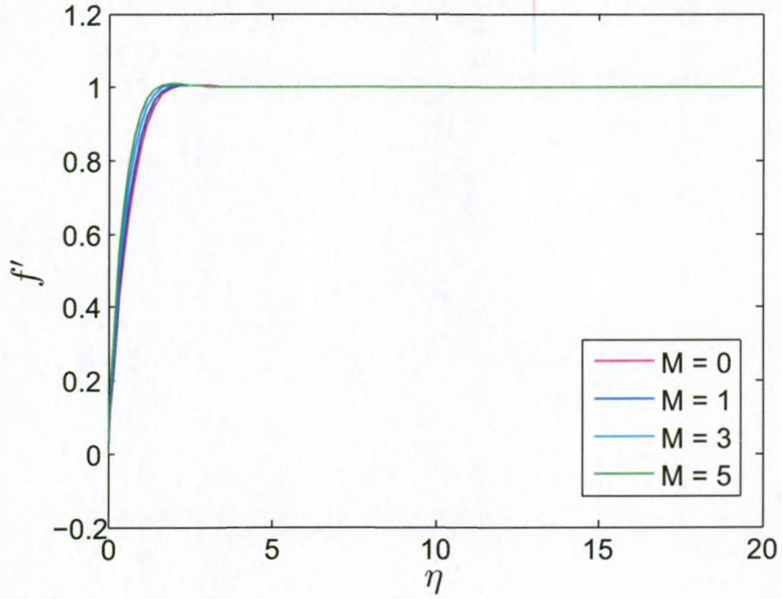

FIGURE 5.8: The impact of the various values of M upon f' where $\lambda = 1$, Pr = 0.7 and $\alpha = 1$.

In Figure 5.7, an increase in the rotation parameter increases the velocity distribution but not by a significant amount; due to λ not appearing explicitly in equation (5.11) and hence the velocity profile will rely weakly on λ. A similar effect on f' is depicted in Figure 5.8 when the magnetic parameter increases, this could be because M is halved in equation (5.11).

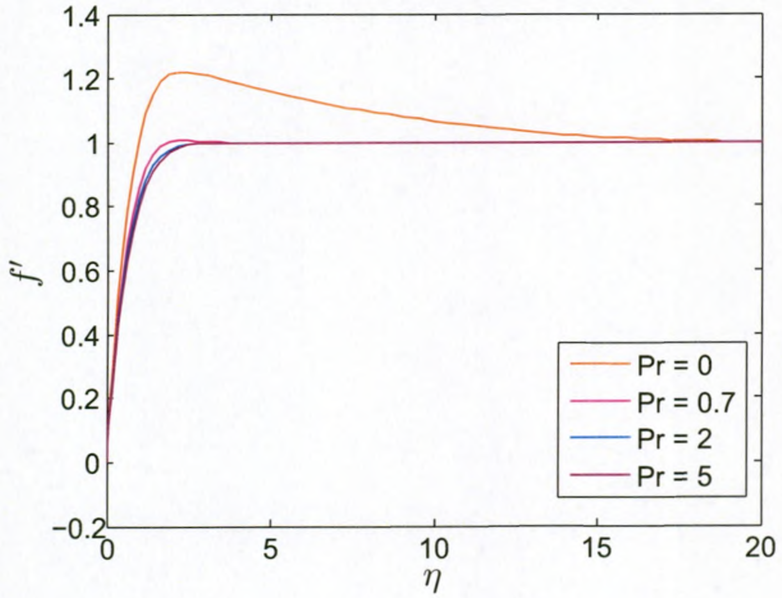

FIGURE 5.9: The influence of Prandtl's number on the velocity distribution where $\lambda =$ 1, M = 1 and $\alpha = 1$.

Initially the various plots of f' with varying Prandtl's numbers are increasing, then visible peaks occur for Pr = 0.7, the greatest being at Pr = 0. This means that either the presence of momentum diffusivity (kinematic viscosity) is not there or the fluid responds very quickly to a change in temperature.

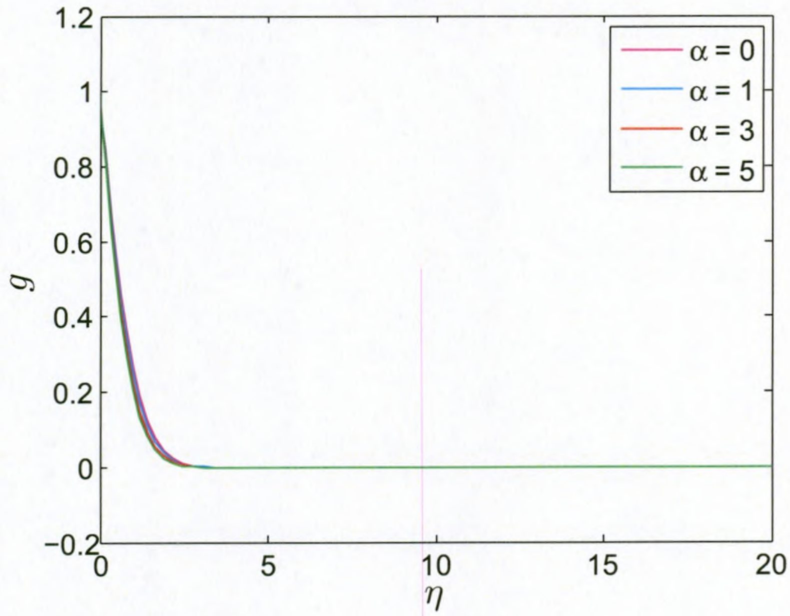

FIGURE 5.10: Plots for g for varying values of α where λ= 1, M = 1 and Pr = 1.

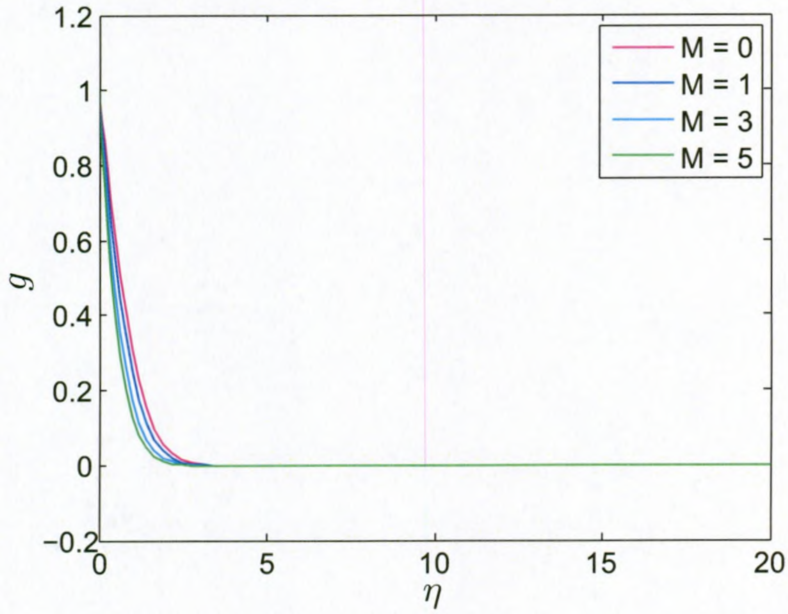

FIGURE 5.11: The effect of M on g where α= 1, λ = 1 and Pr = 1.

In Figure 5.10 above, the effect of the different values of α display a very minimal increase in g. For increasing values of M in Figure 5.11 g decreases. This coincides with the components that describe M. The distinct values of α have a meager impact on the temperature (increasing values of α slightly decrease θ) in Figure 5.12.

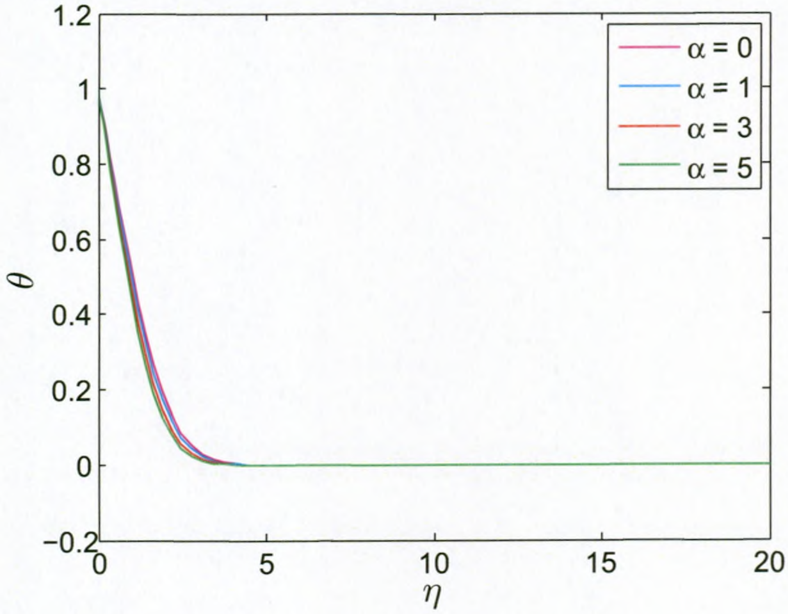

FIGURE 5.12: The various values of α plotted for its influence upon temperature (θ) where M $= 1$, $\lambda = 1$ and Pr $= 1$.

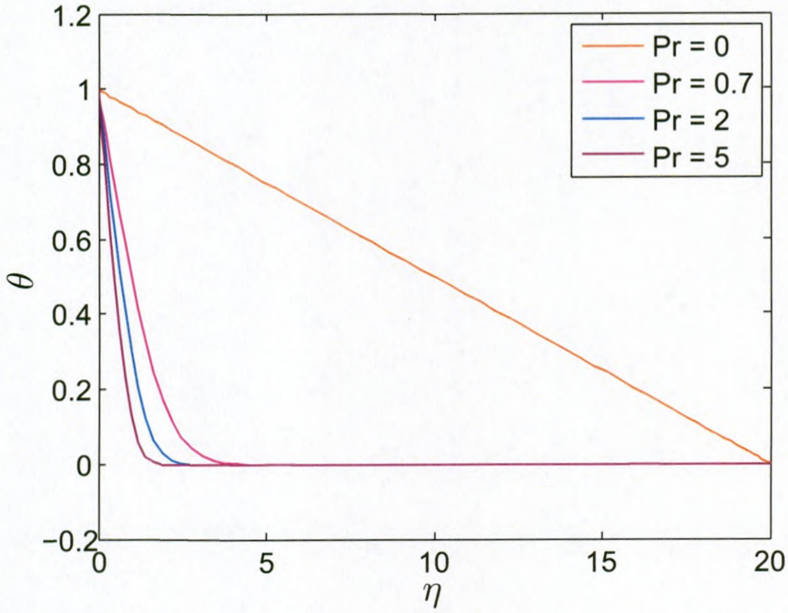

FIGURE 5.13: The influence of Pr upon θ where $\alpha = 1$, $\lambda = 1$ and Pr $= 1$.

Prandtl's number is the parameter that makes a visible impact on θ; with rising values of Pr, θ declines. This means that there is a strong presence of thermal diffusivity.

5.3.1 Convergence and error analysis

Convergence is shown after five iterations for solutions of f, g and θ and the derivatives of f, g and θ. The errors are below 10^{-10} for both the dervatives and results of f, g and θ; this is depicted in Figures 5.14 and 5.15 below.

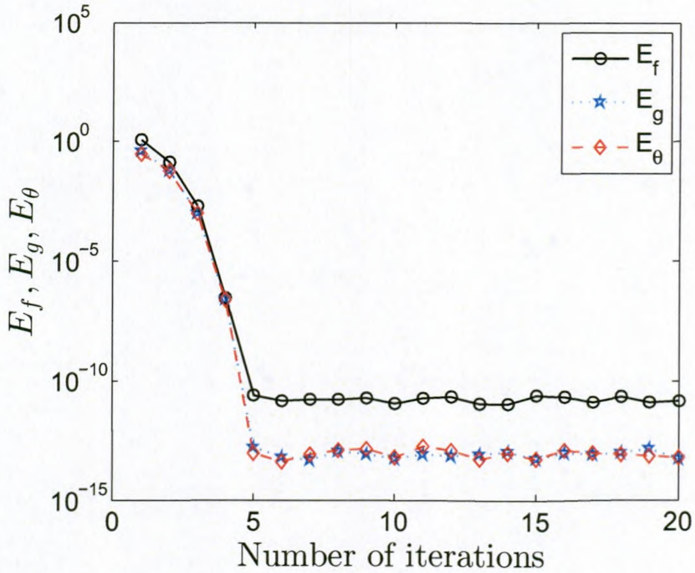

FIGURE 5.14: Error and convergence for f, g and θ.

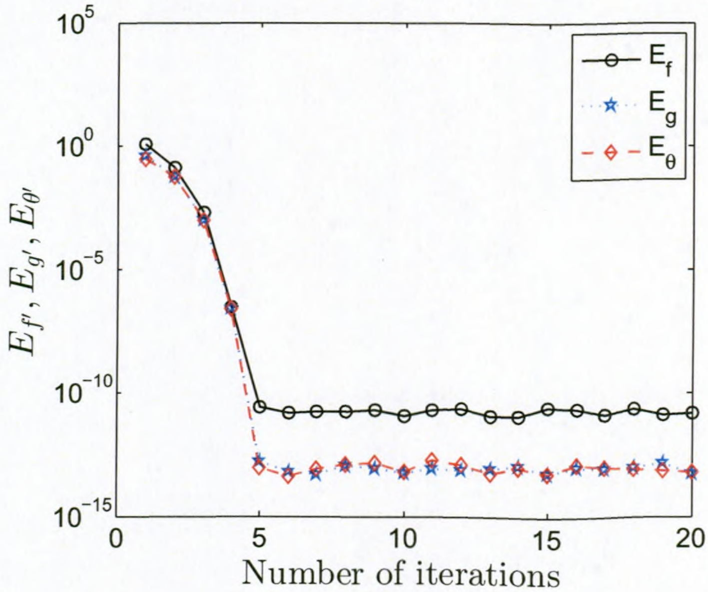

FIGURE 5.15: Error and convergence for the derivatives of f, g and θ.

Chapter 6

Conclusion

In this research the Chebyshev collocation spectral method was proposed for the solution of decoupled and coupled non-simliar boundary layer equations. The BI-SQLM was formulated by conflating the quasi-linearisation method and Chebyshev spectral collocation method with bivariate Lagrange interpolation. With all the research models that were considered the BI-SQLM was relatively easy to implement, computationally efficient and solutions reached convergence rapidly, equivalently in the space and time domains, $\xi \in [0, 1]$ and $\eta \in [0, \infty)$ respectively. Furthermore it was observed that the residual errors were close to zero. When model II was examined, the BI-SQLM proved to be comparable with previous methods employed [62].

Initial solutions were calculated for the three models considered in this dissertation. Also the initial guesses used by Ali and Mehmood [57] for model I and Dinarvand et al. [66] for model III were tested on the corresponding models. It was found that the convergence was slightly slower than the initial solutions that we computed.

6.1 Further work

The employment of the bivariate spectral relaxation method (BI-SRM) on the research models covered in this dissertation would be an interesting extension to the work conducted here. The BI-SRM is an improvement on the spectral relaxation method (SRM). The SRM discretizes derivatives in space and finite differences discretize the time domain. The BI-SRM combines the relaxtion scheme of the spectral relaxation method, bivariate Lagrange interpolation and Chebyshev spectral collocation method. This technique has been used on four non-linear partial diffential equations [68] and the results were deemed to be good, if not superior to other methods such as the Keller-box method. The main advantage is better accuracy which stems from coarser grids and improves the computational speed of the method. Another benefit would be faster convergence to the required solution.

Another avenue to explore is applying the BI-SQLM to an equation or sets of equations, where the dependent variable(s) is/are contingent upon three or more independent variables. An intriguing model to look into would be the model considered in the article by Chakravarty and Mandal entitled *Mathematical modelling of blood flow through an overlapping arterial stenosis* [69]. A stenosed artery comprised of viscoelastic fluid (blood) is described as a thin elastic cylindrical tube, where (r, θ, z) are the coordinates with the z-axis taken along the axis of the artery, while r and θ are the radial and circumferential directions respectively. The overlapping stenosis is depicted by [69]

$$\frac{R(z,t)}{a} = \begin{cases} 1 - a_1(t)\left(\frac{11}{32}(z-d)l_0^3 - \frac{47}{48}(z-d)^2 l_0^2 - \frac{1}{3}(z-d)^4\right), \\ 1 \quad \text{if} \quad d \leq z \leq d + \frac{3l_0}{2}, \end{cases}$$

where $R(z,t)$ is the radius of the arterial segment in the stenotic region, d is the location of the stenosis, a is the constant radius of the normal artery in the non-stenotic region, $3l_0/2$ indicates the length of the stenosis and $a_1(t)$ which is the time-dependent parameter. The unsteady, axisymmetric, laminar stenotic blood flow considered is of the form

$$\rho\frac{\partial w}{\partial t} = \mu^*\left(\frac{1}{R(z,t)}\frac{\partial^2 w}{\partial \xi^2} + \frac{1}{\xi R(z,t)^2}\frac{\partial w}{\partial \xi}\right) - \frac{\partial p}{\partial z} + \frac{\rho\xi}{R(z,t)}\frac{\partial R}{\partial T}\frac{\partial w}{\partial \xi}, \tag{6.1}$$

where $w = w(r, z, t)$ is the axial velocity of the flowing blood, p is the pressure, ρ is the density, μ^* is the complex viscosity of blood and $\xi = r/R(z,t)$.

The boundary conditions are given as

$$\frac{\partial w}{\partial \xi} = 0, \qquad \text{on } \xi = 0, \tag{6.2}$$

$$w(\xi, z, t) = 0, \qquad \text{at } \xi = 1, \tag{6.3}$$

$$w(\xi, z, t) = w_0, \qquad \text{at } t = 1. \tag{6.4}$$

Bibliography

[1] M. Hussaini. Spectral methods in fluid dynamics. *Fluid Mechanics*, 19:339–367, January 1987.

[2] B. Ogundare. On the pseudo-spectral method of solving linear ordinary differential equations. *Department of Pure Mathematics and Applied Mathematics, Mathematics and Statistics*, 5(2):136–140, March 2009.

[3] S. Motsa, V. Magagula, and P. Sibanda. A bivariate chebyshev spectral collocation quasilinearization method for nonlinear evolution parabolic equations. *World Scientifc Journal*, August 2014.

[4] D. Gottlieb. Spectral methods. *Scholarpedia*, 4(2):7504, 2009.

[5] L. Trefethen. Fourier spectral methods. 1994.

[6] D. Kopriva A. Hussaini and A. Patera. Spectral collocation methods. 1987.

[7] L. Delves and J. Mohamed. Computational methods for integral equations. *Cambridge University Press*, page 388, 1985.

[8] T. Cebeci and P. Bradshaw. Physical aspects of convective heat transfer. *Springer-Verlag, Berlin*, 1984.

[9] T. Cebeci and P. Bradshaw. Physical and computational aspects of convective heat transfer. *Springer, New York*, 1984.

[10] S. Nakamura. Iterative finite difference schemes for similar and non-similar boundary layer equations. *Advances in Engineering Software*, 21:123–131, 1994.

[11] E. Mureithi and D. Mason. Local non-similarity solutions for a forced free boundary layer flow with viscous dissipation. *Mathematical and Computational Applications*, 15(4):558–573, 2010.

[12] M. Asgharinia and M. Heydari. The analysis of the boundary layer flow on walls of ducts of a training wind tunnel with flow mach of subsonic test. *Scientific Research*, 3(1):57–71, 2014.

[13] S. Nakamura R. Gorla, J. Lee and I. Pop. Effects of transverse magnetic field on mixed convection in wall plume of power law fluids. *Engineering and Science*, 31 (7):1035–45, 1993.

[14] S. Nakamura R. Gorla, J. Lee and I. Pop. Mixed convection in wall plume of powerlaw fluid. *Mechanics*, 101:47–58, 1993.

[15] N. Kafoussias and E. Williams. An improved technique to obtain numerical solution of a class of two-point boundary value similarity problems in fluid mechanics. *Numerical Methods Fluids*, 17:145–62, 1993.

[16] M. Mustafa T. Hayat and S. Asghar. Unsteady flow with heat and mass transfer of a third grade fluid over a stretching surface in the presence of chemical reaction. *Non-linear Analysis: Real World Applications*, 11:3186–3197, 2010.

[17] S. Liao H. Xu and I. Pop. Series solutions of unsteady three-dimensional mhd flow and heat transfer in the boundary layer over an impulsively stretching plate. *Mechanics B/Fluids*, 26:15–27, 2007.

[18] Z. Lin Y. Zhao and S. Liao. A modified homotopy analysis method for solving boundary layer equations. *Applied Mathematics*, 4:11–15, 2013.

[19] P. Dlamini S. Motsa and M. Khumalo. Spectral relaxation method and spectral quasilinearization method for solving unsteady boundary layer flow problems. *Advances in Mathematical Physics*, June 2014.

[20] Z. Makukula S. Motsa, F. Awad and P. Sibanda. The spectral homotopy analysis method extended to systems of partial differential equations. *Applied Analysis*, April 2014.

[21] V. Epifanov. Boundary layer. March 2011. URL www.thermopedia.com.

[22] Porosity and permeability. April 2016. URL https://www.classzone.com/books/earth_science/terc/content/investigations/es1401/es1401page04.cfm.

[23] Suction. April 2016. URL http://www.thefreedictionary.com/suction.

[24] Injection. April 2016. URL http://www.thefreedictionary.com/injection.

[25] Hydrodynamic. April 2016. URL http://www.merriamwebster.com/dictionary/hydrodynamics.

[26] Thermal. April 2016. URL http://www.thefreedictionary.com/thermal.

[27] Magnetic force parameter. May 2016. URL http://www.thefreedictionary.com/magneticforceparameter.

[28] Buoyancy parameter. May 2016. URL http://www.thefreedictionary.com/buoyancyparameter.

[29] Prandtl number. May 2016. URL http://www.engineeringtoolbox.com.

[30] Rotation parameter. May 2016. URL http://docs.autodesk.com.

[31] McGraw-Hill Dictionary. Skin-friction coefficient. September 2017. URL https://encyclopedia2.thefreedictionary.com/skin-friction+coefficient.

[32] Nusselt number. September 2017. URL http:\auworkshop.autodesk.com/library/convection-heat-lemaster/nusselt-number-relationship.

[33] R. Goldstein. Eckert number. *Heat and mass transfer and fluid engineering*, February 2011.

[34] A. Kau and M. Keteltas. Lagrange interpolation. *General engineering*, December 2009.

[35] Lagrange interpolating polynomials. December 2015. URL http://pegasus.cc.ucf.edu.

[36] S. Motsa. New developments in spectral method based numerical solutions of pdes: A bi-variate spectral collocation approach. *University of KwaZulu-Natal*, July 2014.

[37] J. Shen and T. Tang. Spectral and high-order methods with applications. 2006.

[38] J. Shen. Efficient chebyshev-legendre galerkin methods for elliptic problems. *Houston Journal of Mathematics*, 1996.

[39] S. Liao. A new branch of solutions of boundary layer flows over an impermeable stretched plate. *Heat and Mass Transfer*, 48:2529–2539, June 2005.

[40] B. Sakiadis. Boundary layer behavior on continuous solid surface. i. boundary layer equations for two-dimensional and axisymmetric flow. *AIChE*, 7:26–8, March 1961.

[41] E. Sparrow F. Tsou and R. Glodstein. Flow and heat transfer in the boundary layer on a continuous moving surface. *Heat and Mass Transfer*, 7:219–35, February 1967.

[42] L. Crane. Flow past a stretching plate. *ZAMP*, 21(4):645–647, July 1970.

[43] W. Banks. Similarity solutions of the boundary-layer equations for a stretching wall. *Theoretical and Applied Mechanics*, 2:375–392, 1983.

[44] W. Banks and M. Zaturska. Eigensolutions in boundary layer flow adjacent to a stretching wall. *IMA J. Applied Mathematics*, 36(3):263–273, January 1986.

[45] L. Grubka and K. Bobba. Heat transfer characteristics of a continuous, stretching surface with variable temperature. *ASME J. Heat Transfer*, 107(1):248–250, February 1985.

[46] M. Ali. Heat transfer characteristics of a continuous stretching surface. *Heat and Mass Transfer*, 29(4), March 1994.

[47] L. Fan L. Erickson and V. Fox. Heat and mass transfer on a moving continuous flat plate with suction or injection. *Industrial Chemical Engineering*, 5, 1966.

[48] E. Elbashbeshy. Heat transfer over a stretching surface with variable surface heat flux. *Physics and Applied Physics*, 31:1951–1954, 1998.

[49] C. Chen and M. Char. Heat and mass transfer on a continuous stretching surface with suction or blowing. *Mathematical Analysis and Applications*, 135:568–580, 1988.

[50] E. Magyari and B. Keller. Exact solutions for self-similar boundary-layer flows induced by permeable stretching walls. *Eur. J. Mechanics - B/Fluids*, 19:109–122, 2000.

[51] J. Merkin M. Chaudhary and I. Pop. Similarity solutions in the free convection boundary-layer flows adjacent to vertical permeable surfaces in porous media. *Eur. J. Mechanics - B/Fluids*, 14:217–237, 1995.

[52] K. Vajravelu. Hydromagnetic flow and heat transfer over a continuous, moving, porous, flat surface. *Acta Mathematica*, 64, 1986.

[53] N. Amin N. Nazar and I. Pop. Unsteady boundary layer flow due to stretching surface in a rotating fluid. *Mechanics Research Communications*, 31:121–8, 2004.

[54] S. Liao and H. Xu. Series solutions of unsteady magnetohydrodynamic flows of non-newtonian fluids caused by an impulsively stretching plate. *Non-Newtonian Fluid Mechanics*, 129:46–55, 2005.

[55] S. Liao. An analytic solution of unsteady boundary-layer flows caused by an impulsively stretching plate. *Communications in Nonlinear Science and Numerical Simulation*, 11:326–39, 2006.

[56] J. Williams and T. Rhyne. Boundary layer developed on a wedge impulsively set into motion. *SIAM J. Applied Mathematics*, 38:215–24, 1980.

[57] A. Ali and A. Mehmood. Homotopy analysis of unsteady boundary layer flow adjacent to permeable stretching surface in porous medium. *Communications in Nonlinear Science and Numerical Simulation*, 13:340–349, 2008.

[58] L. Walker. Discrete equations. September 2017. URL http://www.maths.manchester.ac.uk/~lwalker/MATH10000/project-05-lecture-notes.pdf.

[59] A. Raptis. Flow of a micropolar fluid past a continuously moving plate by the presence of radiation. *Heat and Mass Transfer*, 41:2865–2866, 1998a.

[60] A. Raptis. Radiation and free convection flow through a porous medium. *Communications in Heat and Mass Transfer*, 25:289–295, 1998b.

[61] K. Yih. Mhd forced convection flow adjacent to a non-isothermal wedge. *Communications in Heat and Mass Transfer*, 26:819–827, 1999.

[62] A. Quadri A. Chamkha, M. Mujtaba and C. Issa. Thermal radiation effects on mhd forced convection flow adjacent to a non-isothermal wedge in the presence of a heat source or sink. *Heat and Mass Transfer*, 39:305–312, 2003.

[63] R. Rajasekaran and M. Palekar. Mixed convection about a rotating sphere. *Heat and Mass Transfer*, 28:959–965, 1985.

[64] H. Hatzikonstantinou. Effects of mixed convection and viscous dissipation on heat transfer about a porous rotating sphere. *ZAMM*, 70:457–464, 1990.

[65] M. Ece. The initial boundary layer flow past a translating and spinning rotational symmetric body. *Mathematical engineering*, 26:415–428, 1992.

[66] E. Doosthoseini S. Dinarvand, A. Doosthoseini and M. Rashidi. Series solutions for unsteady laminar mhd flow near forward stagnation point of an impulsively rotating and translating sphere in presence of buoyancy forces. *Nonlinear Analysis: Real World Applications*, 11:1159–1169, 2009.

[67] A. Chamkha H. Takhar and G. Nath. Unsteady laminar mhd flow and heat transfer in the stagnation region of an impulsively spinning and translating sphere in the presence of buoyancy forces. *Heat Mass Transfer*, (37):397–402, 2001.

[68] V. Magagula S Motsa, P. Dlamini and P. Sibanda. Bivariate spectral relaxation method for unsteady three dimensional mhd flow and mass transfer in a porous media. *Heat Mass Transfer*, April 2015.

[69] S. Chakravarty and P. Mandal. Mathematical modelling of blood flow through an overlapping arterial stenosis. *Mathematical Computer Modelling*, 19(1):59–70, July 1994.

[70] C. Boor. A pratical guide to splines. *Springer-Verlag*, 1978.

[71] F. Fritsch and R. Carlson. Monotone piecewise cubic interpolation. *SIAM journal on numerical analysis*, (17):238–246, 1980.